DIFFRACTION AND TRAPPING OF WAVES BY CAVITIES AND SLENDER BODIES

by

GRANT ROBERT BIGG, B.Sc.(Hons.) (Adelaide)

Thesis submitted for the degree of
Doctor of Philosophy at the
University of Adelaide,
Department of Applied Mathematics.

ADELAIDE, OCTOBER 1982

TABLE OF CONTENTS

SUMMARY

This thesis consists of two parts, linked by the use of common mathematical techniques and the consideration of similar physical phenomena. Part I examines the response of cavities to external exciting oscillations, in both two and three dimensions. The cavities are assumed to possess openings whose dimensions are small in comparison to the size of the cavity itself. This assumption enables the technique of matched asymptotic expansions to be employed. For a portion of the analysis the further assumption that the wavelength of the exciting oscillation is small is used. This enables a careful inspection to be made of the Helmholtz resonance of the cavity.

The theory developed is compared to numerical computations, made using a boundary integral equation technique, and work, both analytic and experimental, by other researchers in this field. Several interesting results of the theory are discussed, such as the symmetry property which enables the number of cavities treatable by this analysis to be extended and the difference in response curve for cavities of the same volume.

The second part of the thesis examines the scattering of waves by slender bodies which are either transparent to the incident radiation or opaque to it. The specific application of the work is to an oceanographic situation but simple extensions may be made to include acoustic, electromagnetic and elastic problems. The work of Mei and Tuck (1980), which employed the parabolic approximation to study scattering by (mostly) transparent bodies, is analyzed critically using matched asymptotic expansions and numerical comparisons; these using boundary integral equation

methods. The existence of a special class of "barely submerged islands" is verified but it is shown that the theory is not useful when energy is trapped over the feature, producing resonance.

Part II also examines, both numerically and analytically, the scattering of waves by slender opaque bodies, or "islands". Matched asymptotic expansion analysis reveals that the parabolic approximation, which essentially says that the amplitude of the wave varies more rapidly in one direction than another, is useful over a range of incident wavelengths but not uniformly.

SIGNED STATEMENT

This thesis contains no material which has been accepted for the award of any other degree or diploma in any University. To the best of my knowledge and belief, the thesis contains no material previously published or written by any other person, except where due reference is made in the text.

GRANT R. BIGG.

ACKNOWLEDGEMENTS

I would like to express my appreciation for the encouragement and guidance given by my supervisor Professor E.O. Tuck during the course of this research. . I also wish to acknowledge the helpful discussions on the work of this thesis that I had with Professor C.C. Mei and Dr. R. Yeung during their sabbaticals at Adelaide from the Massachusetts Institute of Technology. Lastly, I would like to acknowledge the excellent typing of Elizabeth Henderson.

P A R T I

CAVITY RESONATORS

CHAPTER 1

REVIEW OF CAVITY RESONATOR THEORY

Cavity resonators, both two and three dimensional, have a number of important applications, ranging from the design of musical instruments to the operation of man-made and natural harbours. The mathematics of the physical processes involved has thus received considerable attention since the pioneering work of Helmholtz (1860) and Rayleigh (1870, 1896) last century. However, while a degree of progress has been achieved, especially in the two dimensional harbour problem, the theory of cavity resonance is far from complete. The first part of this thesis will look at a branch of this field, namely the linear theory of externally excited resonators with small openings, and attempt to place it on a firm basis by use of the technique of matched asymptotic expansions.

1.1 Previous Work

The theory of cavity resonators has in recent years split into two separate fields: the study of harbour resonance, a basically hydrodynamically-oriented discipline, often working within a two dimensional framework; and acoustic-cavity theory. This division, while obscuring to some extent the similarities between the two classes of problem, has some advantages and will be used in this discussion.

The aim of much of the work in the theory of nearly-closed cavity resonators is to describe the response curve of a given cavity to an external excitation. This response contains peaks at frequencies close to the natural resonant frequencies of the

fully closed cavity; that is, at wavelengths comparable to, or smaller than, the dimensions of the cavity. In addition, there is a single low-frequency peak, unrelated to any non-trivial natural frequency of the cavity, and corresponding to a wavelength in excess of the dimensions of the cavity. When subject to this mode, the cavity is said to be responding as a "Helmholtz resonator". It is this aspect of the response which has caused most discussion and will be examined in detail in Chapters 3 and 4.

The physical nature of this mode, first realised by Helmholtz and Rayleigh in their three dimensional studies mentioned above, may be most easily thought of in the acoustic problem, where it corresponds to a uniform compression of the air in the entire cavity. Thus, it is quite different from a natural frequency mode, in which density variations across the cavity play a prominent role. A common portrayal of the Helmholtz mode is in terms of a "spring and mass" system, see for instance Rayleigh (1896), Kinsler and Frey (1962) and Alster (1972), where the mass on the spring represents the mass of the fluid in the aperture, and the spring represents the interior of the cavity. This simple model leads to a relatively accurate leading-order prediction of the Helmholtz resonant wavenumber for three dimensional resonators, namely

$$k_H = \left(\frac{A_N}{(\ell_N + \alpha_E) V} \right)^{1/2} , \qquad (1.1)$$

A_N being the area of the aperture, ℓ_N its length, V the volume of the cavity and α_E the "end correction".

The factor α_E, introduced by Rayleigh to extend his work to resonators with narrow walls near the opening, was recognized by him as varying in value with cavity shape. This property, an important part of his theory, has not always been appreciated in subsequent work, with α_E usually assuming a value which is only a definite multiple, $8\omega/3\pi$, of the aperture radius ω rather than a more complicated expression. It has now been shown that this is a gross simplification, e.g. Ingard (1953a), Hirschwehr (1974).

While Rayleigh's formula (1.1) is useful, it can be inaccurate by about 10%, and for some cavities this error is much greater. In particular, the parameter α_E is often hard to compute, especially for cavities with finite wall curvature near the aperture. The formula is also only formally correct for cavities with large interior-to-opening dimension ratios and long incident wavelengths.

Thus, a good deal of effort has gone into further examination of the phenomenon of cavity resonance. Much of the early work was experimental or aimed at improving Rayleigh's estimates. A bibliography of pre-1950 papers can be found in Chapter 7 of Zwikker and Kosten (1949), which also gives a summary of the standing of the subject at that time. Since then, non-linear aspects of the problem and the study of particular shapes of cavities has become important.

The experimental and mathematical investigation into various cavity shapes has been fairly successful. Panton and Miller (1975a) calculated the frequencies for both the Helmholtz and natural modes in circular cylinders by the use of improved entrance corrections; that is, by effectively modifying α_E. Ingard (1953b) examined spherical cavities both experimentally and by theoretical means.

He was principally concerned with the effect of changing the velocity distribution across the opening, and seeing how this altered the accuracy of the theoretical results. The response of the complex cavities of various musical instruments was investigated by Jansson (1977), with emphasis on particular shapes and the vibration of the casing. Cummings (1973) developed a one dimensional model of the acoustics of a slender wine bottle valid for all frequencies. Another paper, by Tam and Block (1978), in a related field dealt with low subsonic grazing flow past a two dimensional rectangular cavity. Recently, the design of automobile passenger compartments was reviewed by Nefske, Wolf and Howell (1982), with emphasis on finite element prediction of modes of acoustic vibration for both rigid and elastic walls.

The non-linear investigations of resonator response have involved both studies of damping, and the role of jets or turbulent boundary layers in the generation of resonance. Zinn (1970) used viscosity to give a theoretical model of the damping of the motion in a two dimensional cavity as well as considering the damping from jets formed at the ends of the orifice. Covert (1970) used vortex sheets to determine the velocity required in a shearing flow to induce cavity oscillations, finding that the induced vibrations corresponded to the natural vibrational modes. In 1973, Tang and Sirignano presented a "theory of a generalized Helmholtz resonator" using non-linear one dimensional gas dynamics equations. They gave both a first and a second order theory. Panton and Miller (1975b) experimentally tested the effect of a turbulent boundary layer on the resonance properties of cavities, finding that the resonant frequencies shifted and had larger amplitudes in the presence of

the boundary layer. Elder (1978) examined the Helmholtz resonance, both experimentally and theoretically, in a cavity subject to turbulent shear grazing flow, in which the mouth of the resonator was considered to be small compared to the wavelength of the external field. Nelson, Halliwell and Doak (1981) also examined resonator dynamics experimentally, looking at aperture characteristics, such as velocity and Reynold's stresses, in particular.

A prominent worker in the field of non-linear investigations of Helmholtz resonators is M.S. Howe. In a series of papers he has considerably advanced the state of knowledge in this field. In 1975, in an article dealing with the theory of aerodynamic sound, he applied matching techniques, which are similar to some of the methods used in the present Chapters 3 and 4, to grazing flow in the vicinity of a lateral opening in a flute. Then, in 1976, he developed a three dimensional theory for the excitation of a Helmholtz resonator by external disturbances located close to the mouth of the resonator. This paper also considered the response due to a shear layer of turbulent eddies near the aperture. Still considering grazing flow problems, in 1979(a) he presented an essentially two dimensional analytic examination of flow past a circular cavity set in a wall. In 1981(a) he looked at the dynamics of the flue organ pipe, postulating that it is driven by jets found near the lateral openings.

This researcher has also been prominent in the associated field of study which examines flow through apertures. For a discussion of the literature on this topic see Appendix IB.

Other workers have attempted a general linear theory. For example, Alster (1972) derived an improved formula for resonant

frequencies in axially symmetric Helmholtz resonators using ideas developed from the simple spring-mass concept mentioned earlier. Another investigator was Tuck (1975), who applied basic matched asymptotic expansion theory to the prediction of the Helmholtz frequency, via use of an aperture parameter s, similar in nature to the "conductivity" parameter c of Rayleigh. This parameter will play a large role in the later work of this thesis.

As noted earlier, the problem of harbour resonance is a special case of general resonator theory, which has been vigorously pursued by workers in oceanography and hydrodynamics since the beginning of the century (see e.g. Honda, Terada, Isitani (1908)). Both numerical and analytic approaches to this problem have been used; for several early studies see Lee (1971).

The numerical attacks have employed techniques such as finite elements, boundary integral equation (b.i.e.) methods and hybrids of these. Hwang and Tuck (1970) used a b.i.e. method to examine the oscillations in harbours of arbitrary shape and constant depth, as did Lee (1969, 1971). These studies are used as a basis for the numerical method in Chapter 2. An example of a finite element approach is that of Chen and Mei (1976). They examined resonance in man-made harbours detached from the coast. Shaw and Falby (1978) developed a hybrid method for variable depth harbours, employing finite elements in the harbour and b.i.e. techniques outside. Rahman (1981) also looked at a variable depth harbour. By considering a number of zones to have different constant depths, he was able to determine the free surface movement by employing a combination of matching at the junctions and a b.i.e. method.

Mattioli has used b.i.e. methods of conventional design (see Chapter 2) and some of his own genesis, (1978a), (1981), in studying

resonance in harbours. He has examined the oscillations in rectangular harbours with various bottom profiles (1978b), constant depth harbours of arbitrary shape (1979) and such harbours with external coasts being of complex, rather than the conventional linear, design (1980). Most of Mattioli's work is an attempt to simplify the integrals involved in b.i.e. methods by removing the frequency component from the kernels.

Another prolific worker in the field of harbour resonance is J.W. Miles, who often uses variational approaches to a problem to obtain analytic results. In 1971 he performed an equivalent-circuit analysis of harbour resonance for both the Helmholtz mode and the natural modes. He examined circular, rectangular and semi-circular harbours in particular. Then, in 1974, he published a review article on harbour seiching in general. In collaboration with Y.K. Lee (1975), he used variational principles to study the Helmholtz resonance of harbours of variable depth. This study considered the effects of entry separation and bottom friction, and used a parameter M, related to the parameter b of Chapter 3, in calculations. Recently, in 1981(a), Miles has used Hamiltonian mechanics to investigate non-linear behaviour of Helmholtz resonance in harbours and coupled basins.

A problem similar to harbour resonance is the seiching of basins separated from the open sea by a submerged barrier. Both Tuck (1980) and Miles (1981b) have investigated this class of problem.

It is also worth mentioning that some work on cavity resonators in an electromagnetic context has been done. The paper of Hamilton and Kerdemelidis (1982) gives references to work on transmission

through slits while Harrington (1982) discusses cavity resonance. This latter paper is interesting in its own right, as the effect of an isolated body inside the cavity on the response to an external excitation is examined. This analysis leads to the conclusion that such a body increases the response at resonance.

1.2 Problem Formulation

In many fields of application the problem breaks down into the solution of the same set of equations, providing we assume linearity. These equations will first be presented and then several physical problems will be discussed to demonstrate the truth of the above statement.

An external exciting oscillation will be assumed to produce a time-harmonic potential, $e^{-i\,wt}\phi(x_j)$, $j=1,2$ or $j=1,2,3$ depending on the dimensionality of the problem. This time dependence will be neglected in what follows. Our governing equation is then

$$\nabla^2\phi(x_j) + k^2\phi(x_j) = 0, \tag{1.2}$$

where the wavenumber k is a fixed positive constant, in a region R bounded by a surface or curve Γ across which there is no flow; that is,

$$\frac{\partial\phi}{\partial n} = 0 \quad \text{on} \quad \Gamma \ . \tag{1.3}$$

R includes both the external region and the cavity.

To obtain the radiation condition at infinity, assume that at a great distance from the cavity the external oscillation is $\phi_\infty(x_j)$ so that, as $r = \sqrt{x_j^2} \to \infty$,

$$\phi(x_j) \to \phi_\infty(x_j) + e^{ikr} \cdot O(r^{-(n-1)/2}), \tag{1.4}$$

where n is the dimension of the problem. This is Sommerfeld's radiation condition.

We now turn to some physical problems to demonstrate how (1.2) comes about. Firstly, consider the irrotational flow of an incompressible fluid, with velocity potential $\Phi(x,y,z,t)$, under a free surface in the presence of a gravitational acceleration g. Then the governing equation is

$$\nabla^2\Phi = 0, \tag{1.5}$$

but if we let

$$\Phi(x,y,z,t) = -\frac{1}{i\omega}\phi(x,y)Z(z)e^{-i\omega t} \tag{1.6}$$

then (1.5) may be transformed to (1.2) with respect to the ϕ component, with k being the solution of

$$\omega^2 = gk \cdot \tanh(kh), \tag{1.7}$$

h, the depth of the fluid, being assumed constant. The z-component of (1.6) is given by

$$Z(z) = \frac{-A_i\, g \cosh(k(h+z))}{\cosh(kh)}, \tag{1.8}$$

where A_i is the amplitude of the incident wave and $z=0$ is the undisturbed free surface. For more details see Stoker (1957; pp. 110, 414).

As a second example consider the irrotational flow of a *compressible* fluid with velocity potential $\Phi(x,y,z,t)$. That is,

we are now looking at an acoustic problem. From Lamb (1932; §§ 285, 287, 289) the governing equation is found to be the wave equation

$$\frac{\partial^2 \Phi}{\partial t^2} = c^2 \nabla^2 \Phi \ , \tag{1.9}$$

c being the speed of sound in the fluid. So, if the time harmonic component of (1.8) is removed, Helmholtz's equation is derived with

$$k = \frac{\omega}{c} \ . \tag{1.10}$$

The final application to be considered is to the theory of electromagnetism. If the propagation of monochromatic electromagnetic waves through a non-conducting homogeneous medium is examined, then the governing equation is found to be

$$\nabla^2 E(x,y,z,t) = \varepsilon/\mu \, \frac{\partial^2 E(x,y,z,t)}{\partial t^2} \ , \tag{1.11}$$

where E is the electric field strength, ε is the permittivity and μ is the permeability of the medium. Upon invoking the time harmonic property of E, equation (1.2) is derived with

$$k = \omega(\varepsilon\mu)^{\frac{1}{2}} \ . \tag{1.12}$$

For further details see Lorrain and Corson (1970; §§10.10, 11.2, 11.3).

CHAPTER 2

THE BOUNDARY INTEGRAL EQUATION METHOD

In Chapter 3, as throughout Part II, considerable use will be made of numerical solutions to various problems by means of boundary integral equation techniques. As the basic mathematics of each problem is similar, this chapter deals, in depth, with the method employed in Chapter 3. In the use of subsequent numerical methods, only the different framework will be examined. It should also be noted that the numerical formulation, in particular the matching procedure at the cavity entrance, owes much to J.-J. Lee (1969), (1971).

2.1 Green's Function Solution

For the purpose of the numerical formulation, consider a cavity set in a plane wall, as in Figure 2.1. The boundary Γ can be decomposed into

$$\begin{aligned} \Gamma &= \Gamma_E + \Gamma_C \\ &= (\Gamma_E - \Gamma_0) + (\Gamma_C + \Gamma_0) \end{aligned} \tag{2.1}$$

where Γ_C is the cavity wall, Γ_E the exterior curve and Γ_0 is an artificial boundary across the opening. We let $\Gamma_E - \Gamma_0$ be taken as the y-axis and assume that a plane wave is normally incident on the wall from the left, that is,

$$\phi_i = \frac{1}{2} e^{ik_1 x} \quad . \tag{2.2}$$

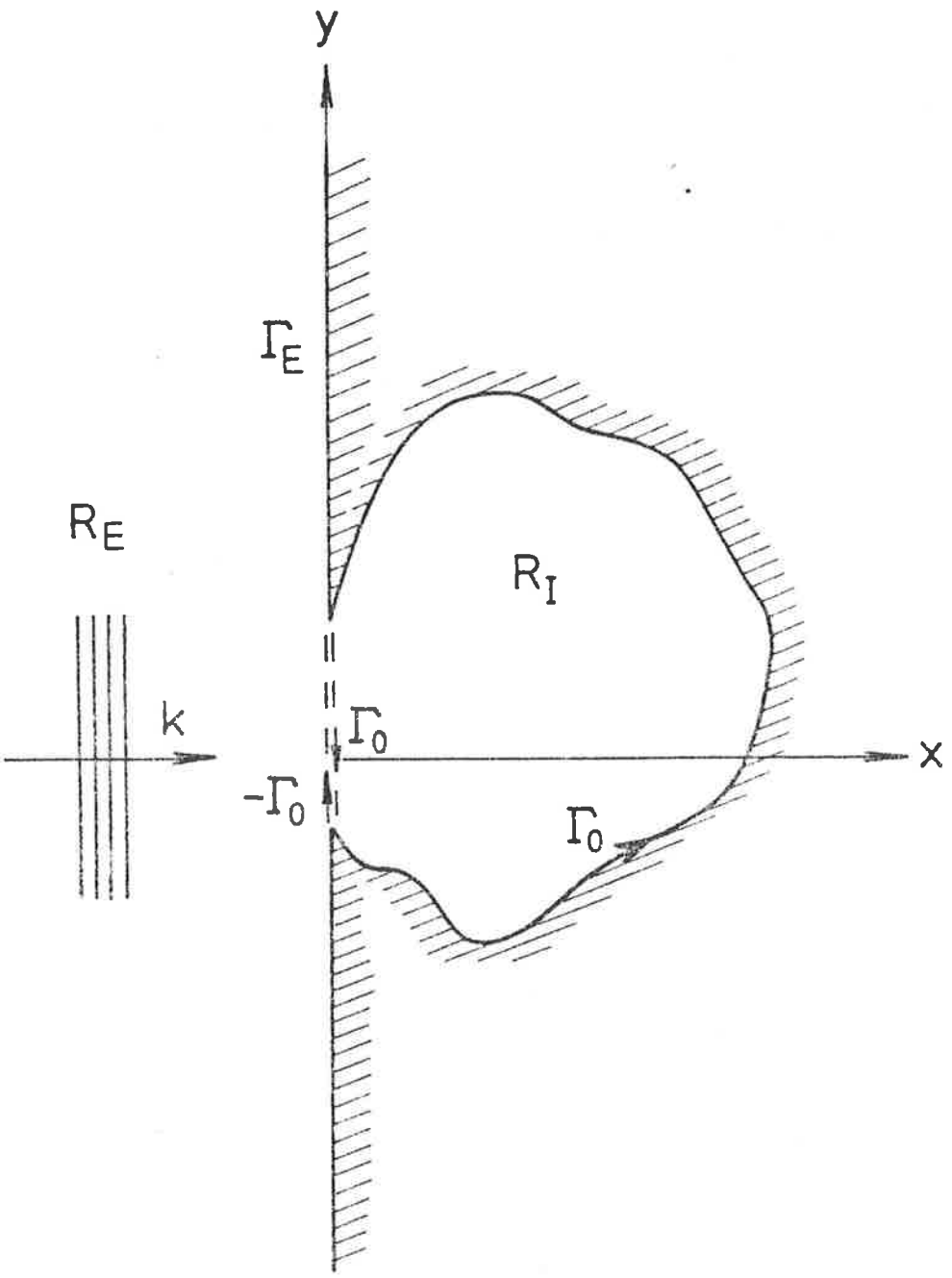

Figure 2.1: Schematic of cavity considered by numerical method.

Note that the assumption of normal incidence is not necessary but only used for convenience.

The potential flow in this problem is subject to (1.2)-(1.4) and may therefore be given a Green's integral representation in both the interior (cavity) and exterior regions. If the analytic closed curve $\Gamma_C + \Gamma_0 = \Gamma_I$, then the potential inside this curve, ϕ_I, may be written, by use of a version of Green's theorem

$$\iint_S (\beta\nabla^2 A - A\nabla^2\beta)\,dxdy = \oint_C (\beta\frac{\partial A}{\partial n} - A\frac{\partial\beta}{\partial n})\,d\ell \ , \qquad (2.3)$$

(1.2) and the properties of the Green's function, as

$$\phi_I(\underset{\sim}{x}_i) = \int_{\Gamma_I} [\phi_I(\underset{\sim}{x}')\frac{\partial G(\underset{\sim}{x}';\underset{\sim}{x}_i)}{\partial n} - G(\underset{\sim}{x}';\underset{\sim}{x}_i)\frac{\partial \phi_I(\underset{\sim}{x}')}{\partial n}]\,d\ell(\underset{\sim}{x}'), \quad \underset{\sim}{x}_i \in \{R_I - \Gamma_I\}, \qquad (2.4)$$

where $G(\underset{\sim}{x}';\underset{\sim}{x}_i)$ is the appropriate Green's function, $\partial/\partial n$ is an outward normal derivative with respect to $\underset{\sim}{x}'$ and R_I is the region enclosed by Γ_I. As, from (1.3), the normal derivative of ϕ_I vanishes on Γ_C, (2.4) may be simplified. We still need to find $\partial\phi_I/\partial n$ on Γ_0, and to do this the flow will be matched with the exterior solution across the aperture.

However, as (2.4) is not valid on Γ_I it must be modified, by a limiting process outlined in Lee (1969), to enable the boundary potential on Γ_I to be found. The potential may then be represented as

$$\phi_I(\underset{\sim}{x}_i) = 2\int_{\Gamma_I} [\phi_I(\underset{\sim}{x}')\frac{\partial G(\underset{\sim}{x}';\underset{\sim}{x}_i)}{\partial n} - G(\underset{\sim}{x}';\underset{\sim}{x}_i)\frac{\partial \phi_I(\underset{\sim}{x}')}{\partial n}]\,d\ell(\underset{\sim}{x}'), \quad \underset{\sim}{x}_i \in \Gamma_I, \qquad (2.5)$$

the integral taking its Cauchy Principal Value.

The Green's function for this problem is a multiple of the zeroth order Hankel function of the first kind (see, for instance,

Shaw (1979)), that is, using the notation of Abramowitz and Stegun (1972),

$$G(\underset{\sim}{x}';\underset{\sim}{x}_i) = -\frac{i}{4}H_0^{(1)}(kr'), \tag{2.6}$$

where

$$r' = |\underset{\sim}{x}_i - \underset{\sim}{x}'| \ . \tag{2.7}$$

To find $\partial\phi_I/\partial n$ on Γ_0, as noted above, the exterior solution must be found. Now in R_E, the region external to the cavity, where

$$\phi_E = \phi_\infty + \bar{\phi}_E \ , \tag{2.8}$$

$\bar{\phi}_E$ being the cavity radiation correction and where, for (2.2),

$$\phi_\infty = \cos kx, \tag{2.9}$$

the boundary condition

$$\frac{\partial\bar{\phi}_E}{\partial n} = \begin{cases} 0 & y \in \Gamma_E \\ \dfrac{-\partial\phi_I}{\partial n} & y \in -\Gamma_0 \end{cases} \tag{2.10}$$

applies, assuming continuity of flux. There is an integral equation, analogous to (2.5), satisfied by $\bar{\phi}_E$ on $\Gamma_E - \Gamma_0$, the contribution from the semi-circle at infinity being zero (see Appendix IA), but as this boundary is the y-axis, $\partial r'/\partial n$, and thus $\partial G/\partial n$, is zero. Therefore, using (2.10),

$$\phi_E(0,y_i) = 1 - \frac{i}{2}\int_{\Gamma_0} H_0^{(1)}(kr')\frac{\partial\phi_I(y')}{\partial n}\,dy' \ . \tag{2.11}$$

Assuming continuity of potential across Γ_0, (2.11) gives an expression for ϕ_I in the mouth of the resonator.

2.2 Discretization

Having expressed the problem in integral form, we can now discretize (2.5) and (2.11), noting that use of (1.3) simplifies the second term of (2.5). In discretizing, ϕ_I and $\partial\phi_I/\partial n$ are considered to be constant on a given segment and representable by the value at the segment's midpoint. In the opening, where these assumptions might be thought to be severe, it will be seen in Chapters 3 and 4 that ϕ is approximately constant in the aperture and while $\partial\phi/\partial n$ is singular at the edges, the singularity is weak and does not produce difficulties. So, dividing Γ_I into N segments with the first p across Γ_0, (2.5) and (2.11) may be rewritten as

$$\phi_I(\underset{\sim}{x}_i) = \sum_{j=1}^{N} \phi_I(\underset{\sim}{x}_j) \int_{\Delta\ell_j} -\frac{i}{2}\frac{\partial H_0^{(1)}(kr')}{\partial n}\, d\ell(\underset{\sim}{x}') - \sum_{j=1}^{p} \frac{\partial\phi_I(y_i)}{\partial n} \int_{\Delta\ell_j} -\frac{i}{2}H_0^{(1)}(kr')dy' \qquad i=1,\ldots,N, \quad (2.12a)$$

with $\underset{\sim}{x}_i = (0,y_i)$ for $i \leq p$, and

$$\phi_I(\underset{\sim}{x}_i) = 1 + \sum_{j=1}^{p} \frac{\partial\phi_I(y_j)}{\partial n} \int_{\Delta\ell_j} -\frac{i}{2}H_0^{(1)}(kr')dy' \qquad i=1,\ldots,p. \quad (2.12b)$$

Note that $\underset{\sim}{x}_i$ is the midpoint of the ith segment.

These two equations may be rewritten in matrix form, that is,

$$\begin{aligned} \Psi_1 &= A\Psi_1 - B\Psi_2 \\ \Psi_{1p} &= e + B_p\Psi_2 \end{aligned} \qquad (2.13)$$

where

$$[\Psi_1]_i = \phi_I(\underset{\sim}{x}_i), \quad i=1,\ldots,N$$

$$[\Psi_2]_i = \frac{\partial \phi_I}{\partial n}(\underset{\sim}{x}_i), \quad i=1,\ldots,p$$

$$[A]_{ij} = \int_{\Delta \ell_j} -\frac{i}{2}\frac{\partial H_0^{(1)}(kr')}{\partial n} d\ell(\underset{\sim}{x}'), \quad i,j=1,\ldots,N$$

$$[B]_{ij} = \int_{\Delta \ell_j} -\frac{i}{2}H_0^{(1)}(kr')dy', \quad i=1,\ldots,N;\ j=1,\ldots,p \qquad (2.14)$$

$$[\Psi_{1p}]_i = [\Psi_1]_i, \quad i=1,\ldots,p$$

$$[e]_i = 1, \quad i=1,\ldots,p$$

$$[B_p]_{ij} = [B]_{ij}, \quad i,j=1,\ldots,p.$$

If we write

$$\Psi_{1p} = K\Psi_1 \qquad (2.15)$$

where

$$[K]_{ij} = \delta_{ij}, \quad i=1,\ldots,p;\ j=1,\ldots,N, \qquad (2.16)$$

δ_{ij} being the Kronecker delta, then eliminating Ψ_2 from (2.13) and rearranging gives

$$\Psi_1 = (A-I-BB_p^{-1}K)^{-1}BB_p^{-1}e, \qquad (2.17)$$

I being the $N\times N$ identity matrix. Thus, assuming the coefficients of A and B are known, (2.17) gives a means of evaluating the potential at N points on the cavity boundary Γ_0.

2.3 Evaluation of Matrix Coefficients

The coefficients of the matrices A and B may be evaluated by a combination of numerical and analytic techniques. If the

kernels of each integral are split into their singular and non-singular components, then the singular parts may be integrated exactly, as in Hwang and Tuck (1970). The remaining non-singular terms are then numerically integrated.

So, consider $H_0^{(1)}(kr')$, which may be split up to give

$$\frac{i}{2}H_0^{(1)}(kr') = \frac{-1}{\pi}\ln(r') + M(k,r'), \tag{2.18}$$

$M(k,r')$ being the non-singular component. The general coefficient of A then becomes

$$[A]_{ij} = \int_{\Delta\ell_j}\left[-\frac{\partial M(k,r')}{\partial n} + \frac{1}{\pi}\nabla\ln(r').\underset{\sim}{n}\right]d\ell(\underset{\sim}{x}') \quad i,j=1,\ldots,N. \tag{2.19}$$

If we let the segment have the parametric representation

$$\underset{\sim}{\ell}(t) = \xi(t)\underset{\sim}{i} + \eta(t)\underset{\sim}{j}, \tag{2.20}$$

then, recalling the definition of r' from (2.7), the singular part of (2.19) may be written as

$$I_1 = -\frac{1}{\pi}\int_{t_j}^{t_{j+1}} \frac{(x_i-\xi(t))\eta'(t) - (y_i-\eta(t))\xi'(t)}{(x_i-\xi(t))^2 + (y_i-\eta(t))^2}\,dt, \tag{2.21}$$

because $\underset{\sim}{x}_i = (x_i, y_i)$ and $\underset{\sim}{n} = (\eta'(t), -\xi'(t))$. Making the change of variable

$$\gamma = (y_i-\eta(t))/(x_i-\xi(t)), \tag{2.22}$$

where

$$d\gamma = dt\left[\frac{\xi'(t)(y_i-\eta(t)) - \eta'(t)(x_i-\xi(t))}{(x_i-\xi(t))^2}\right], \tag{2.23}$$

(2.21) becomes

$$I_1 = \frac{1}{\pi}\int_{t_j}^{t_{j+1}} \frac{1}{1+\gamma^2}\, d\gamma \tag{2.24}$$

$$= \begin{cases} \frac{1}{\pi}\left[\arctan\left(\frac{y_i - Y_{j+1}}{x_i - X_{j+1}}\right) - \arctan\left(\frac{y_i - Y_j}{x_i - X_j}\right)\right] & i \neq j, \\ 0 & i = j, \end{cases} \tag{2.25}$$

where (X_j, Y_j) is the coordinate of the jth grid-point. Note that

$$(X_{N+1}, Y_{N+1}) = (X_1, Y_1). \tag{2.26}$$

The non-singular component of (2.19) may be integrated by Simpson's three point rule, with Bessel functions being evaluated by use of polynomial approximations in Abramowitz and Stegun (1972) modified to eliminate the singular terms.

Turning now to the general component of B, use of (2.18) gives

$$[B]_{ij} = \int_{\Delta\ell_j} [\frac{1}{\pi}\ln(r') - M(k,r')]dy' \qquad i=1,\ldots,N;\ j=1,\ldots,p. \tag{2.27}$$

The non-singular part of (2.27) may be integrated using Simpson's rule, as for the coefficients of A, but the singular component requires different treatment, using complex variables. Thus, from Hwang and Tuck (1970),

$$I_2 = \frac{1}{\pi}\int_{\Delta\ell_j} \ln(r')dy' = Re\{\frac{1}{\pi}\int_{z_1}^{z_2} \ln z dz e^{-i\alpha}\} \tag{2.28}$$

where

$$e^{-i\alpha} = [(X_{j+1} - X_j) - i(Y_{j+1} - Y_j)]/\Delta\ell_j \tag{2.29}$$

$$z_1 = (X_j - x_i) + i(Y_j - y_i) \tag{2.30}$$

and

$$z_2 = (X_{j+1} - x_i) + i(Y_{j+1} - y_i) \quad . \tag{2.31}$$

Simplifying (2.28) gives

$$I_2 = \frac{1}{\pi} Re\{e^{-i\alpha}[z_2(\ln z_2 - 1) - z_1(\ln z_1 - 1)\} \quad . \tag{2.32}$$

Having now formulated the method of solution we see that storage space is a significant problem. This is due to our having to invert two complex matrices, one a small $p \times p$ matrix the other a large $N \times N$ matrix, which exhibit no properties, such as symmetry or bandedness, allowing simple inversion. To partially solve this handicap only cavities symmetric about the x-axis were examined, so that the number of segments in which ϕ_I is explicitly evaluated is halved. This imposition of symmetry does however give rise to more complicated matrix coefficients, as two terms, with sign exchanges, different radii, etc., are now required for each coefficient.

2.4 Off-Boundary Potential

Equation (2.17) evaluates ϕ_I on Γ_I but it may also be of interest to be able to calculate ϕ_I at some arbitrary point of $\{R_I - \Gamma_I\}$. It will be recalled that (2.4) is designed for just such a purpose and so we may discretize this equation in the same manner as (2.5) to give the matrix equation

$$\Xi = \frac{1}{2}(\bar{A}\Psi_1 - \bar{B}B_p^{-1}(\Psi_{1p} - e)), \tag{2.33}$$

where Ξ is the vector of the interior ϕ values at n selected points and the barred matrices have coefficients which contain

integrals of regular, rather than C.P.V., interpretation. So, once the potential on Γ_I is known, the potential at any point in R_I may be found by simple matrix multiplications.

CHAPTER 3

TWO-DIMENSIONAL RESONATORS WITH SMALL OPENINGS

This chapter develops a theory for the acoustic response of a two-dimensional nearly-closed cavity to an excitation through a small opening, using the method of matched asymptotic expansions. The Helmholtz mode of vibration will be examined in some detail and the numerical model outlined in Chapter 2 will be employed to test the usefulness of the theory.

Much of the material in this chapter has appeared in Bigg and Tuck (1982).

3.1 Introduction

A general class of small-opening problems will first be studied. For these, the complete response curve of the cavity will be computed, as a theory is obtained which is asymptotically valid for small opening size, compared to both wavelength and cavity size, but which does not yet assume that the wavelength is far in excess of the dimensions of the cavity. This theory is therefore, in principle, capable of predicting all resonances in the response, namely the Helmholtz mode and all of the peaks corresponding to natural frequencies of the fully-closed cavity.

The results depend on two length parameters s and b, the former associated with the geometry of the opening, and the latter with the geometry of the cavity. The opening parameter s is independent of frequency and was introduced in its present form

by Tuck (1975), although Rayleigh (1870) had used a related quantity. In this chapter the use of s will be extended to cavities in which the interior and exterior walls, in the neighbourhood of the opening, are non-planar; specifically, to allow the opening to be at the apex of a wedge-like region of general angle. Computation of s is relatively straightforward, and examples are given for various opening geometries.

On the other hand, for general cavities, the computation of the cavity shape parameter b, which is dependent on frequency, is not at all straightforward. However, exact results for b are obtainable for circular-sector cavities and are used to compute the response of this particular type of cavity as a function of frequency. These computations are compared to those obtained by direct numerical solution of the problem, using the theory of Chapter 2.

Restricting our attention to the Helmholtz mode, it is found not to be necessary to know the cavity parameter b at all frequencies, but only its zero-frequency limit. The problem of determining this limit can be reduced to that of solving a Poisson equation in the closed cavity; a much simpler computational problem. The resulting value of the natural logarithm of b is related to a parameter M introduced by Miles and Lee (1975), and further examples of its computation are presented.

Once b is known for a cavity, the response of the cavity to excitation at frequencies in the neighbourhood of the Helmholtz mode can be computed to a consistent order of approximation. This response will be discussed for several types of cavity and the

important features of Helmholtz resonance noted.

3.2 Flow Through Small Openings

The matching procedures discussed in Tuck (1975) will be adapted to the present problem. The general scheme of the process is as follows:

The flow in the vicinity of the opening is discussed, using the assumption that ks is small, in terms of an incompressible motion. Then the disturbance in the exterior region, far from the cavity aperture, is considered and the small r expansion of this field is matched with the exterior far field of the opening flow. The appearance of the orifice to the observer far into the cavity is then examined, and the small r expansion of this motion is matched with the far field interior expansion of the flow in the aperture.

The opening geometry which may be considered by our theory is quite general, as sketched in Figure 3.1. This opening is a transition between an asymptotically converging wedge of angle θ_- on the left, and a corresponding diverging wedge of angle θ_+ on the right. The length scale of the aperture is some measure of its linear size, and the requirement of smallness of the opening is that s be small compared to all other significant length scales, notably the wavelength $2\pi/k$ and the linear size of the cavity. Although s could be taken initially as any typical length dimension of the aperture, such as the minimum width w, we will determine a special measure s, that uniquely characterizes this opening geometry, as seen in its own far field.

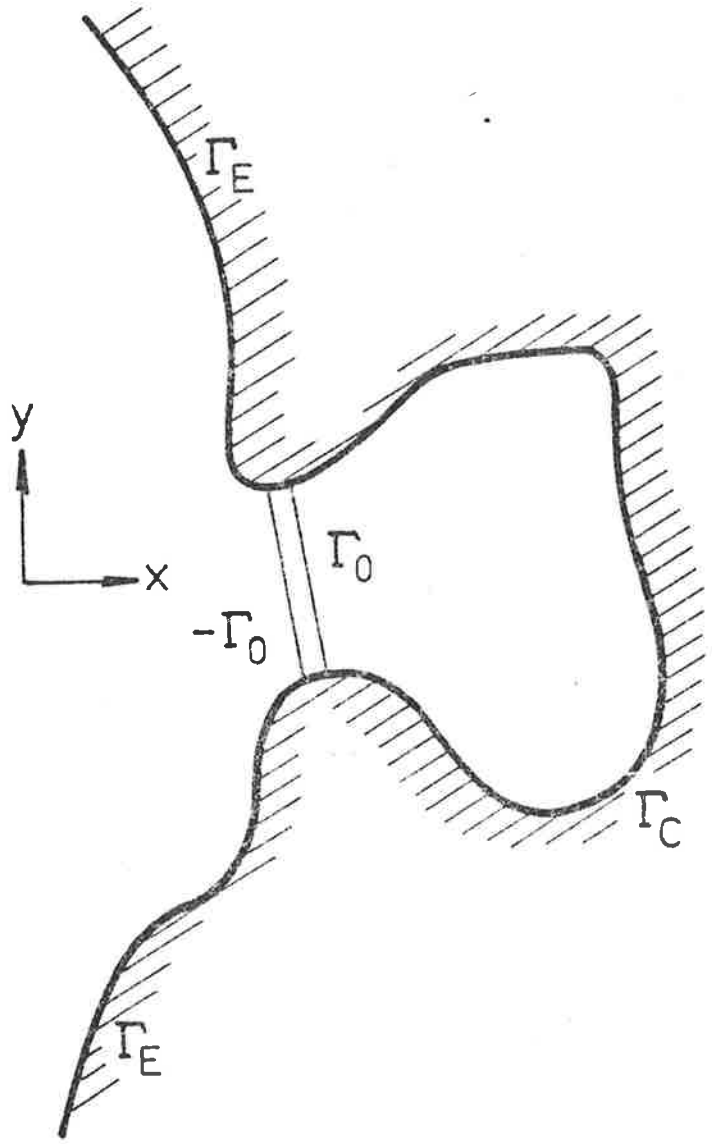

Figure 3.1: Sketch of boundary geometry.

Since ks is small the flow in the opening is approximately incompressible, and thus we have to solve Laplace's equation for a flow through the opening. The behaviour at infinity is that corresponding to a source-sink pair. Without loss of generality, we may normalize the net flux through the opening, seeking, therefore, a scaled potential $\bar{\phi}$ satisfying, as $r \to \infty$,

$$\bar{\phi} \to \pm \ln(r)/\theta_{\pm} + C_{\pm}, \quad x \gtrless 0. \tag{3.1}$$

The constants $C_{\pm}$ do not necessarily take the same value, and the effective size s is defined in terms of the change in value between C_- and C_+, that is, (3.1) is written as

$$\bar{\phi} \mp \ln(r/s)/\theta_{\pm} \to 0 \quad \text{as} \quad x \to \pm\infty . \tag{3.2}$$

So, for any appropriate opening geometry, $\nabla^2\bar{\phi} = 0$ must be solved, subject to $\partial\bar{\phi}/\partial n = 0$ on the aperture boundaries and (3.2) at infinity. In the process of solving the problem, s will be determined uniquely. Examples of the calculation of s are given in Tuck (1975) and Appendix IB, which includes discussion of other approaches to this problem, but it can be usefully stated here that s varies only slightly for fixed aperture width and is $O(w)$ in magnitude.

The opening potential $\bar{\phi}$ is now used in the full acoustic problem. In the exterior region there is an incident wave field $\phi_\infty(x,y)$ which, in the absence of the aperture, takes the value $\phi_\infty(0,0)$ at the cavity entrance.

In the limit as $ks \to 0$, the disturbance due to the cavity vanishes and $\phi \to \phi_\infty$. The residual effect of the cavity, as seen

by an exterior observer, must be that of an acoustic source. That is, if m is the apparent strength of that source, we set in $x < 0$, $r \gg s$,

$$\phi = \phi_\infty - \frac{1}{4} i m H_0^{(1)}(kr), \tag{3.3}$$

and seek m by matching with the flow in the cavity, via the opening region. Note that m is the flux of the source through an arbitrary *complete sphere* about the origin, while the actual flux in $x < 0$ is $\theta_- m/4\pi$, as the outflow is restricted by the exterior wedge-like boundary.

In order to perform the matching of the exterior and opening solutions, let $kr \to 0$ in (3.3), to obtain

$$\phi = \phi_\infty(0,0) - \frac{1}{4} i m [1 + \frac{2i}{\pi} \ln(\frac{1}{2}\bar{\gamma} kr)] + O(mk^2 r^2 \ln(kr)), \tag{3.4}$$

where $\ln\bar{\gamma} = 0.577...$ is Euler's constant. The expression (3.4) must match with a boundary condition, as $x/s \to -\infty$, for a through-opening flow, and for that purpose (3.4) can be rewritten as

$$\phi \to \phi^0 + \frac{m}{2\pi} \ln\left(\frac{r}{s}\right) \quad \text{as } x/s \to -\infty, \tag{3.5}$$

where the constant ϕ^0 is given by

$$\phi^0 = 1 - \frac{1}{4} i m + \frac{m}{2\pi} \ln\left(\frac{1}{2}\bar{\gamma} ks\right), \tag{3.6}$$

$\phi_\infty(0,0)$ being normalized to unity. Therefore, using (3.2), the solution for the incompressible flow through the opening is

$$\phi(x,y) = \phi^0 - \frac{\theta_- m}{2\pi} \bar{\phi}(x,y), \tag{3.7}$$

$\bar{\phi}$ being the canonical potential defined above.

Having solved for this opening flow, we may now proceed all the way into the cavity, by letting $x/s \to \infty$, that is, again using (3.2),

$$\phi \to \phi^0 - \frac{\theta_- m}{2\pi\theta_+} \ln\left(\frac{r}{s}\right) \quad \text{as} \quad \frac{x}{s} \to +\infty \ . \tag{3.8}$$

To complete the solution, we now match with an interior solution by observing that, if the opening size s is small compared to a typical dimension β of the cavity, the opening will appear to the cavity as a sink of strength $\theta_- m/\theta_+$; that is, (3.8) will provide a singularity condition as $r/\beta \to 0$. The potential in the cavity can therefore be written as

$$\phi = \frac{-\theta_- m}{\theta_+} \phi_c(x,y) \ , \tag{3.9}$$

where ϕ_c satisfies (1.2), and (1.3) on the limiting (closed as $s \to 0$) boundary of the cavity, except that ϕ_c behaves like a source of *unit* strength at the point on that boundary corresponding to the vanishing opening. That is, as $r \to 0$ we require

$$\phi_c \to \frac{1}{2\pi} \ln r + \varepsilon \ . \tag{3.10}$$

The constant ε is uniquely determined by these conditions and we define a parameter b by choosing ε to satisfy

$$\varepsilon = \lim_{r \to 0}[\phi_c - \frac{1}{2\pi} \ln r] = \frac{\theta_+}{2\pi k^2 A} - \frac{1}{2\pi} \ln b, \tag{3.11}$$

where A is the area of the cavity. The parameter b measures the size of the cavity as seen in the neighbourhood of its opening; it has the dimensions of a length, and may be expected to be comparable in value to the linear dimensions of the cavity,

that is, $b = O(A^{1/2}) = O(\beta)$. For the rest of this section it will be assumed that ϕ_c, and hence b, can be determined for any given cavity.

To conclude our solution, consider the cavity potential as $r \to 0$, namely,

$$\phi \to \frac{-\theta_- m}{2\pi\theta_+}\left[\ln\left(\frac{r}{b}\right) + \frac{\theta_+}{k^2 A}\right] , \tag{3.12}$$

which matches with (3.8), the far field opening potential, if

$$\phi^0 + \frac{\theta_- m}{2\pi\theta_+}\ln s = \frac{\theta_- m}{2\pi\theta_+}\ln b - \frac{\theta_- m}{2\pi k^2 A} . \tag{3.13}$$

Upon use of (3.6) the required formula for the source strength m is obtained, namely,

$$2\pi m^{-1} = \frac{-\theta_-}{k^2 A} - \ln\left(\frac{1}{2}\gamma k s\right) + \frac{\theta_-}{\theta_+}\ln\left(\frac{b}{s}\right) + \frac{\pi i}{2} . \tag{3.14}$$

The small gap resonator theory is now complete. In summary, the exterior potential is given by (3.3), the opening potential by (3.7), the interior potential by (3.9) and the apparent source strength m by (3.14). As constituents of these equations we need the canonical potentials $\bar{\phi}$ in the opening and ϕ_c in the cavity. Associated with $\bar{\phi}$ is a single effective size parameter s, with dimensions typical of the opening. Associated with ϕ_c is a single parameter b, with dimensions typical of the cavity. Since $\bar{\phi}$ satisfies Laplace's equation, s is frequency-*independent* but, as ϕ_c satisfies Helmholtz's equation, b will be frequency-*dependent*. It is also as a result of the governing equations for $\bar{\phi}$ and ϕ_c that $\bar{\phi}$, and hence s, is easier to compute than ϕ_c. This fact has a significant bearing on the development of further

theory.

It is worth reiterating at this point that the only approximation made thus far is that the effective size s of the orifice is small compared to all other length scales. It has not yet been assumed that the cavity size β is small compared to the wavelength. Consequently, the error in expressions like (3.14) is at most a factor of order $1 + O(ks, s/\beta)$.

3.3 Large Circular-sector Cavities

Determining the canonical potential $\phi_c(x,y)$, which satisfies (1.2), (1.3) and (3.10), is a difficult problem and exact analytic solutions are few. One case in which a solution may be found is that for a cavity consisting of a sector of a circle, with the opening at the apex. That is, if (r,θ) are polar coordinates centred at the location of the aperture, the boundary consists of a circular arc $r=a$ and radial lines $\theta = \pm\frac{1}{2}\theta_+$, the cavity having area $A = \frac{1}{2}\theta_+ a^2$. In particular, if $\theta_+ = \pi$ the cavity is semi-circular, with the opening at the centre of the diameter.

It is easily shown that all the necessary conditions on ϕ_c are satisfied if

$$\phi_c = \frac{1}{4}\left(Y_0(kr) - \frac{Y_1(ka)}{J_1(ka)} J_0(kr)\right), \tag{3.15}$$

and the parameter b is given by

$$\ln\left(\tfrac{1}{2}\bar{\gamma}kb\right) = \frac{2}{k^2a^2} + \frac{\pi}{2}\frac{Y_1(ka)}{J_1(ka)}, \tag{3.16}$$

this being seen from the small argument expansions of the Bessel functions in Abramowitz and Stegun (1972). The source strength m can now be evaluated using (3.14). Assuming $\theta_- = \pi$, that is,

that the outer wall is planar, the potential on the cavity wall $r=a$ is

$$\phi = \frac{-m}{2ka\theta_+ J_1(ka)}$$

$$= \frac{-2}{\pi ka}[Y_1(ka) + J_1(ka)\{\frac{i\theta_+}{\pi} - \frac{2}{\pi}(1 + \frac{\theta_+}{\pi})\ln(\tfrac{1}{2}\bar{\gamma}ks)\}]^{-1}. \qquad (3.17)$$

An illustrative plot of $|\phi|$ against ka is given in Figure 3.2, for the case of a semi-circular cavity with $s/a = 0.05$.

Peaks in the response curve occur whenever the quantity in the square brackets of (3.17) is small. Since ks is small, that is $-\ln(\frac{1}{2}\bar{\gamma}ks)$ is large, this quantity is usually dominated by its second term, and hence peaks occur when $J_1(ka) \simeq 0$. This merely says that when the opening is small, the cavity behaves almost as if it were closed, as the condition $J_1(ka) = 0$ precisely determines those natural eigenmodes of the closed cavity without θ-dependence. This cavity can also support modes with θ-dependence, but these possess a node at $r=0$ and hence are not excited through a vanishingly small opening there.

However, the term in the square brackets of (3.17) can also become small when ka is small, as the leading term $Y_1(ka)$ then becomes large and may cancel the second term. This occurs during the Helmholtz mode of resonance, the first and highest peak in Figure 3.2. This mode will be discussed in detail in the following section, where a theory applicable to more general cavities is to be presented. For the present, the expansion of the "exact" cavity potential ϕ_c for $ka \to 0$ will be noted, namely

$$\phi_c = \frac{1}{\pi k^2 a^2} + \frac{1}{2\pi}[\ln(\frac{r}{a}) - \frac{1}{2}\frac{r^2}{a^2} + \frac{3}{4}]$$

$$- \frac{k^2a^2}{8\pi}[\frac{r^2}{a^2}\ln(\frac{r}{a}) - \frac{1}{4}\frac{r^2}{a^2} - \frac{1}{8}] + \mathcal{O}(k^4a^4), \qquad (3.18)$$

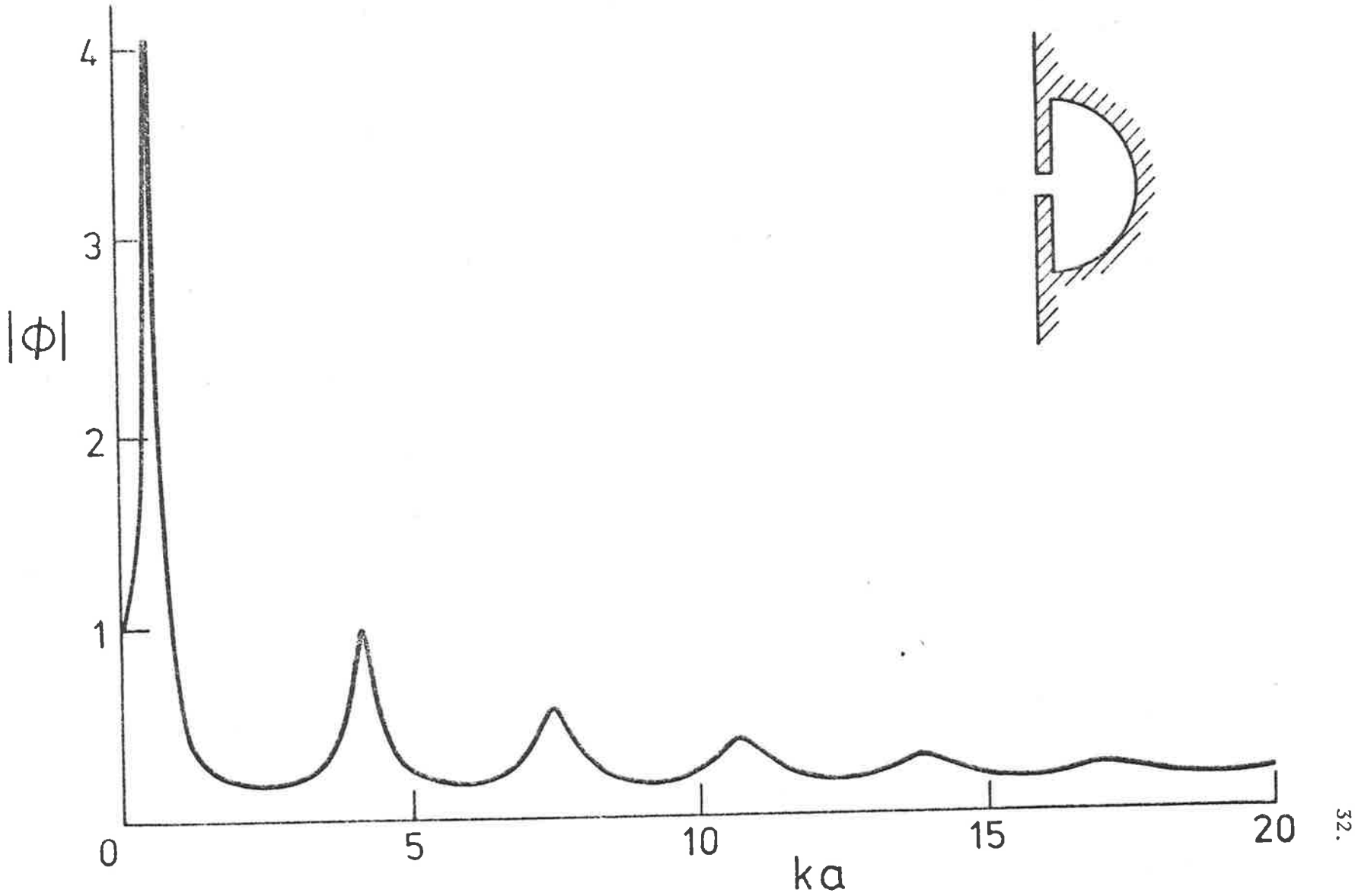

Figure 3.2: Response of semi-circular cavity of radius a and opening of effective size s=0.05a, computed by asymptotic theory for small s/a and evaluated on the curved boundary.

which implies, from (3.10) and (3.11), that

$$b/a = e^{-\frac{3}{4}} + O(k^2a^2). \tag{3.19}$$

The corresponding formula for the source strength m follows directly from (3.14), and the small-ka expansion of the response on the cavity wall $r=a$ can then be written

$$\phi = \frac{1 + \frac{1}{8}k^2a^2 + O(k^4a^4)}{1 - 2k^2A[\frac{-1}{2\pi}\ln(\frac{1}{2}\gamma ks) + \frac{1}{2\theta_+}\ln(\frac{a}{s}) - \frac{3}{8\theta_+} + \frac{i}{4}] + O(k^4a^4)}. \tag{3.20}$$

Equation (3.20) may also be obtained by a careful direct small-ka expansion of (3.17). In performing this expansion the quantity $-\ln(\frac{1}{2}\gamma ks)$ must be assumed to be a very large quantity, indeed at least as large as $(ka)^{-2}$. This is necessary if we are to be able to discuss the Helmholtz resonance mode, in which substantial cancellation must occur between the leading order terms in the denominator of (3.20). The advantage of the particular form adopted for (3.20) (as the ratio between two separate expansions with respect to ka), is that the error terms quoted as $O(k^4a^4)$ for both numerator and denominator are errors resulting *only* from expansions of ϕ_c, and are completely independent of the opening parameter s.

The accuracy of (3.17) may be checked by comparison with computations made for a semi-circular cavity, using the numerical method of chapter 2. For that purpose, the cavity wall was divided into a maximum of 80 segments. That is, at most 30 segments were needed in each half of the symmetric cavity boundary Γ_c, and 10 on each half of the artificial boundary Γ_0 across the opening. About 3-figure accuracy was always achievable, even close to the

resonance peaks, with this discretization, since ϕ varies only slowly around the boundary, except at the junction between Γ_c and Γ_0. Segment distribution was generally uniform, but with a certain amount of accumulation near that junction. As found by Lee (1969), the number of segments across the opening had little effect on the computations.

The numerical results for $s/a < 0.02$ are in agreement to 2 or 3 significant figures with the asymptotic results from (3.17), for all treated k. Even for considerably larger s the approximation of the Helmholtz and radially symmetric natural modes by (3.17) is very good. However, as the cavity mouth increases in width, the θ-dependent modes, mentioned above, begin to appear. In Figure 3.3 the velocity potential at $(a,0)$ is shown for $s/a = 0.05$, to illustrate this phenomenon. The two plots are in excellent agreement everywhere, except in the vicinity of $ka \simeq 3.05$. The sharp spike in the numerical results near this point is the resonance of a θ-dependent mode with two nodal lines $\theta = \pm\pi/4$, intersecting at right angles at $r=0$.

Having confirmed the good agreement of (3.17) with an independent numerical solution to the problem, we now consider the effect of the opening size s on the response curves. In Figure 3.4 the first two resonance peaks for a semi-circle are shown, computed from (3.17), for several s values. As expected from this equation and (3.20), a reduction in the size s of the opening shifts the Helmholtz mode peak to a smaller wavenumber k, and increases the peak amplitude dramatically. It is also to be noted that, as s is reduced, the position of the first natural eigenmode frequency also changes, its bandwidth decreases and its maximum amplitude increases.

Figure 3.3: Comparison of numerical and asymptotic results for semi-circular cavity at s/a = 0.05.

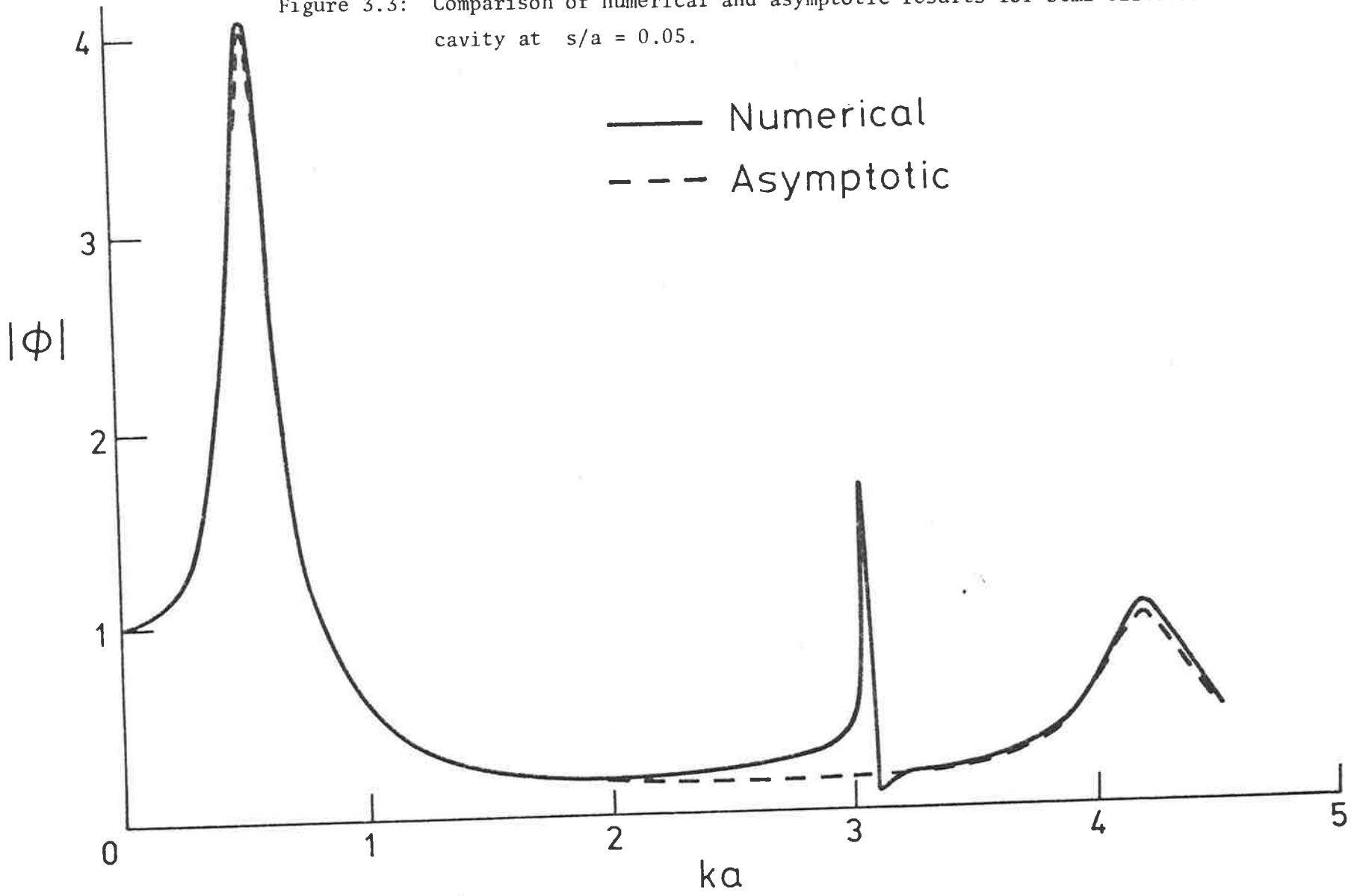

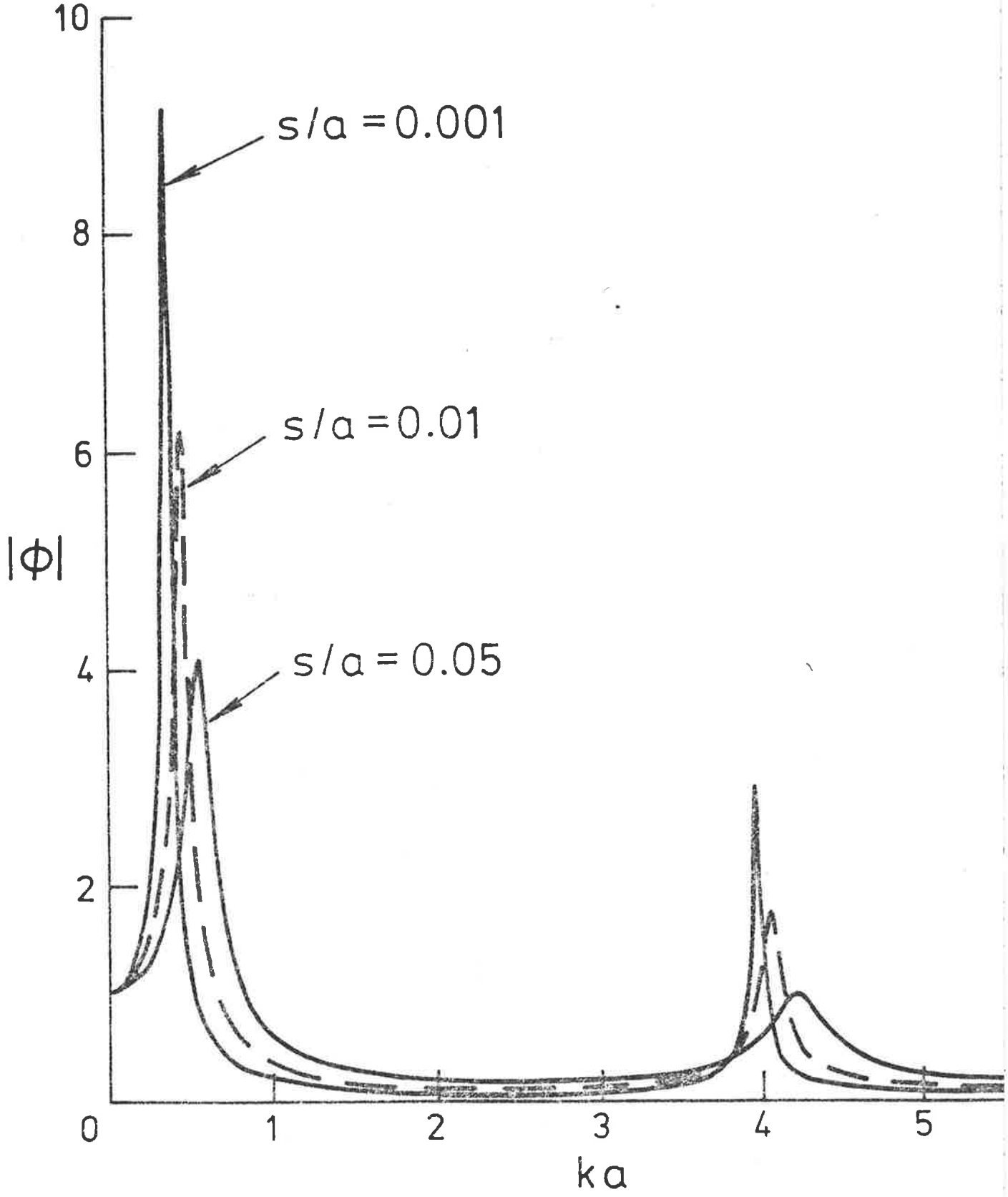

Figure 3.4: Variation in response of semi-circular cavity with opening size s.

Figure 3.5: Response of 90° circular sector cavity, cf. curve in Figure 3.4 for s/a = .001.

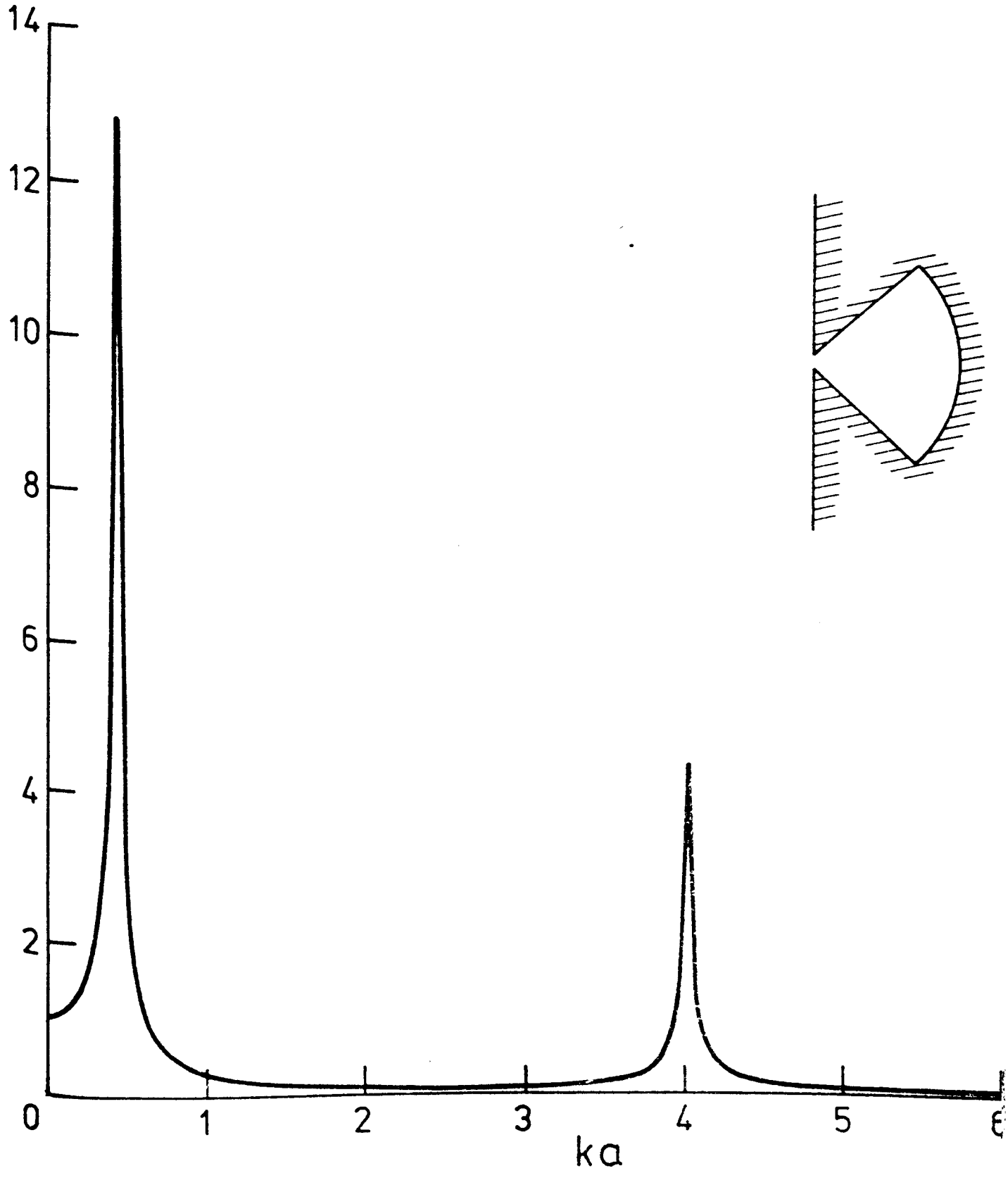

The quantitative nature of these changes, however, differs from the alterations to the Helmholtz peak. While the Helmholtz mode exhibits the "harbour paradox" of Miles and Munk (1961), namely, that narrowing the aperture increases $k_H A_H^2/Q_H$, where A_H is the peak value of the Helmholtz resonance and Q_H is the ratio of the Helmholtz frequency to the half-power bandwidth of the resonance curve, the natural modes do not. In fact, as shown by Garrett (1970) and Miles (1971), the quantity $k_n A_n^2/Q_n$ is invariant for the natural modes, $n \geq 1$.

The effect of the variation of the interior cavity angle θ_+ is also of interest. This is depicted in Figure 3.5 for $\theta_+ = 90^\circ$. As θ_+ is decreased, the magnitude of the response increases. This indicates that the energy entering the cavity is not decreasing as quickly as the cavity area, which is consistent with the expression for m given in (3.14). Figure 3.5 also shows the position of the resonance altering slightly, as is consistent with (3.17).

3.4 The Helmholtz Mode

Although the determination of the cavity potential ϕ_c is formidable in general, in discussing the Helmholtz mode only the small-ka expansion of ϕ_c is of interest, as typified by (3.18) for the circular-sector cavity. Using (3.18) as a guide, consider a power series in $k^2\beta^2$ of the form

$$\phi_c = \phi_0 + \phi_1 + \phi_2 + \ldots \tag{3.21}$$

where $\phi_0 = O(k^{-2}\beta^{-2})$, $\phi_1 = O(1)$, $\phi_2 = O(k^2\beta^2)$ and so on. The leading term ϕ_0 is expected to be constant throughout the cavity, both by analogy with (3.18) and by physical arguments, since this

corresponds to uniform compression over the whole cavity, the only possible form of motion in the low frequency limit $k \to 0$.

If the series (3.21) is substituted into the Helmholtz equation (1.2), there results a sequence of Poisson equations for $\phi_1, \phi_2, \ldots$, that is

$$\nabla^2\phi_1 = -k^2\phi_0 \ , \tag{3.22}$$

$$\nabla^2\phi_2 = -k^2\phi_1 \ , \tag{3.23}$$

and so on. Similarly, the wall boundary condition (1.3) implies that

$$0 = \frac{\partial\phi_1}{\partial n} = \frac{\partial\phi_2}{\partial n} = \ldots \qquad \text{on} \quad \Gamma_c \ . \tag{3.24}$$

An important set of integral relations follow if we integrate both sides of (3.22) and (3.23) over the cavity, R_I, with boundary Γ_I. Thus, from (3.22),

$$\iint_{R_I} \nabla^2\phi_1 dxdy = \oint_{\Gamma_I} \frac{\partial\phi_1}{\partial n} d\ell = -k^2\phi_0 A \tag{3.25}$$

is the net flux of ϕ_1 produced by the constant forcing term on the right. However, as $\partial\phi_1/\partial n = 0$ on the cavity wall Γ_c, the only contribution to the line integral in (3.25) comes from the flow through the aperture Γ_0, which has shrunk to a point. The opening is represented now by a source of unit apparent strength in a sector of angle θ_+, which therefore produces a net, outgoing, flux of $-\theta_+/2\pi$. That is,

$$k^2\phi_0 A = \frac{\theta_+}{2\pi} \tag{3.26}$$

or, isolating the leading term of (3.21),

$$\phi_0 = \frac{\theta_+}{2\pi k^2 A} \quad . \tag{3.27}$$

Since the term ϕ_1 in (3.21) already accounts for the unit-source character of ϕ_c, further terms $\phi_2, \phi_3, \ldots$ in the series do not produce any net flux through the opening. Hence, for example,

$$\iint_{R_I} \nabla^2 \phi_2 dxdy = \oint_{\Gamma_I} \frac{\partial \phi_2}{\partial n} d\ell = -k^2 \iint_{R_I} \phi_1 dxdy = 0. \tag{3.28}$$

The resulting integral condition,

$$\iint_{R_I} \phi_1 dxdy = 0 \ , \tag{3.29}$$

is a normalization for the potential ϕ_1 that ultimately determines the zero frequency limit b_0 of the cavity parameter. In the next section solutions to (3.22) are presented, but if we assume for now that $b = O(\beta)$ is a known quantity to leading order, with relative error $O(k^2\beta^2)$, we can give expressions for ϕ in the cavity and aperture.

The potential in the cavity interior is, from (3.9),

$$\phi = -\frac{\theta_- m}{\theta_+}\left[\frac{\theta_+}{2\pi k^2 A} + \phi_1 + O(k^2\beta^2)\right] \tag{3.30}$$

where m is given by (3.14). In the neighbourhood of the opening, where (3.30) is singular, we use (3.7) to give us the aperture potential

$$\phi = 1 - m\left(\frac{i}{4} - \frac{1}{2\pi}\ln\left(\frac{1}{2}\bar{\gamma}ks\right) + \frac{\theta_-}{2\pi}\bar{\phi}(x,y)\right) \ . \tag{3.31}$$

Both equation (3.30) and (3.31) predict only second order spatial effects on the response. However the constant terms in these equations are not equal and using the expression for m (3.14),

replacing b by its zero frequency limit b_0, it may be shown that

$$\frac{\phi_{\text{opening}}}{\phi_{\text{cavity}}} = 1 - \frac{k^2 A}{\theta_+}\ln\left(\frac{b_0}{s}\right) + O(k^2\beta^2) \quad . \tag{3.32}$$

This ratio is significantly less than unity, since $-\ln(b/s)$ is large, so the potential in the aperture is less than that in the cavity.

The order of the error in these results is of interest as the Helmholtz mode is of practical importance. Such a resonance corresponds to large magnitudes for k^2A/m in (3.14). Since the imaginary part of this quantity is small and provides damping, such a resonance will occur for wavenumbers k close to the value at which the real part of the quantity will vanish, that is, where

$$k^2 A = \left(-\frac{1}{\theta_-}\ln\left(\frac{1}{2}\gamma ks\right) + \frac{1}{\theta_+}\ln\left(\frac{b_0}{s}\right)\right)^{-1} . \tag{3.33}$$

Although (3.33) is a transcendental equation for the resonant wavenumber k, it is clear that the order of magnitude of this k is given by

$$k\beta = O\left\{\left(\ln\left(\frac{b_0}{s}\right)\right)^{-1/2}\right\} . \tag{3.34}$$

Hence, in this range of wavenumbers, the error in the present results is a factor of the order of $1 + O\left\{\left(\ln\left(\frac{b_0}{s}\right)\right)^{-2}\right\}$.

An approach giving results similar to this theory is that of Miles and Lee (1975). Using variational methods, they define a parameter M, found from solution of a Poisson equation, which incorporates the parameters s and b_0. In fact, it appears that

$$M = \frac{1}{\pi}\ln\left(\frac{b_0}{s}\right) . \tag{3.35}$$

Thus, both the cavity and aperture geometry are involved in the specification of the parameter M. Miles and Lee have some difficulty in defining and computing M, in the general case, and construct a lower bound which seems to approximate their parameter adequately. The treatment we have discussed in the preceding sections, however, differentiates between the opening and cavity geometry, and thus indicates separately the relative importance of these quantities in the final solution.

3.5 Determination of the Second Order Potential

The second order potential in the cavity may be found by solving the Poisson equation, from (3.22) and (3.27),

$$\nabla^2\phi_1 = -\frac{\theta_+}{2\pi A}, \tag{3.36}$$

in R_I, subject to (3.24), that is

$$\frac{\partial\phi_1}{\partial n} = 0 \quad \text{on} \quad \Gamma_c \tag{3.37}$$

and, from (3.10) and (3.11),

$$\phi_1 \to \frac{1}{2\pi}\ln\left(\frac{r}{b_0}\right) \quad \text{as} \quad r \to 0, \tag{3.38}$$

where $r=0$ defines the vanishingly small opening on the wall of the cavity. The system of equations (3.36) - (3.38) possesses a solution for any value of the constant b_0, but the value of b_0 is rendered unique by the normalization condition (3.29).

Solving this system is still a non-trivial task but separation of variables, conformal mapping techniques and inverse methods enable a number of cavity geometries to be studied, examples of

which we consider below. However, there is a symmetry property which enables more cavity geometries to be treated, especially if the aperture is in a plane wall. These symmetry considerations apply to the parameter b_0. Suppose the cavity R_I under consideration possesses symmetry about the x-axis, with the opening, whose geometry is immaterial for the computation of ϕ_1 and b_0, located at the origin. If we now place a rigid wall along this x-axis, and consider only one of the identical chambers $R_I^{\pm}$ created by this action, this half-chamber has the same shape parameter b_0 as the original full cavity. This is because:

(i) The ratio θ_+/A in (3.36) is unchanged, the new opening lying in the corner of angle $\pi/2$,

(ii) the potential ϕ_1 for R_I will satisfy all required conditions for R_I^+, and

(iii) the normalization integral (3.29) over R_I^+ is just half that over R_I, and therefore also vanishes.

Now suppose that we create a third cavity R_I^*, whose axis of symmetry is the y-axis, by reflecting R_I^+ with respect to that axis. Now, by the same arguments, R_I^* has the same value of b_0 as does R_I^+, and therefore the same value of b_0 as does the original cavity R_I. Figure 4.4 illustrates this property in action for three-dimensional cavities; see also Bigg (1982a).

The first, and simplest, cavity to be considered is the circular-sector cavity of radius a, already discussed in §3.3. It can be quickly seen that an appropriate solution of the Poisson system (3.36)-(3.38) is

$$\phi_1 = \frac{1}{2\pi}\ln\left(\frac{r}{b_0}\right) - \frac{r^2}{4\pi a^2}\,, \qquad (3.39)$$

and if the integral in (3.29) is evaluated, as in Appendix IC, it is found that

$$b_0 = ae^{-\frac{3}{4}} \quad , \tag{3.40}$$

as in (3.19). The expression (3.39) also agrees with the $O(1)$ term in the expansion (3.18) of ϕ_c in powers of ka.

If the cavity wall is the *complete* circle $r = 2a \cos\theta$, then $\theta_+ = \pi$ and a solution to (3.36)-(3.38) can be derived as for the circular-sector cavity to give

$$\phi_1 = \frac{1}{2\pi}\ln\left(\frac{r}{b_0}\right) - \frac{r^2 - 2ar\cos\theta}{8\pi a^2} \quad , \tag{3.41}$$

which satisfies (3.29) if, from Appendix IC,

$$b_0 = ae^{\frac{1}{8}} \quad . \tag{3.42}$$

This circular cavity can be used to illustrate dependence of the response on position in the cavity. Figure 3.6 shows $|\phi|$ at $s/a = 0.05$, computed from (3.31), using (3.41) to give ϕ_1, for two positions within the cavity. The graph shows the, essentially, spatially invariant nature of the response for non-resonant exciting frequencies, but also the significant variation in the magnitude, if not the frequency, of the Helmholtz peak. The response in the aperture is shown on this figure as well, using (3.31) with $\bar{\phi}$ taken to be zero, indicating, as predicted by (3.32), a significantly reduced response at all frequencies. The uniform response within the cavity is to be expected, due to the physical nature of the Helmholtz resonance being a uniform compression of the fluid within the resonator. Some second order variation, evident close to the resonant frequency in the response curves, is due to the geometry

Figure 3.6: Helmholtz response of a complete circular cavity of radius a at s/a = 0.05, for various positions within the cavity.

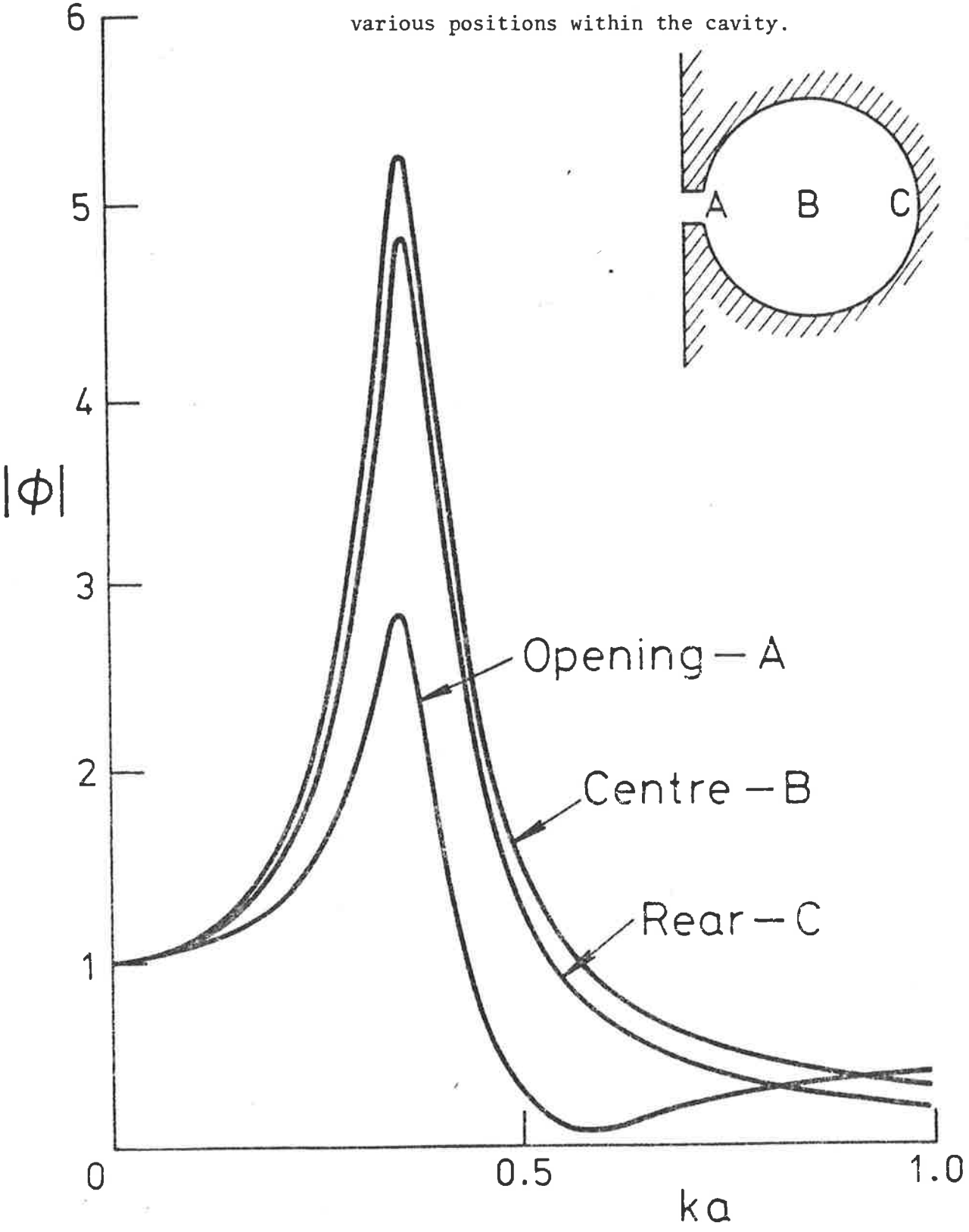

of the cavity, but does not conceal this basic uniformity.

A rectangular cavity of length L and breadth 2h, the opening being located at the centre (x,y) = (0,0) of one of the sides of breadth 2h, may also be examined. An appropriate solution to the problem can be constructed in the form

$$\phi_1 = \frac{1}{2\pi}\ln\left[\sinh^2\left(\frac{\pi x}{2h}\right)+\sin^2\left(\frac{\pi y}{2h}\right)\right] - \frac{x^2}{8hL} + \frac{1}{4hL}\sum_{n=0}^{\infty} a_n \cosh\left(\frac{n\pi x}{h}\right)\cos\left(\frac{n\pi y}{h}\right) \qquad (3.43)$$

for suitable real coefficients a_n, n=0,1,2,..., as shown in Appendix IC. The expression (3.43) satisfies (3.38) if

$$\sum_{n=0}^{\infty} a_n = \frac{2Lh}{\pi}\ln\left(\frac{2h}{\pi b_0}\right) . \qquad (3.44)$$

As demonstrated in Appendix IC, the boundary condition on x=L yields formulae for a_n, n=1,2,..., as coefficients in a Fourier-cosine series. The remaining coefficient a_0, and hence b_0, is determined by the normalization integral (3.29) to give

$$a_n = \begin{cases} -\dfrac{2hL}{\pi^2 n}\cdot\dfrac{\tanh\left(\frac{\pi L}{h}\right)}{\sinh\left(\frac{n\pi L}{h}\right)}\cdot\sum_{j=0}^{\infty} T_{jn}\left(\cosh\left(\frac{\pi L}{h}\right)\right)^{-1} & n \geqslant 1 \\ \dfrac{-L^2}{3}+\dfrac{2hL}{\pi}\ln 2 & n = 0, \end{cases} \qquad (3.45)$$

where

$$T_{jn} = \left[1+(-1)^{n+j}\right]\cdot\begin{cases} \dfrac{f_{nj}\,.\,j!}{(n-j)(n-j+2)\ldots(n+j)} & j < n \\ \dfrac{\pi}{2^{j+1}}\binom{j}{\ell} & n \leqslant j,\ j-n=2\ell \\ \dfrac{j!}{(2\ell+1)!!\,(2n+2\ell+1)!!} & n < j,\ j-n=2\ell+1, \end{cases} \qquad (3.46)$$

$$(2n+1)!! = (2n+1)(2n-1)\ldots 3.1 \qquad (3.47)$$

and

$$f_{nj} = \begin{cases} 0 & n-j = 2\ell \\ 1 & n-j = 4\ell+1 \\ -1 & n-j = 4\ell-1 \end{cases} . \qquad (3.48)$$

The final expression for b_0, (3.44), is thus a double sum, which, fortunately, converges rapidly.

These results for the rectangular cavity can be used to illustrate the dependence of the Helmholtz resonator on cavity shape, via the aspect ratio $\delta = 2h/L$, holding the area $A = 2hL$ fixed. Figure 3.7 shows $|\phi_0|$ plotted against $kA^{1/2}$ for various δ, at $s/A^{1/2} = 0.025$. Note that ϕ_1, the spatial variation of the potential has been neglected, as Figure 3.6 showed its second order effect. The most striking feature in Figure 3.7 is the variation, with δ, of both the position and magnitude of the Helmholtz resonance peak. As all the plots are for cavities of the same area, it is clear that the classical view, of resonance characteristics, being independent of the cavity area, as stated by Tuck (1975) in connection with three dimensional cavities, is not tenable. This conclusion also follows for Helmholtz resonance in three dimensional resonators, as will be shown in Chapter 4. However, it should be appreciated that significant alteration to the resonance properties occurs only once the cavity is somewhat elongated - for rectangular resonators which are approximately square, the classical interpretation is a useful one. This fact generalizes to the principle that, for resonators of the same area, which do not possess a dominate axis of distortion, the Helmholtz resonance characteristics are virtually identical.

The symmetry property described at the beginning of this section is useful when studying the response of rectangular cavities

Figure 3.7: Helmholtz response of rectangular cavities of constant area A, at constant opening size $s/A^{1/2} = 0.025$, for various aspect ratios $\delta = 2h/L$.

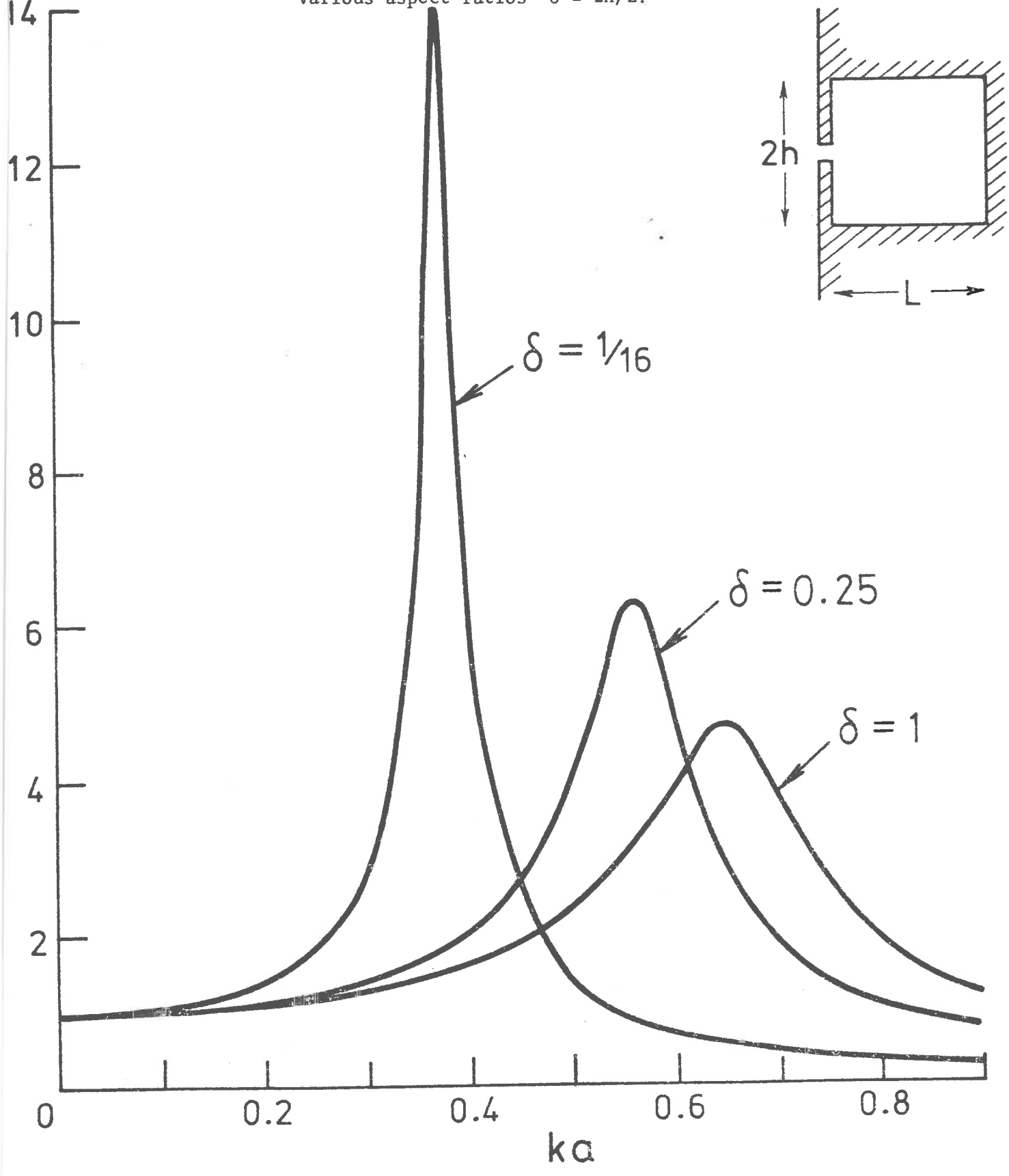

and leads to some interesting consequences. Thus a cavity with aspect-ratio δ has the same response curve, neglecting second order differences, as the resonator with an aspect-ratio of $4/\delta$. Note that this implies that a square, with its opening in the middle of a side, has the same response characteristics as a rectangle of aspect ratio $\delta=4$, with its opening in the middle of the long side.

To end this section a discussion of inverse methods is presented. To demonstrate how these work, a particular class of problems will be examined.

Consider the generalization of equation (3.41)

$$\phi_1 = \frac{1}{2\pi}\ln(\frac{r}{b_0}) - \frac{r^2}{8A} + \Phi \ , \tag{3.49}$$

where Φ is any solution of Laplace's equation vanishing at $r=0$. For a given Φ, we can construct inverse solutions of our problem, satisfying (3.36)-(3.38) and (3.29), the cavity's boundary curve $r = r(\theta)$ being determined by solving the ordinary differential equation

$$\frac{dr}{d\theta} = \frac{r^2\phi_{1r}(r,\theta)}{\phi_{1\theta}(r,\theta)} \ , \tag{3.50}$$

which follows from (3.37). For example, if

$$\Phi = -\frac{1}{4\pi a^2\lambda}r^2\cos 2\theta \tag{3.51}$$

for some constant λ, it is found in Appendix IC that (3.50) gives

$$r^2\sin 2\theta = 2a^2\lambda\tan^{-\lambda}\theta\int_0^\theta \tan^\lambda\theta'd\theta' \ . \tag{3.52}$$

Figure 3.8 shows the constant area cavity shapes, and corresponding

Figure 3.8: A class of inversely-determined cavity shapes with known cavity parameter b.

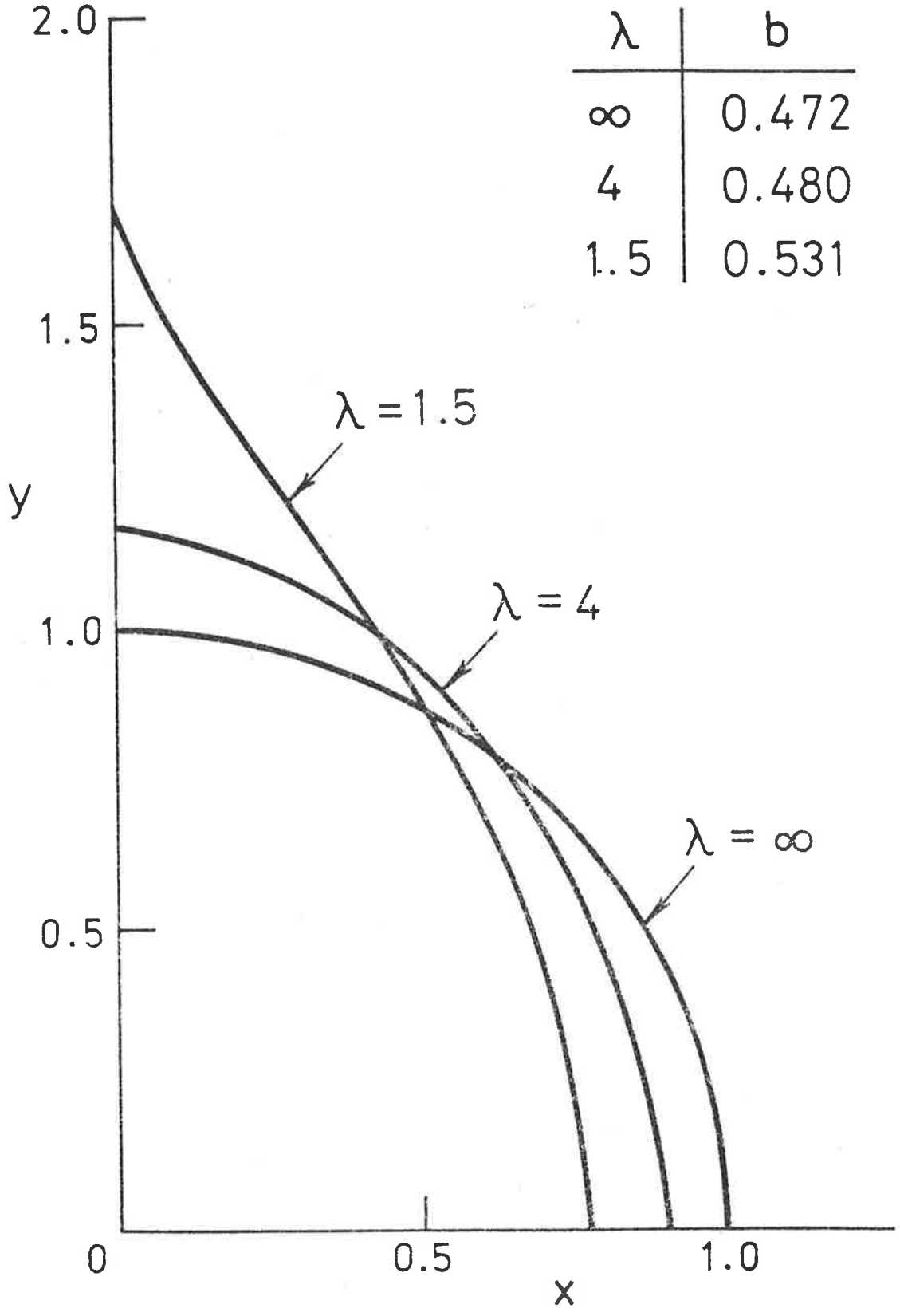

values of b_0, for various λ. Note that if $\lambda = \infty$ the potential, and cavity boundary, for a semi-circle of unit radius is given. Use of the symmetry property discussed above gives additional cavity geometries.

3.6 Summary

In this chapter we have obtained asymptotic expansions for the response of two dimensional cavities of arbitrary shape with small openings, also of arbitrary shape. The effect of the boundary geometry is introduced via two independent length parameters, one related to the opening and the other to the cavity.

The opening parameter s is well known to be an important influence on the response of the cavity, and was, in effect, used by Rayleigh in his analysis of the Helmholtz resonator. However, it is conventional to assume that, at least for the Helmholtz mode, the shape of the cavity is not important, only its net area influencing the response. The present results, being expressed in terms of a uniquely-defined cavity shape parameter b, are capable of testing this assumption.

In fact, if, for cavities of constant area and constant opening parameter s, the geometry, and hence b, is allowed to vary, the variation in response, while usually small, may be significant, especially for exciting frequencies near resonance. For example, quite large variations are obtained by varying the aspect-ratio of a rectangular cavity from unity through values as high as 16, as shown in Figure 3.7.

In addition, it was seen how the response varies from point to point within the cavity, whereas the classical analysis for a

Helmholtz resonator predicts a uniform response. Again, the variation is not, in general, large, but near resonance, and in the vicinity of the aperture at all frequencies $k = o(\beta^{-1})$, the difference in response is significant.

A symmetry property, which connects the response characteristics of cavities of related geometry, has also been described. This is a useful tool for extending the range of cavities to which this theory may be usefully applied.

CHAPTER 4

THE THREE DIMENSIONAL CAVITY RESONATOR

This chapter, the material of which has appeared in Bigg (1982a), (1982b), extends the theory of Chapter 3 to three dimensional cavity resonators with small openings. The extension to three dimensions is not trivial due to the presence of an extra, unexpected term in the asymptotic expansions, brought about by aperture curvature considerations.

4.1 Introduction

The structure of this chapter is much like that of the previous chapter. That is, we first present a theory which is asymptotically valid for small openings, compared to both wavelength and cavity dimensions, and then examine in detail the long wave limit of this presentation. It is found that there are five parameters of importance, compared to the two employed in the two dimensional theory. Of these five, two, s and b are analogous to the parameters of Chapter 3. However, the necessity to consider the curvature of the cavity walls in the vicinity of the opening introduces three further parameters: $\gamma_{\pm}$, which is an indicator of the local curvature near the aperture, and Ω and Λ, which are introduced to the problem through the extra term in the asymptotic expansions that is a result of curvature. Various examples of the computation of these parameters will be given.

The effect of the curvature of the aperture geometry, not of significance to the order of approximation in the previous chapter, will be discussed. The variation of response within the cavity is

also examined and the symmetry property will be used further. The phenomenon of cavities of equal volume having differing responses is shown to occur in three dimensions as well as two.

The theoretical results presented here are also compared with classical predictions and experimental results to check the validity of the approach.

4.2 Flow Through Small Holes

As in Chapter 3, matched asymptotic expansion techniques will be used to solve the problem of flow through small holes. The procedure for forming these expansions is as explained in the first paragraph of §3.2.

The geometry of the aperture will be assumed to be locally axisymmetric, as in Figure 4.1, unless it lies in a plane (or conical) wall. No such assumption is necessary if the orifice is in such a wall. As $r_c/w \to \infty$, r_c being the cylindrical radius, we require the surfaces shown in Figure 4.1 to approach cones of solid angle $\theta_\pm$, for $z \gtrless 0$, or, alternatively, paraboloids of revolution such that

$$r_c^2 = \pm\alpha_\pm z, \quad z \gtrless 0. \tag{4.1}$$

The characteristic size of the opening is given by two parameters, s and Ω, of which s is the more important. The condition determining smallness of the aperture is that s and Ω be small compared to all other length scales, notably the wavelength of the incident wave and the linear dimension $\beta = V^{\frac{1}{3}}$ of the cavity, V being the volume of the resonator. The parameters s and Ω will be chosen to characterize uniquely the opening geometry, as seen in its far field, as in Chapter 3.

Figure 4.1: Geometry of cavity mouth axisymmetric about z-axis.

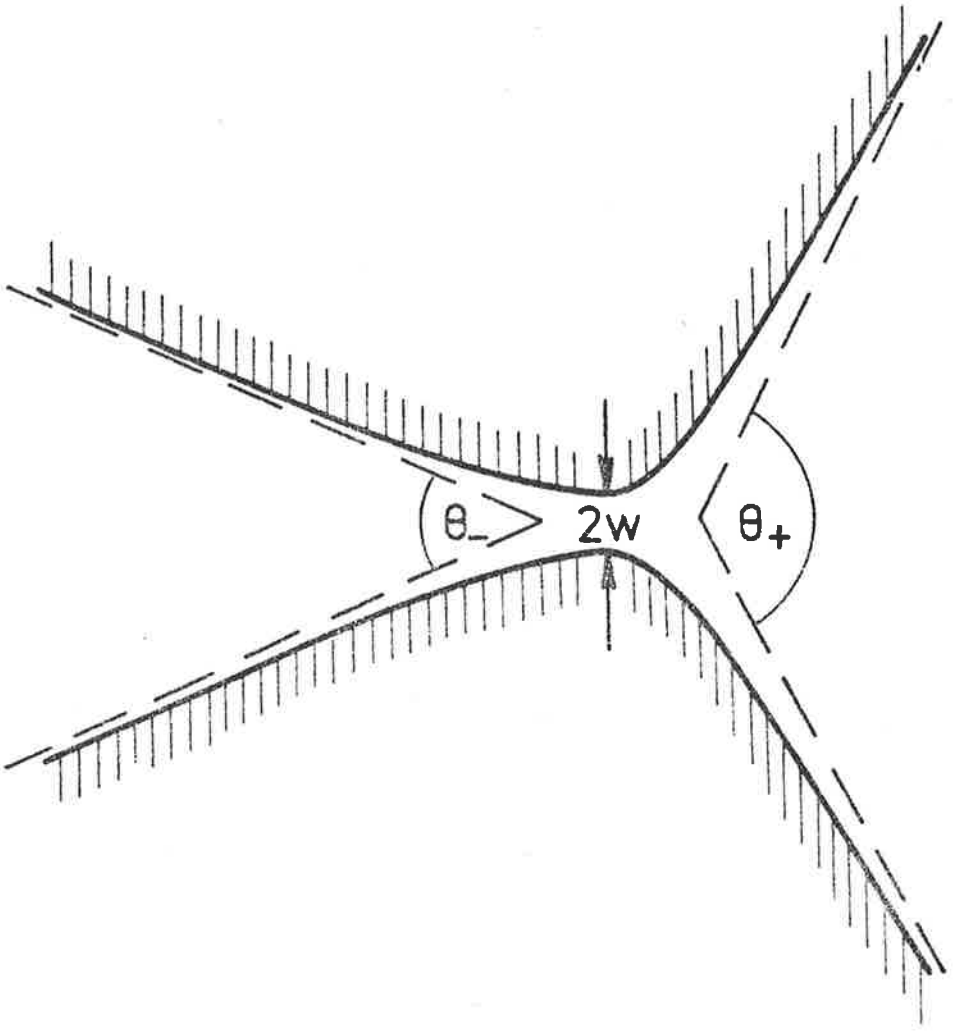

If ks is small, k being the wavelength of the exciting wave, the flow in the gap is approximately incompressible, and we must therefore solve Laplace's equation in this region. The behaviour at plus (minus) infinity corresponds to a sink (source) combined, if the aperture is not in a plane or conical wall, with a semi-infinite line sink (source) aligned along the negative (positive) z-axis*. So, normalizing the potential, we have, in the vicinity of the opening,

$$\bar{\phi} \to \pm \frac{1}{\theta_{\pm} r} \mp \frac{\gamma_{\pm}}{\theta_{\pm}} \ln(r \pm z) + C_{\pm}, \qquad z \gtrless 0, \tag{4.2}$$

where

$$r = (x^2+y^2+z^2)^{1/2} \tag{4.3}$$

and, from Appendix ID,

$$\gamma_{\pm} = \frac{1}{\alpha_{\pm}} \quad . \tag{4.4}$$

The constants $C_{\pm}$, not necessarily being the same, will be used to define s and Ω, that is, we write (4.2) as

$$\bar{\phi} \mp \frac{1}{\theta_{\pm}}\left[\left(\frac{1}{r} - \frac{1}{s}\right) - \gamma_{\pm} \ln\left(\frac{r \pm z}{\Omega}\right)\right] \to 0, \qquad z \to \pm\infty \ . \tag{4.5}$$

Thus, for any appropriate aperture geometry, $\nabla^2\bar{\phi} = 0$ must be solved, subject to $\partial\bar{\phi}/\partial n = 0$ on the opening boundaries and (4.5) at infinity. In the process of solving the problem, s and Ω will be uniquely determined. Note that if curvature is absent from the local geometry then $\gamma_{\pm} = 0$.

---

* Appendix ID examines the semi-infinite line source.

This problem is, however, rather difficult to solve, mostly because of the three dimensionality and the consequent lack of conformal mapping techniques. Thus only a few geometries can be fully examined. Tuck (1975) details some of these and several others are discussed in Appendix IB. However, as is the case for its two dimensional counterpart, s varies only slightly for fixed aperture area, while Ω is of the same order as s.

We consider now the exterior region in which there is an incident wave field $\phi_\infty(x,y,z)$ taking, in the absence of the aperture, the value $\phi_\infty(0,0,0)$ at the cavity entrance. In the limit as $ks \to 0$, the disturbance due to the cavity vanishes and $\phi \to \phi_\infty$. The residual effect of the cavity, as seen in its own far field, must be that of an acoustic source, if, as will be assumed from now on, the exterior boundary asymptotes to a cone of solid angle θ_-, so that $\gamma_- = 0$. Note that if $\theta_- = 2\pi$ the outer boundary is a plane wall. Letting m be the apparent strength of that source, we set in $z < 0$, $r >> s$,

$$\phi = \phi_\infty - \frac{me^{ikr}}{4\pi r} \tag{4.6}$$

and seek m by matching with the flow in the cavity, via the aperture. It is important to realize, before proceeding, that m is the flux of the source through an arbitrary *complete* sphere about the origin while the actual flux in $z < 0$ is $\theta_- m/4\pi$, as the outflow is restricted by the exterior conical boundary.

To perform the matching through the aperture, let $kr \to 0$ in (4.6) to obtain

$$\phi = \phi_\infty(0,0,0) - \frac{m}{4\pi r}(1+ikr) + O(mk^2 r), \tag{4.7}$$

which may be written as

$$\phi \to \phi^0 - \frac{m}{4\pi}\left(\frac{1}{r} - \frac{1}{s}\right), \quad \frac{z}{s} \to -\infty \tag{4.8}$$

where

$$\phi^0 = 1 - \frac{m}{4\pi}\left(\frac{1}{s}+ik\right) , \tag{4.9}$$

$\phi_\infty(0,0,0)$ being normalized to unity. The strength m, it should be noted, has the dimensions of a length.

The solution for incompressible flow through the aperture is therefore, using (4.5),

$$\phi(x,y,z) = \phi^0 + \frac{\theta_- m}{4\pi} \bar{\phi}(x,y,z) , \tag{4.10}$$

$\bar{\phi}$ being the canonical potential defined earlier.

Proceeding into the cavity, let $z/s \to +\infty$ to give

$$\phi \to \phi^0 + \frac{\theta_- m}{4\pi\theta_+}\left[\left(\frac{1}{r} - \frac{1}{s}\right) - \gamma_+ \ln\left(\frac{r+z}{\Omega}\right)\right], \quad \frac{z}{s} \to +\infty. \tag{4.11}$$

This expansion is matched with an interior solution by noting that, if $s \ll \beta$, β being the linear dimension of the cavity, the opening will appear to the cavity as an acoustic point sink of strength $\theta_- m/\theta_+$, coupled with an acoustic semi-infinite line sink of magnitude $m\gamma_+\theta_-/\theta_+$. That is, (4.11) provides a singularity condition as $r/\beta \to 0$. The potential in the cavity can therefore be written as

$$\phi = \frac{\theta_- m}{\theta_+} \phi_c (x,y,z) , \tag{4.12}$$

where ϕ_c satisfies (1.2), and (1.3) on the limiting boundary of the cavity, except that as $r \to 0$

$$\phi \rightarrow \frac{1}{4\pi}\left(\frac{1}{r} - \gamma_+ \ln(r+z)\right) + A \ . \qquad (4.13)$$

The constant A in (4.13), is uniquely determined by these conditions and two parameters, Λ and b, will be defined by

$$A = \lim_{r \to 0}\left[\phi_c - \frac{1}{4\pi}\left(\frac{1}{r} - \gamma_+ \ln(r+z)\right)\right] = \frac{-1}{4\pi}\left(\frac{\theta_+}{k^2 V} + \frac{1}{b} - \gamma_+ \ln\Lambda\right) \ . \qquad (4.14)$$

These parameters, b and Λ, have the dimensions of a length and are *frequency dependent* since ϕ_c satisfies the Helmholtz equation. They are also of the order of β. It is worth noting at this point that b is the three dimensional counterpart of the parameter b of Chapter 3.

Now, using (4.14) in (4.13), the limiting condition for ϕ_c becomes

$$\phi_c \rightarrow \frac{1}{4\pi}\left[\left(\frac{1}{r} - \frac{1}{b}\right) - \gamma_+ \ln\left(\frac{r+z}{\Lambda}\right) - \frac{\theta_+}{k^2 V}\right], \quad r \rightarrow 0, \qquad (4.15)$$

so, matching (4.11) with (4.12) as $r \rightarrow 0$ to find m, the relation

$$\phi^0 - \frac{\theta_- m}{4\pi\theta_+}\left(\frac{1}{s} - \gamma_+ \ln\Omega\right) = -\frac{\theta_- m}{4\pi\theta_+}\left(\frac{1}{b} - \gamma_+ \ln\Lambda + \frac{\theta_+}{k^2 V}\right) \qquad (4.16)$$

is obtained, which gives m, upon use of (4.9), as

$$4\pi m^{-1} = \frac{\theta_-}{\theta_+}\left[\left(\frac{1}{s} - \frac{1}{b}\right) - \gamma_+ \ln\left(\frac{\Omega}{\Lambda}\right)\right] + \frac{1}{s} + ik - \frac{\theta_-}{k^2 V} \ . \qquad (4.17)$$

The small gap theory, the results of which are encapsulated in equations (4.6), (4.10), (4.12) and (4.17), is now complete, subject to determination of $\bar{\phi}$ and ϕ_c. In the solution for $\bar{\phi}$ the two parameter s and Ω will be defined. These are associated with the opening and have values of the order of the aperture dimensions. They are also *frequency independent* since $\bar{\phi}$ is a

solution of Laplace's equation. Note that if the aperture is in a plane, or conical, wall then Ω can be neglected. The solution for ϕ_c defines the two parameters b and Λ, which are associated with the cavity and consequently possess properties which reflect this. It is of interest to record that Λ is neglected in the same instances in which Ω is disregarded. This is due to the vanishing of γ_+ when the orifice is set in a plane, or conical, wall.

4.3 Conical Cavities

As with the two dimensional theory, the problem of finding ϕ_c for a given cavity is a difficult one. However, the three dimensional analogue of the circular arc cavity, namely a conical sector of a sphere with its opening at the apex, is one of the few types of cavities for which an exact solution can be found. Thus we shall examine the response of this resonator in some detail.

If we define a spherical coordinate system (r,ψ,v) centred at the cavity opening, then the surface of our resonator is the cone generated by rotating the arc $v = \arccos(1-\theta_+/2\pi)$ (see Appendix IB) about the z-axis, plus the cap $r=a$. Note that because of the conical boundary near the aperture, $\gamma_+=0$ for these cavities and that if $\theta_+ = 2\pi$ the cavity is a semisphere.

The conditions (1.2), (1.3) and (4.13) are satisfied if

$$\phi_c = \frac{-k}{4\pi}\left(y_0(kr) - \frac{y_1(ka)}{j_1(ka)}\, j_0(kr)\right), \qquad (4.18)$$

where j_0, j_1 are spherical Bessel functions of the first kind and y_0, y_1 are spherical Bessel functions of the second kind. To

find b, the limit of (4.18) is taken as $kr \to 0$ and related to (4.15), that is,

$$\frac{1}{4\pi r} - \frac{\theta_+}{4\pi k^2 V} - \frac{1}{4\pi b} = \frac{1}{4\pi r} + \frac{1}{4\pi}\left(\frac{y_1(ka)}{j_1(ka)}k - \frac{k^2 r}{2} - O(k^3 r^2)\right), \quad (4.19)$$

using the expansions for y_0, j_0 in Abramowitz and Stegun (1972, Chapter 10). For this geometry

$$V = \frac{1}{3}\theta_+ a^3 , \quad (4.20)$$

so

$$b^{-1} = \frac{-3}{k^2 a^3} - k\frac{y_1(ka)}{j_1(ka)} . \quad (4.21)$$

Observe that b contains terms representing both the singular nature of the solution, $y_1(ka)$, and the non-singular natural modes, $j_1(ka)$.

Using (4.12) and (4.17), the potential along the boundary r=a is

$$\phi = \frac{(\theta_-/\theta_+)m}{4\pi k a^2 j_1(ka)}$$

$$= \frac{1}{ka^2}[ky_1(ka)+j_1(ka)\{\frac{1}{s}(1+\frac{\theta_+}{\theta_-})+ik\}]^{-1} . \quad (4.22)$$

An illustrative plot of $|\phi|_{r=a}$ against ka is given in Figure 4.2 for the semispherical resonator with $\theta_+ = \theta_- = 2\pi$, s=0.1 and a=1. As with the two dimensional problem, resonance occurs when the quantity in the square brackets of (4.22) is small, which, because s is small, usually occurs when the second term vanishes. These peaks in the response are close to the zeroes of $j_1(x)$, the natural frequencies of the conical sector geometry, $j_1(x)$ being introduced to the solution via the cavity shape parameter b.

Figure 4.2: Response curve for unit radius semisphere with $s = 0.1$ (first peak has a maximum value of 33).

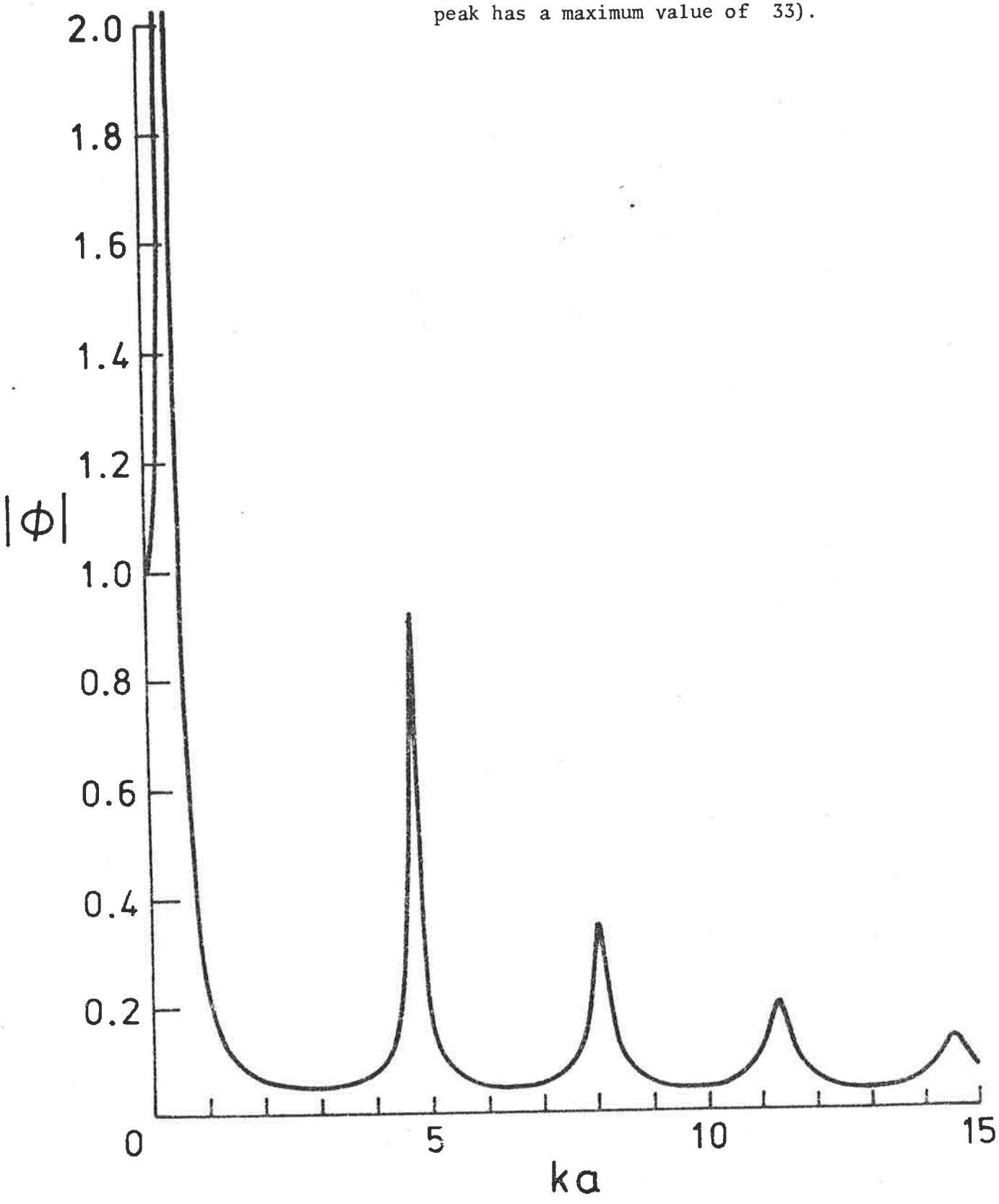

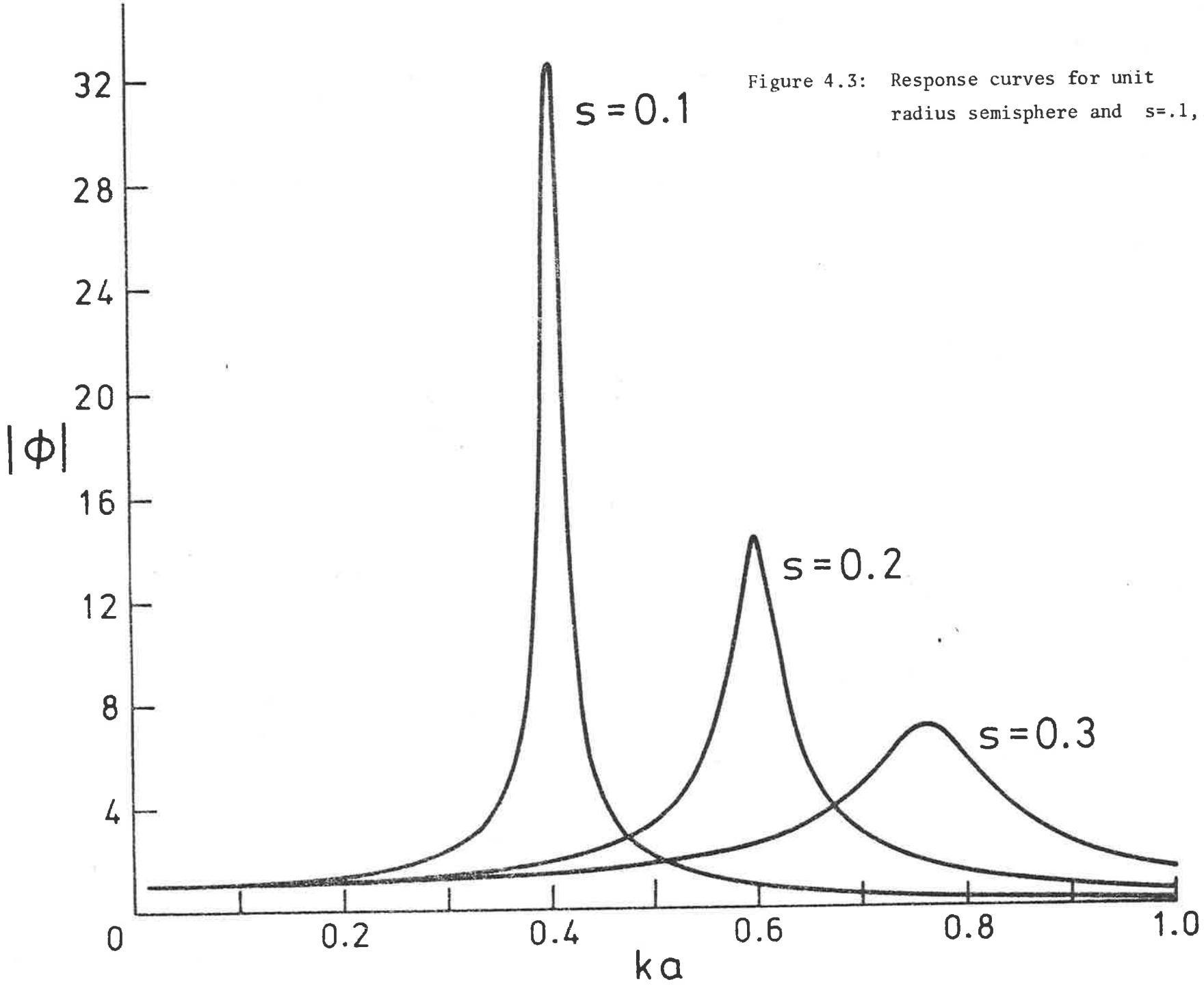

Figure 4.3: Response curves for unit radius semisphere and s=.1,.2,.3.

The first and most prominent peak is, of course, the Helmholtz resonance and it is due to the two terms of (4.22) almost cancelling each other, which occurs only for small ka. This mode of resonance will be treated in more detail in the next section.

The effect of changing s/a is quite considerable, as shown in Figure 4.3. Decreasing s/a pushes all resonant peaks to lower frequency and increases their magnitude. Indeed, for $s/a \lesssim 0.05$ this increase in amplitude for the Helmholtz mode is very large - up to 10,000 times the amplitude of the incoming disturbance. Viscous and non-linear effects must play a considerable damping role in this resonance. As with the two dimensional example, the natural vibrational modes, not shown in Figure 4.3, change in a quantitatively different manner; the "Harbour paradox", discussed in §3.3, does not apply to these modes.

It is worth comparing, at this point, the two dimensional response, as shown in Figures 3.2, 3.4 and 3.5, with the above results. The major differences are in the magnitudes and the bandwidths of the resonant peaks, respectively smaller and wider in the two dimensional as opposed to the three dimensional resonator. It is also of interest that the response between resonance peaks is much greater in the 2-D case than in the 3-D, where there is practically no response.

4.4 The Helmholtz Mode

To enable the Helmholtz mode to be discussed in some detail, use will be made of the fact that resonance occurs for small $kV^{\frac{1}{3}}$ to simplify the investigation.

The problem in the interior of the cavity consists of solving (1.2) subject to $\partial\phi_c/\partial n = 0$ on the limiting cavity walls, with condition (4.15) holding as $r \to 0$. We may expand ϕ_c in the series

$$\phi_c = \phi_0 + \phi_1 + \phi_2 + \ldots , \tag{4.23}$$

where $\phi_0 = O((k^2V)^{-1})$, $\phi_1 = O(V^{-\frac{1}{3}})$, $\phi_2 = O(k^2V^{\frac{1}{3}})$, etc., remembering that ϕ_c has dimensions of inverse length. Note that the leading term ϕ_0 is expected to be a constant, from physical arguments, as in the two dimensional theory.

Substituting (4.23) into Helmholtz's equation (1.2) gives rise to a sequence of Poisson equations

$$\nabla^2\phi_1 = -k^2\phi_0, \tag{4.24}$$

$$\nabla^2\phi_2 = -k^2\phi_1, \tag{4.25}$$

etc., with accompanying boundary conditions

$$\frac{\partial\phi_1}{\partial n} = \frac{\partial\phi_2}{\partial n} = \ldots = 0 . \tag{4.26}$$

If (4.24) and (4.25) are integrated over the interior of the cavity some useful results follow.

Firstly, integrating (4.24) it is found that

$$\iiint_V \nabla^2\phi_1 dV = \iint_S \frac{\partial\phi_1}{\partial n} ds = -k^2\phi_0 V , \tag{4.27}$$

S being the interior surface of the cavity plus the plane of the aperture. Using (4.26), the surface integral in (4.27) is reduced to an integral over the cavity opening only. This represents the net flux transported through the aperture. If the opening is now represented as a point sink of unit apparent strength

combined with a semi-infinite line sink of magnitude γ_+, as in §4.2, this flux is $\theta_+/4\pi$. The semi-infinite line sink does not contribute to the flux as it is exterior to the cavity. Thus, the leading term in (4.23) is the constant

$$\phi_0 = \frac{-\theta_+}{4\pi k^2 V} . \tag{4.28}$$

Integrating (4.25) over V gives

$$\iiint_V \nabla^2\phi_2 dV = \iint_S \frac{\partial\phi_2}{\partial n} dS = -k^2 \iiint_V \phi_1 dV . \tag{4.29}$$

But $\partial\phi_2/\partial n = 0$ everywhere on S, as ϕ_2 makes no contribution to the net flux through the opening, so (4.29) gives the normalization condition analogous to (3.29), namely,

$$\iiint_V \phi_1 dV = 0 . \tag{4.30}$$

This condition is used to determine the parameters b and Λ, in conjunction with (4.15).

Leaving the solution of the problem for ϕ_1 to the next section, we assume that ϕ_1 is known and give expressions for ϕ in the cavity and aperture.

Using (4.12), the velocity potential in the interior of the cavity is

$$\phi = \frac{\theta_- m}{\theta_+}\left(- \frac{\theta_+}{4\pi k^2 V} + \phi_1(x,y,z) + O(k^2 V^{\frac{1}{3}}) \right), \tag{4.31}$$

where m is given by (4.17). In the vicinity of the aperture, where (4.31) becomes singular, (4.10) gives

$$\phi = 1 - \frac{m}{4\pi}\left(\frac{1}{s} + ik - \theta_- \bar{\phi}(x,y,z)\right) . \tag{4.32}$$

Note that in both (4.31) and (4.32) m has an error $O(k^2V)$, as only the leading terms in the small-k expansion of b and Λ are found through (4.30). Thus the overall error in both equations is $O(k^4V^{4/3})$.

As with the two dimensional equivalents of (4.31) and (4.32), namely (3.30) and (3.31), spatial variations of second order only are predicted for the velocity potential in both the aperture and the interior of the cavity. Thus the leading order constant is generally more important. However, the constant terms of (4.31) and (4.32) are not the same, their ratio being

$$\frac{\phi_{opening}}{\phi_{cavity}} = 1 - \frac{k^2V}{\theta_+}\left[\left(\frac{1}{s} - \frac{1}{b_0}\right) - \gamma_+ \ln\left(\frac{\Omega}{\Lambda_0}\right)\right] , \qquad (4.33)$$

where b_0 and Λ_0 are the zero frequency limits of the parameters b and Λ respectively. The ratio, as for two dimensional cavities, is less than unity for non-zero k, as s^{-1} is larger than the other terms in the square brackets of (4.33). Therefore the response in the opening is less than that in the cavity.

The effect of aperture curvature, not of importance in two dimensional resonator theory, is of interest as the classical end-correction does not take it into account. As Rayleigh (1896) states, the end-correction is dependent on the cavity shape, not just the aperture width as commonly accepted. If aperture curvature is considered, however, the leading order approximation to the Helmholtz wavenumber becomes, from consideration of (4.17),

$$k_H = \left\{\left(\frac{\theta_+ \theta_-}{\theta_+ + \theta_-}\right)\frac{s}{V}\right\}^{1/2} , \qquad (4.34)$$

assuming $\Omega = O(s) << \Lambda_0$, which reduces to the classical expression

$$k_H = \left(\frac{\pi s}{V}\right)^{1/2} \tag{4.35}$$

if $\theta_- = \theta_+ = 2\pi$ (see Bigg (1982a)). Thus aperture curvature has *no* effect on the leading order estimate of the Helmholtz wavenumber.

It is possible to derive an explicit expression for this modal wavenumber by considering the mean potential in the cavity, $m\phi_0$ $(\theta_-=\theta_+=2\pi)$, and differentiating its magnitude with respect to k, so that

$$k_H = \left(-\frac{\tau^2}{3} + \frac{1}{3}(\tau^4+\tau\eta)^{1/2}\right)^{1/2}, \tag{4.36}$$

where

$$\tau = \frac{2}{s} - \frac{1}{b_0} - \gamma_+ \ln\left(\frac{\Omega}{\Lambda_0}\right) \tag{4.37}$$

and

$$\eta = \frac{12\pi}{V} . \tag{4.38}$$

Note that the classical result is contained within (4.36) for large τ. From (4.36) it can be seen that the effects of b_0, Ω and Λ_0 are smaller than those of s and non-uniform, that is, for some cavities they act to increase the Helmholtz frequency in comparison with the classical frequency, while for others we see the opposite tendency. Examples of this are given in the next section.

4.5 Determination of First Order Potential

To complete the solution, ϕ_1 must be found. This quantity satisfies

$$\nabla^2\phi_1 = \frac{\theta_+}{4\pi V} \tag{4.39}$$

in the limiting cavity, subject to

$$\frac{\partial \phi_1}{\partial n} = 0 \tag{4.40}$$

on S, except at the opening where

$$\phi_1 \to \frac{1}{4\pi}\left(\frac{1}{r} - \frac{1}{b_0}\right) - \frac{\gamma_+}{4\pi}\ln\left(\frac{r+z}{\Lambda_0}\right), \qquad r \to 0. \tag{4.41}$$

The normalization condition (4.30) is used to uniquely define b_0 and Λ_0, the cavity potential being given finally by (4.31).

As with two dimensional resonator theory, solving this system is still a difficult task but solutions may be found by various methods, some of which are presented here. The symmetry property, so useful in the analysis of §3.5, is still applicable and is even more valuable, as three dimensionality has removed complex analysis from our repertoire of solution techniques. The role of cavity symmetry is illustrated in Figure 4.4.

We will begin our discussion of the solution of the system of equations (4.39)-(4.41) by considering the conical sector geometry of §4.3. Due to the conical nature of the cavity walls near the opening the parameter $\gamma_+=0$, so the potential satisfying the necessary conditions is

$$\phi_1 = \frac{r^2}{8\pi a^3} + \frac{1}{4\pi r} - \frac{1}{4\pi b_0}, \tag{4.42}$$

where, from Appendix IE,

$$b_0 = \frac{5a}{9}. \tag{4.43}$$

Upon substitution of (4.42) into (4.31) to give the interior potential, it can be seen that this potential is identical with the small-ka expansion of the exact potential of §4.3.

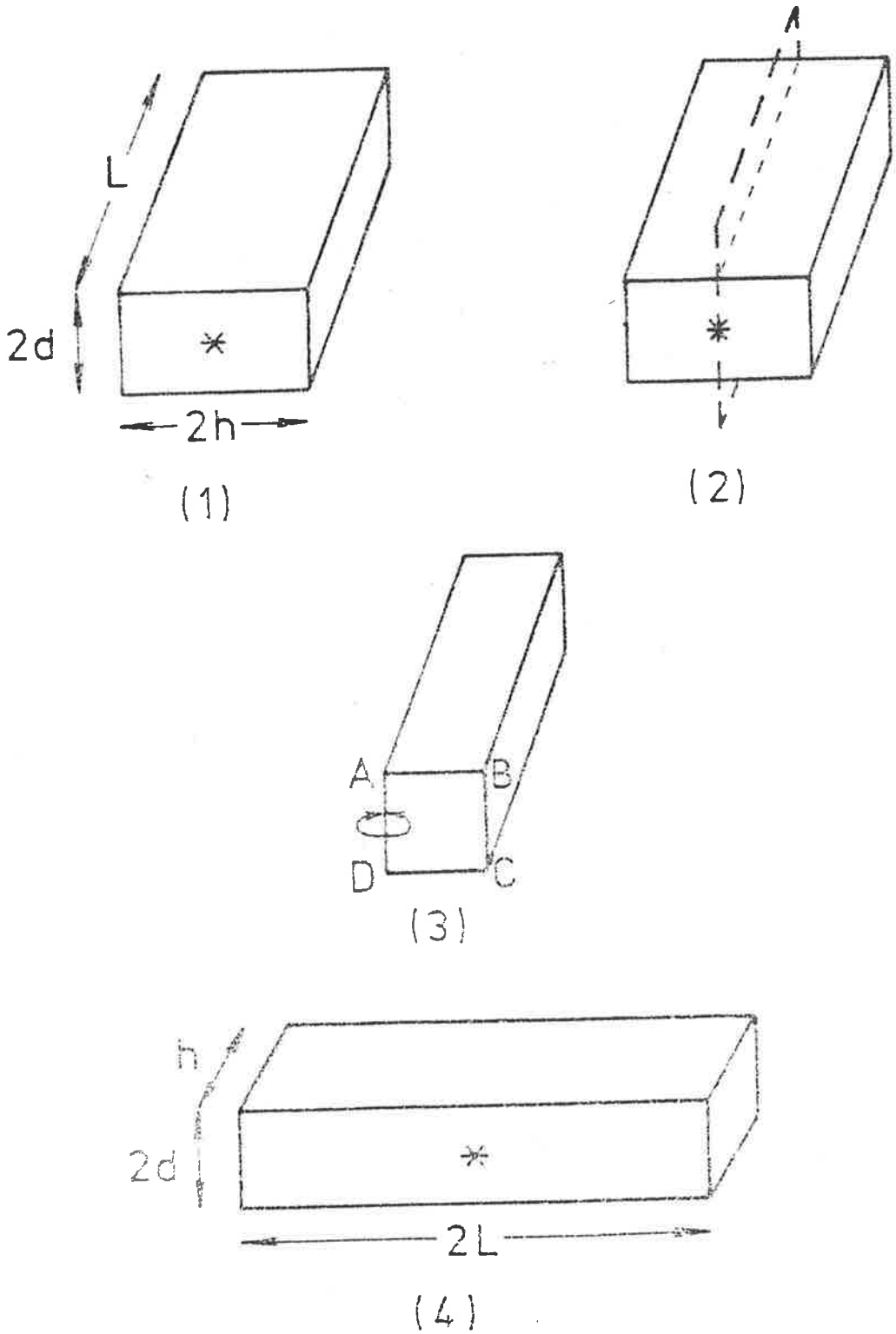

Figure 4.4: Example of symmetry property. (1) original cavity; (2) wall placed on symmetry plane; (3) aperture moved to edge of long wall; (4) new cavity ((3) reflected in ABCD).

This resonator will be used to demonstrate the variation of ϕ within the cavity. In Figure 4.5 the potential along three constant radius arcs in the cavity is shown. It is clearly seen that the magnitude of the response at the mouth of the resonator is considerably smaller than that in the interior, as predicted by (4.33). The other important feature is the spatial invariance of $|\phi|$ within the cavity, except at resonance where a 5-10% difference in magnitude is found. Note that the resonance occurs at the same frequency throughout the cavity. It is also interesting to compare Figure 4.5 with Figure 3.6, the corresponding diagram for two dimensional resonators, as we see that three dimensional resonance is more uniform over the cavity than is two dimensional resonance.

Another cavity to be examined is the finite length circular cylinder of radius a and length L, whose orifice is in the centre of a circular face. It is shown in Appendix IE that a potential satisfying (4.39) - (4.41) is

$$\phi_1 = \frac{z^2}{4\pi a^2 L} + \frac{1}{4\pi\sqrt{r_c^2+z^2}} + \sum_{n=1}^{\infty} a_n J_0\left(\frac{\alpha_n}{a} r_c\right)\cos\left(\frac{\alpha_n}{a} z\right) + C, \qquad (4.44)$$

where α_n is the nth root of $J_0(x)$ and $r_c^2 = x^2+y^2$. The Bessel coefficients, a_n, are given by

$$a_n = \frac{\left[\alpha_n \sin\left(\frac{\alpha_n}{a}L\right)\right]^{-1}}{aJ_1^2(\alpha_n)\pi}\left\{\frac{J_1(\alpha_n)}{\alpha_n} - \frac{1}{2} + \frac{\alpha_n L}{2a}\int_0^{\alpha_n} \frac{J_1(\tau)}{\sqrt{\tau^2+\left(\frac{\alpha_n}{a}L\right)^2}}d\tau\right\} \quad n=1,2,3,\ldots, \qquad (4.45)$$

unless

$$L = \frac{\ell\pi a}{\alpha_n}, \qquad \ell=1,2,3,\ldots \qquad (4.46)$$

when the appropriate a_n vanishes, and, using the normalization condition (4.30), the constant C is given by

Figure 4.5: $|\phi|$ across unit radius semispherical cavity, s=0.1; --- r=1; —— r=0.5; —— —— r=0.

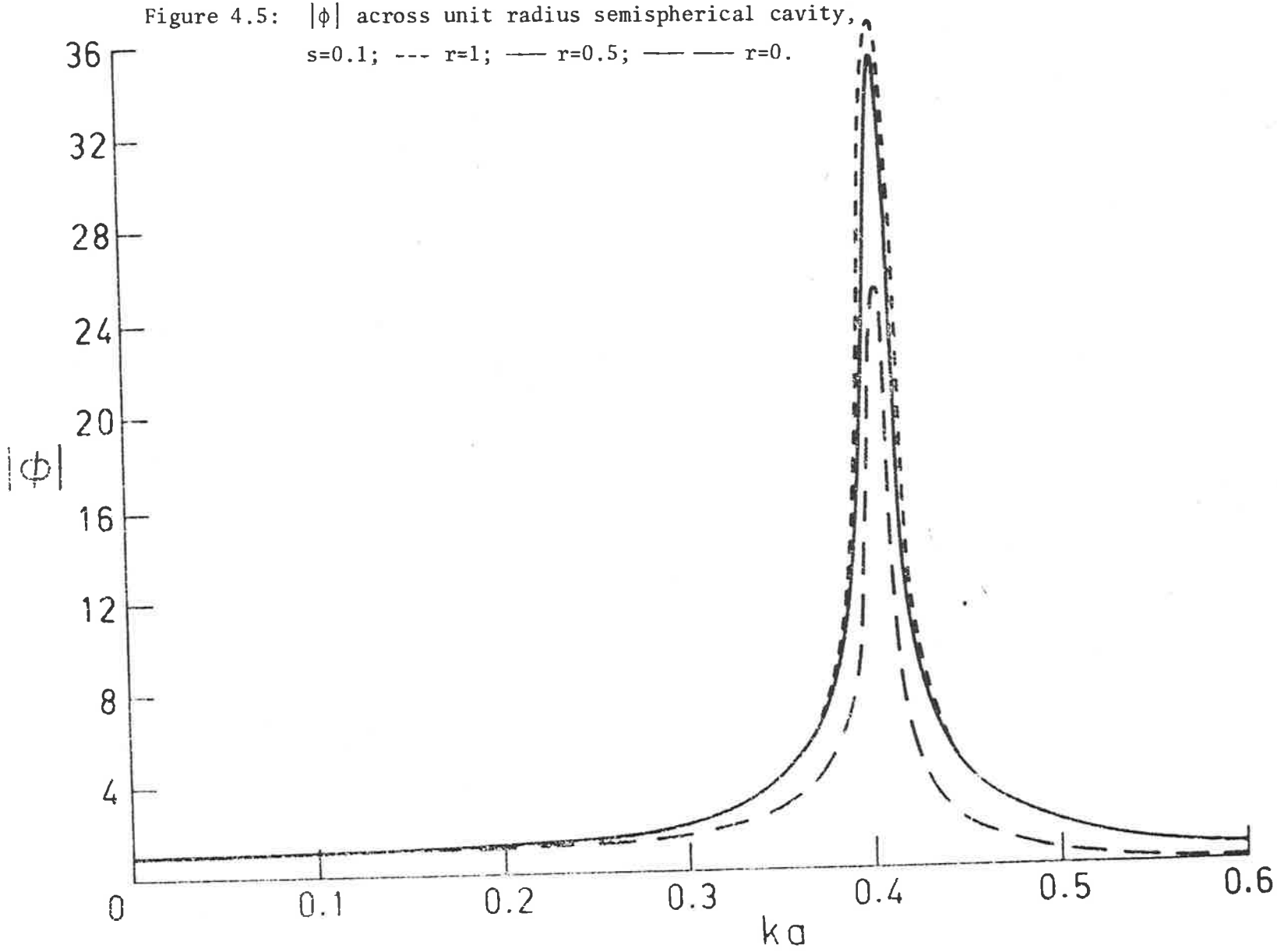

$$C = \frac{-1}{\pi a^2 L}\left\{-\frac{L^2}{6} + \frac{a^2}{4}\left[\operatorname{arcsinh}\left(\frac{L}{a}\right) + \frac{L}{a}\cosh\left(\operatorname{arcsinh}\left(\frac{L}{a}\right)\right)\right]\right.$$

$$\left. + 2\pi a^3 \sum_{n=1}^{\infty} a_n \sin\left(\frac{\alpha_n L}{a}\right)\frac{J_1(\alpha_n)}{\alpha_n^2}\right\} . \qquad (4.47)$$

Using (4.41), noting that $\gamma_+=0$ as the aperture is in a plane wall, it is found that the cavity shape parameter b_0 is given by

$$b_0^{-1} = -4\pi\left(\sum_{n=1}^{\infty} a_n + C\right). \qquad (4.48)$$

The parameter Λ_0 is, of course, zero as $\gamma_+=0$.

Panton and Miller (1975a) considered this geometry and in Table 4.1 the resonant frequencies for several circular cylinders are shown, as computed by both their theory and the present work. It should be noted that Panton and Miller's formula, an adaptation of the classical result with improved entrance corrections, namely

$$k_H = \frac{1}{c}\left(\frac{A_0}{\ell' V + \frac{1}{3}L^2 A_0}\right)^{\frac{1}{2}} , \qquad (4.49)$$

where c is the speed of sound, A_0 the orifice area and ℓ' the effective length of the aperture, requires that no dimension of the cavity be greater than a sixteenth of a wavelength λ. The classical result (1.1) has a similar constraint but it is not a necessary condition in the present theory. In fact, this analysis has the single proviso that $s \ll \beta$; β being a characteristic dimension of the cavity.

The two starred rows in Table 4.1 show the results for cylinders of the same volume, with the second of the two having a length slightly greater than $\lambda/16$. The present work encounters

TABLE 4.1: Comparison with Panton and Miller's (1975b) formula for circular cylinders.

s^+ (m)	Radius (m)	Length (m)	Resonant Wavenumber Present Work	Panton & Miller	Classical
.05	1	1	.221	.219	.224
.05*	2	1	.105	.107	.112
.05*	1	4	.122	.105	.112
.05	1	2	.164	.151	.158
.10	1	1	.308	.315	.316
.10	2	3	.064	.089	.091
.10	3	1	.107	.103	.105

*These two have the same volume.

$^+$Opening is a circular hole of radius $W = \pi s/2$ with no neck.

TABLE 4.2: Helmholtz frequency for spherical cavities.

W (cm)	Radius (cm)	Wall Thickness (cm)	Resonant Frequency (Hz) Classical	Eq.(40)	Ingard's Theory*	Experiment*
.8	9.	.1	116.2	117.6	117	120
1.025	9.	.1	132.6	135.0	134	135
1.55	9.	.1	164.8	170.3	168	168
1.86	9.	.1	180.6	188.4	185.5	190
1.91	9.	.1	183.6	192.0	189	195
$^+$ .0157	.75	0.	703.3	703.7		
.0157	2.	0.	161.5	161.4		
.157	2.	0.	510.7	516.0		
.157	5.	0.	129.2	129.4		

*Taken from Table I, (1953b).

$^+$Last 4 rows theoretical only, s given by (IB.23).

no difficulties with this length and should be accurate. The results therefore demonstrate the important property, already noted in two dimensional resonator theory, that cavities of the same volume, but different geometry, have different response curves. This conclusion has been tested for other volumes not shown here.

It may also be noted that while Panton and Miller's formula gives resonant frequencies consistently less than the classical formula, indicating a standard correction factor, the present theory has no such characteristic, Helmholtz frequency predictions being both above and below those of the classical result.

To illustrate the use of the curvature parameters in the first order theory, we will now examine a cavity which has neither plane nor conical walls near the aperture but a curved surface. Such a cavity is the sphere of radius a. The results for this type of resonator will be compared to the experimental and theoretical results of Ingard (1953b).

It is shown in Appendix IE that a potential satisfying the necessary conditions for spherical geometry is, if r is measured from the aperture,

$$\phi_1 = \frac{1}{4\pi r} - \frac{7}{20\pi a} + \frac{1}{16\pi a^3}(r^2-2az) - \frac{1}{8\pi a}\ln\left(\frac{r+z}{a/2}\right) , \qquad (4.50)$$

with

$$\Lambda_0 = \frac{a}{2} \qquad (4.51)$$

and

$$b_0 = \frac{5a}{7} . \qquad (4.52)$$

In Table 4.2 the Helmholtz frequencies for various spherical cavities, as computed by (4.35), (4.36) and Ingard (1953b), are presented. The aperture parameter s, used in (4.35) and (4.36),

was taken to be the approximation (IB.25) as the walls of the experimental spheres were of non-zero thickness. The parameter Ω was, however, assumed to be unaltered, that is (IB.47) was still used. It should be noted that the detailed calculations for this chapter are for resonators set in a plane outer wall, while the experiments were conducted with isolated spheres. The present theory may, however, be adapted for this cavity with only slight second order changes. Another relevant point is the size of the openings, which were relatively large in the experiment, so the above theory may approach its limit of validity for the spheres of larger aperture.

Having stated the above facts, we see from Table 4.2 that even for moderate s/β values agreement between the present theory and experiment is very good. The results are generally better than the theoretical predictions of Ingard, which were derived explicitly for spherical geometry. Considering all the tabulated results, it is seen that the classical prediction is accurate to within a few percent for small s/β ratios but may be more than 10% in error for larger s/β ratios. It is in this region, when considering such symmetrical bodies, that the second order terms in (4.36) become important. Of course it should be remembered that, as was seen in the examination of cylindrical cavities, some cavity shapes are subject to significant changes in their Helmholtz resonance frequency, in comparison with another cavity of the same volume, due to the effects of cavity and aperture geometry. Therefore the second order parameters are useful to employ if known.

Another paper with which results may be compared is the semi-empirical article of Alster (1972). This paper obtains a formula

for the Helmholtz frequency using extensions of the spring-like arguments used to derive the classical formula, as in Kinsler and Frey (1962, p. 186f.). This formula may be adapted to many different cavities; however, the results given by Alster are consistently 60-70% higher than those obtained by the present theory or by Panton and Miller. If the end-correction used by Alster is adjusted to the classical value of $8\omega/3\pi$, ω being the aperture radius, the resonant frequencies are then comparable. Alster's formula has the same type of restriction as Panton and Miller's, also it should be noted that Alster's experimental data apparently agreed with his formula.

The final cavity shape to be mentioned is the rectangular prism, shown in Figure IE.1. The solution of the system (4.39)-(4.41) uses the ideas of Tuck (1975, §6) and is derived in Appendix IE. Here the potential will be merely stated:

$$\phi_1 = \frac{1}{4\pi r} + \frac{x^2}{16hdL} + \sum_{n=0}^{\infty} a_n \cos\left(\frac{n\pi x}{d}\right)\cos\left(\frac{n\pi z}{h}\right)\cosh\left(\frac{n\pi y\sqrt{d^2-h^2}}{dh}\right)$$

$$+ \frac{1}{16\pi d}\Phi\left(\frac{x}{2d}, \frac{\sqrt{y^2+z^2}}{2d}\right) + \frac{1}{16\pi h}\Phi\left(\frac{z}{2h}, \frac{\sqrt{x^2+y^2}}{2h}\right) , \quad (4.53)$$

where

$$\Phi(X,R) = \sum_{\ell=1}^{\infty} \{[(\ell-X)^2+R^2]^{-\frac{1}{2}} + [(\ell+X)^2+R^2]^{-\frac{1}{2}} - \frac{2}{\ell}\} , \quad (4.54)$$

the coefficients a_n being given in Appendix IE. Note that $\gamma_+=0$, as the orifice is in a plane wall, and that

$$b_0^{-1} = -4\pi \sum_{n=0}^{\infty} a_n . \quad (4.55)$$

Other methods may be used to solve for ϕ_1 than those demonstrated above. The inverse approach used in §3.5 is one,

which, however, is not as successful in three dimensions as in two. This is because non-linear differential equations occur and the cavities resulting from solutions to these equations usually have asymptoting, rather than closed, surfaces.

4.6 Conclusion

The three dimensional resonator theory presented in this chapter agrees with most of the conclusions of the two dimensional theory of chapter 3. However, if the walls of the cavity near the orifice possess finite curvature, that is, if the aperture is not in a plane or conical wall, then the theory requires significant modification. In two dimensional theory, curvature near r=0 caused no peculiar problems but in three dimensions an extra *singular* term must be introduced to the asymptotic expansions. This singular term describes the potential due to a semi-infinite line source and appears to be virtually unknown in previous literature. While the 3-D theory for cavities whose aperture is set in a plane or conical wall is easily carried over from the 2-D theory, cavities possessing aperture curvature require two extra parameters to describe the second order effects on resonance. However, to leading order, aperture curvature has no effect on the classical formula for the Helmholtz frequency.

Another difference between 2-D and 3-D theory is the higher amplitude of resonance in the 3-D resonator, coupled with the lower off-resonance amplitude. A greater uniformity of potential within the cavity at resonance was also encountered in the 3-D cavity. That is, the variation of peak Helmholtz response about the cavity was a smaller percentage of the maximum response in 3-D resonators as compared to 2-D cavities.

As a final remark it is worth observing that the restriction on the use of this theory, namely that the aperture parameter s be small in comparison with a dimension of the cavity, is of a different nature to the classical restriction. Cavities not suitable for classical analysis may therefore be studied theoretically using the present approach, which generally gives better results than the classical theory in any case. It is also worth noting that even for relatively large s the Helmholtz mode is well described by the above theory, although the higher k responses may be altered by the appearance of non-symmetric modes of oscillation, as was seen in chapter 3.

P A R T I I

SCATTERING BY SLENDER BODIES

CHAPTER 5

REVIEW OF BODY DIFFRACTION THEORY

The problem of forward diffraction by bodies in a homogeneous medium has received a great deal of attention, due to the number of fields of application. These fields include shallow-water wave theory, acoustics, anti-plane elastodynamics and electromagnetism in various guises such as optics and radiation theory. This second part of the present thesis will concentrate on the shallow-water wave problems; however all the work could be easily applied to other areas. In particular, we shall examine diffraction by thin bodies which are either transparent to the incident grazing waves (Chapter 6) or opaque (Chapter 7). The parabolic approximation, first introduced by Leontovich and Fock (1946), will be used as the principal tool of any analysis, building on the work of Mei and Tuck (1980). Matched asymptotic expansion theory will also play a pivotal role in the analysis.

5.1 Previous Work

As has already been noted, the problem of diffraction by bodies, especially bodies in an oceanographical context, has received much attention since at least the last century. However, the advent of computers to the resources available to researchers has led to a proliferation of material in the last twenty years. A representative cross-section of the work done will thus be given, rather than an exhaustive survey.

Lamb gives a survey of the early work in this field in Chapter 10, and the latter half of Chapter 9, of his "Hydrodynamics" (1932). Some papers from our field of interest are those of

Proudman (1914), who examined the exact solution for a plane wave incident on a circular island and approximations for waves incident on elliptic islands, Lamb (1906), who solved the problem of diffraction by a parabolic island, and Watson (1919), who considered the diffraction of electric waves by the earth. This latter paper is of interest because of its connection with Keller's theory of geometrical diffraction.

In the post-World War II research done before the widespread use of computers, analytic and experimental techniques dominated the field. Arthur (1946) used ray diagrams to discuss the bending of waves, passing over depths whose contours were of analytic form, around islands of circular symmetry. He later, (1951), discussed the various mechanisms causing alterations to wave patterns near islands including reflection, refraction, diffraction, current interaction and wave variability. Pocinki (1950) used conformal mapping to study refraction and Isaacs, Williams and Eckart (1951) examined total reflection of surface waves in their passage from shallow to deep water. Eckart (1952) also developed an integro-differential equation for gravity waves in shallow water which he tested on known solutions. Laird (1955) conducted an experimental study of waves incident on a cylindrical island.

Following a few years of little attention to island scattering, the mid 1960's saw the beginning of a revival of interest which has continued to the present day. In 1963 Barakat used the theory of Mathieu functions at low frequency to study diffraction by elliptic cylinders. Then, in 1965, Chambers introduced rotation to the problem and discussed free modes of vibration over sills and around islands. Carrier (1966) included non-linear terms in his examination

of long wave propagation near coasts.

The beginning of numerical studies may also be traced to this period, with Richmond's (1965) use of a boundary integral method to consider scattering by dielectric cylinders of arbitrary cross-section and Moimoi's (1967) use of Bessel function expansions of long waves incident on circular islands.

In 1967 a landmark paper by Longuet-Higgins examined the reception of waves on circular sills and the wave energy modes trapped by free and forced waves. This article, which sparked off a considerable amount of research, also discussed various forms of contours around the sill and the effects on the trapped wave modes from asymmetry, rotation and viscosity. This was followed in 1969 by another paper concentrating on the effects of rotation, and, in 1970, by an article demonstrating that the inertial oscillations are resolvable into two waves travelling in opposite directions around the island. This latter paper also showed the presence of a strong direct current mass transport velocity. Longuet-Higgins' papers were extended by Summerfield (1969, 1972), showing that all modes for cylindrically symmetric depth contours leaked energy to the surrounding ocean.

Another paper from 1967 which led to a number of articles in the field of scattering by bodies is that of Handelsman and Keller. While this paper developed a source distribution theory for axially symmetric *potential* flow about a three dimensional object, it was followed by a series of articles by Geer (1968, 1974, 1975, 1978, 1980) in which the ideas of Handelsman and Keller were applied to many problems including the scattering of waves by slender bodies of revolution. However, the use of this technique for two dimensional

scattering problems is much more complicated and has not yet been done.

Following the first Longuet-Higgins paper a number of similar problems were examined. Shen, Meyer and Keller (1968) discussed the spectra of waves in channels as well as around islands, while Rhines (1969) continued the examination of the effects of rotation on oscillatory motion about islands and sills, where bottom topography was either discontinuous or analytic. Miles and Gilbert (1968) discussed the theory of scattering by circular islands which could be floating docks, that is, where the body does not necessarily touch the sea floor. Lautenbacher (1970) considered a numerical solution to the integral equation describing long wave reception for circular or elliptical symmetry.

Another numerical approach to the problem of scattering by oceanographic features is that of Berkhoff (1972) who used finite element techniques on circular islands and parabolic shoals. Shaw (1974) used finite difference techniques to examine the scattering by a circular island surrounded by a region of varying depth. Another finite difference approach is that of Vastano and Reid (1967) who also examined circular island scattering. They were principally interested in the response to tsunamis.

Articles from related fields during the early seventies include Chen and Mei's (1973) discussion of wave forces on an elliptic platform, using Mathieu functions, and the beginnings of slender ship theory. Faltinsen (1972) examined the first order theory applicable to restrained ships in head-sea waves while Maruo and Sasaki (1975) extended this to second order.

Since the mid seventies a great deal has been done on the scattering problem. We will first examine the work which is mostly

analytical and then discuss the purely numerical articles.

Christiansen (1974) examined diffraction around arbitrary shaped islands using Green's functions. This work was followed up, in 1976, by an investigation involving ray methods. The latter research focussed on islands with a parabolic topography with or without discontinuities. Smith and Sprinks (1975) used the geometrical optics mild slope approximation to give an equation which is an asymptotic approximation to the behaviour of waves. The model was tested using topography similar to that in Lautenbacher (1970).

In 1976 Jonsson, Skovgaard and Brink-Kjaer discussed diffraction and refraction as separate phenomena and compared the two theories for a circular island surrounded by a parabolic shoal. Provis (1976) conducted an experimental study of island diffraction which showed that Keller's geometrical optics theory (see later) is not complete enough to describe the phenomena observed. Roseau (1976) examined the scattering caused by a wedge in a rotating ocean. Note that his analysis is not valid for a wedge in a non-rotating ocean.

In a continuation of the work done by Longuet-Higgins and Summerfield, Losano and Meyer (1976) showed that some trapped waves demonstrate exponentially small leakage properties, which means that these modes are highly resonant. They gave examples of edge waves of large radial wavenumber, which had this characteristic using a circular island geometry. As an extension, Meyer and Painter (1979) allowed absorption at the shore instead of the perfect reflection condition used in the first paper. While some elements of the response changed because of this boundary condition it was found that the peak amplitude remained high. Meyer (1979) has also written a review article on the theory of wave refraction

which, using a geometrical optics approach, covered simple ray theory, resonant wave trapping and extensions for caustics. This latter topic was also examined by Shen and Keller (1975). In another paper (1980) Meyer has studied reflection coefficients from the reflection of waves incident on a continuous sloping bottom.

In 1977 Pite introduced damping into a discussion of waves diffracted over a circular sill. Dotsenko and Cherkesov (1979) have looked at an asymptotic solution for diffraction over small irregularities. In the same year, Kriegsmann (1979) used geometrical optics on a topography described by a quartic equation - this was unsuccessful to some degree because of the prediction of infinite amplitude at the shore. Non-linear wave diffraction has been examined by Hunt and Baddour (1981), using asymptotic expansions, while Möhring (1982) has considered extremely slender body theory.

A worker prominent in the field of slender body diffraction in recent years is Mei. Originally interested in elastic scattering (1979), he has since used the parabolic approximation to solve diffraction problems in a fluid mechanics context. In collaboration with Tuck (1980), scattering by thin bodies was investigated leading to the conclusion that strong resonances occur over sills. With Yue (1980), Stokes waves were considered as incident waves rather than simple time-harmonic surface waves, while Haren and Mei (1981) look at diffraction by a slender raft. All of these papers use the parabolic approximation, which will be discussed in the next section.

Throughout the discussion above the theory of geometrical optics has been cited. This theory, mainly used in electromagnetic

problems, is useful in the applications of interest here but will not be discussed. For an account of the theory see Keller (1962) who summarizes the method, as formulated up to then. While further refinement is always occurring, the basic ideas of Keller's theory are presented in the article.

We turn now to the latest numerical approaches to scattering by bodies. An important work in this area is the paper by Houston (1978, see also Houston, Carver and Markle (1977)) in which a hybrid finite element technique is applied to tsunami reception by the Hawaiian Islands. Triangular elements are distributed around the islands in a circular mesh and analytic expressions are used outside this region leading to very fast computations. As agreement between numerical prediction and observed wave heights is good this method is promising. Another method, using finite differences, is that of Bernard and Vastano (1977).

Two papers have used the parabolic approximation in forming numerical solutions. Radder (1979) uses finite differences on a circular shoal, after applying the approximation to the mild slope equation, while Candel (1979) uses a similar numerical scheme in an acoustic problem.

Another approach is that of Berhault (1980), who uses an integro-variational method which he compares to boundary integral and finite element methods. Each method is seen to have advantages under different circumstances.

The field of tsunami research, occasionally mentioned above, is of some interest to scattering problems. Many of the techniques used are found in both fields and a knowledge of work in this area is an advantage in considering diffraction by islands. As a

discussion of this field is beyond the scope of the present thesis the reviews by Hammack (1972), Chen (1976) and Bigg (1979) are noted for the reader's reference.

To conclude this section an interesting application of scattering theory will be considered, namely, the navigational techniques used by Pacific Islanders based on the observing of wave patterns formed by particular islands acting as scatterers. These techniques were observed as early as the last century by the German sea captain Winkler (1899) who discussed the meaning of sea charts, produced by the Marshall Islanders, with the navigators who used them. The effects of scattering of waves driven by the prevailing winds are seen in these charts and were useful for intra-archipelago sailing, though inter-archipelago navigation mostly relied on other techniques such as star fixes. Krieger (1943) found other island groups in Micronesia and Melanesia used similar charts while Arthur (1951) noted the use Maori navigators made of the technique. An interesting account of the modern day revival of the various navigational features of pre-European Pacific exploration can be found in Lewis (1978). This book convincingly shows that these methods are practical and details their zones of use. The wave pattern recognition technique, of immediate interest in the present context, is shown to be a meso-scale rather than a macro-scale navigational aid.

5.2 Problem Formulation

Only the shallow-water wave problem will be formulated here. As the basic equations are similar to those of Part I the application of the theory to other fields may easily be seen by referring to §1.2.

We consider the irrotational time-harmonic motion of an incompressible fluid bounded by a free surface, whose undisturbed level is $z=0$, and horizontal seabeds at $z=-h_1$ in the region R_1 and $z=-h_2$ in the region R_2, as shown in Figure 5.1. The surface connecting the two seabed levels is a vertical cylinder. An incident plane surface wave of wavenumber k_1 and unit amplitude is assumed to be travelling along the x-axis from the left.

As the flow is simple harmonic in time, the problem may be described in terms of a potential $\phi(x,y)$, after removal of the z and time elements as in §1.2. The equations describing the motion are now Helmholtz equations of the form

$$\nabla^2\phi_j(x,y) + k_j^2\phi_j(x,y) = 0 \quad j=1,2, \tag{5.1}$$

where k_j is the wavenumber, and ϕ_j is the potential, for region R_j, with the incident wave denoted by

$$\phi_0(x,y) = e^{ik_1x} \quad . \tag{5.2}$$

In R_1 there is also a scattered wave $\bar{\phi}_1$ which obeys Sommerfeld's radiation condition; that is,

$$\lim_{k_1 r \to \infty} [(k_1 r)^{\frac{1}{2}} (\frac{\partial}{\partial r} - ik_1)\bar{\phi}_1] = 0, \tag{5.3}$$

r being the radial distance from an origin in R_2. The flow field is subject to continuity conditions across C, the contour separating R_1 and R_2, namely,

$$\phi_0 + \bar{\phi}_1 = \phi_1(x,y) = \phi_2(x,y) \quad \text{on} \quad C \tag{5.4}$$

and

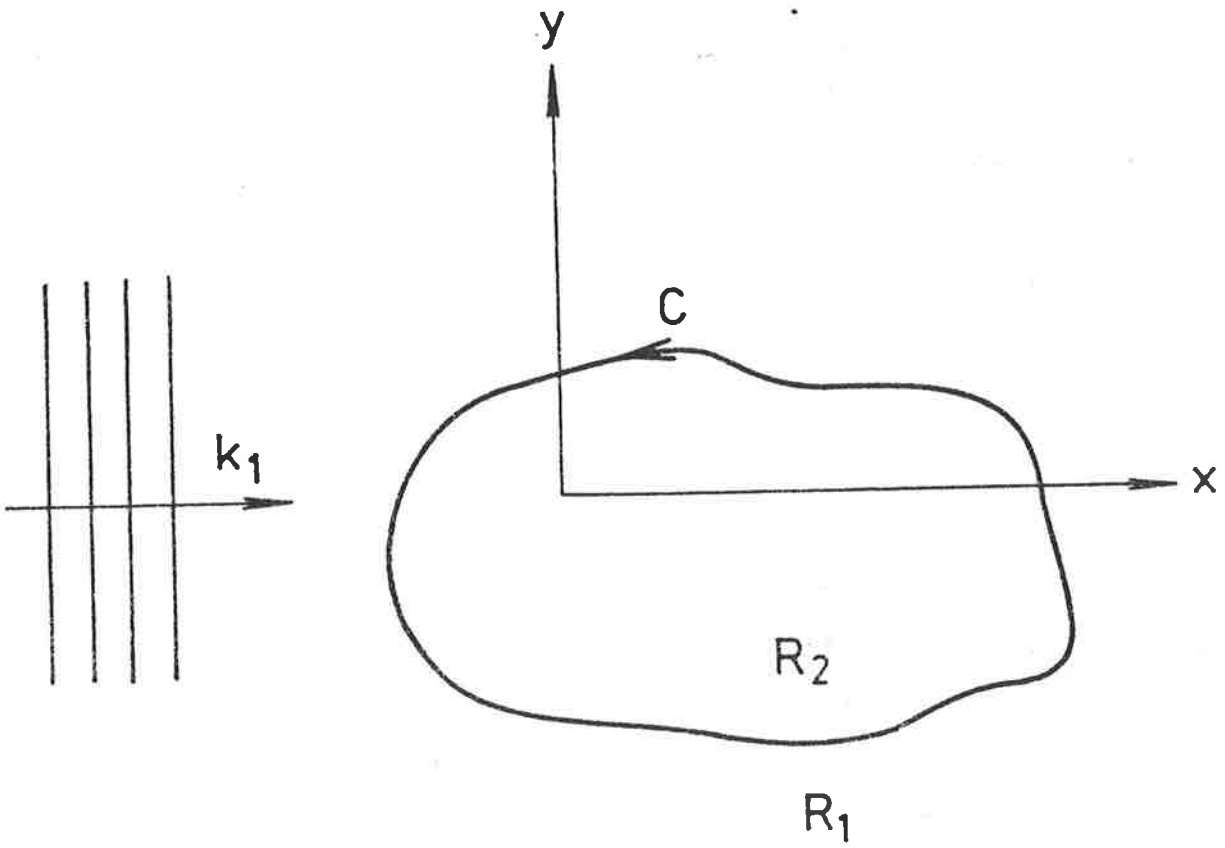

Figure 5.1: Problem formulation.

$$\frac{\partial \phi_1(x,y)}{\partial n} = \left(\frac{k_1}{k_2}\right)^2 \frac{\partial \phi_2(x,y)}{\partial n} \qquad \text{on} \quad C, \tag{5.5}$$

the derivatives in (5.5) being normal derivatives.

Because this thesis is considering shallow-water waves, that is, waves whose wavelength is long in comparison with the depth, then, using Lamb (1932; §228, 229), from equation (1.7) it can be shown that

$$k_2^2 = k_1^2 \frac{h_1}{h_2} . \tag{5.6}$$

Note that if R_2 is a solid body protruding above the sea surface then $k_2 = \infty$.

Having formulated the problem in terms of a potential we will now introduce the parabolic approximation. This essentially says that the amplitude varies slowly in the longitudinal direction as compared to the transverse direction. This disparity of scale leads to a parabolic partial differential equation in which the longitudinal coordinate becomes time-like. Much use has been made of this technique in fields such as underwater acoustics, etc., see for instance McDaniel (1975), Corones (1975), Tappert (1977), Brock, Buchal and Spofford (1977), McCoy (1977) and Kriegsmann and Larsen (1978), as well as in scattering problems, examples of which have already been noted.

If we let

$$\phi_j(x,y) = A^{(j)}(x,y) e^{i k_1 x}, \qquad j=1,2, \tag{5.7}$$

then (5.1) becomes

$$2ik_1 \frac{\partial A^{(1)}}{\partial x} + \nabla^2 A^{(1)} = 0 \quad \text{in} \quad R_1, \tag{5.8a}$$

$$(k_2^2-k_1^2)^2 A^{(2)} + 2ik_1 \frac{\partial A^{(2)}}{\partial x} + \nabla^2 A^{(2)} = 0 \quad \text{in} \quad R_2 \ . \qquad (5.8b)$$

In addition to (5.4) and (5.5) we assume that

$$A^{(1)} \to 1 \quad \text{as} \quad |y| \to \infty \quad \forall x > 0. \qquad (5.9)$$

It will also be assumed that C is symmetric about the x-axis and that it is defined by

$$y = \pm \varepsilon b(x) \ . \qquad (5.10)$$

If R_2 is closed then ε is the width-length ratio of the body and then, for simplicity, we let

$$b(0) = b(1) = 0. \qquad (5.11)$$

If R_2 is not closed we still let $b(0) = 0$.

CHAPTER 6

A CRITICAL ANALYSIS OF THE PARABOLIC APPROXIMATION FOR SCATTERING BY SLENDER TRANSPARENT BODIES

The parabolic approximation theory for scattering by long thin bodies, developed by Mei and Tuck (1980), is analysed critically by both a formal matched asymptotic expansion and a numerical scheme based on the boundary integral equation method of chapter 2. The existence of a special range of parameters, for which the theory is formally valid, is verified, and the use of the parabolic approximation for parameters outside this range is examined. It will be seen that caution must be used in thus employing the parabolic approximation, with breakdown occurring once resonance, or a steep longitudinal gradient in amplitude, appears.

6.1 Formal Asymptotic Theory

As was seen in §5.2, different governing equations are found in R_1 and R_2. The approach to solving the problem here will be to consider separate asymptotic expansions in ε, in R_1 and R_2, and then match them across C. In this theory we will consider R_2 to be a finite closed region, implying that (5.11) is true, and the derivative of the body function $b(x)$ (see (5.10)) will be taken as finite at $x=0$ and $x=1$.

If, in the outer region R_1, we let $x = O(1)$ and, for some positive exponents α,β,γ,

$$\begin{aligned} y &= Y^0\varepsilon^{\gamma} \quad , \\ k_1 &= K\varepsilon^{-\alpha} \quad , \\ A^{(1)}(x,y) &= A_1^0(x,Y^0)+A_2^0(x,Y^0)\varepsilon^{\beta}+A_3^0(x,Y^0)\varepsilon^{2\beta}+\ldots , \end{aligned} \tag{6.1}$$

where

$$A^{(1)}(0,y) = 1 + O(\varepsilon^{\beta}) \quad , \tag{6.2}$$

then (5.8a) gives the leading order outer equation

$$2iK\frac{\partial A_1^0}{\partial x} + \frac{\partial^2 A_1^0}{\partial Y^{0\,2}} = 0 \quad , \tag{6.3}$$

provided

$$\alpha = 2\gamma \quad , \tag{6.4}$$

that is, if $y = O(k_1^{-\frac{1}{2}})$.

Now, examining the inner region R_2, if, for some positive constants δ,μ,

$$\begin{aligned} y &= Y^i \varepsilon \ , \\ h_1/h_2 &= H\varepsilon^{-\delta} \ , \\ A^{(2)}(x,y) &= A_1^i(x,Y^i) + A_2^i(x,Y^i)\varepsilon^{\mu} + A_3^i(x,Y^i)\varepsilon^{2\mu} + \ldots , \end{aligned} \tag{6.5}$$

x being of order unity, then the leading order inner equation from (5.8b) is

$$\frac{\partial^2 A_1^{i\,2}}{\partial Y^{i\,2}} + \bar{k}A_1^i = 0, \tag{6.6}$$

where

$$\bar{k}^2 = \begin{cases} K^2H & 2\alpha+\delta = 2, \quad \delta > 0 & (6.7a) \\ K^2(H-1) & \alpha = 1 \ , \quad \delta = 0 & (6.7b) \\ -K^2 & \alpha = 1 \ , \quad \delta < 0 \ . & (6.7c) \end{cases}$$

The three separate cases in (6.7) correspond to scattering by (a) prominent sills, (b) small sills or shallow canyons, and (c) deep canyons, respectively. It is of use to note that (6.7) implies $\alpha \leqslant 1$ for all δ.

To remove the single degree of freedom δ in the exponents for first order sill scattering, β and μ not appearing in the

leading order equations, and to investigate the canyon further, the matching conditions (5.4) and (5.5) need to be invoked. To do this, (6.3) and (6.6) must be solved in the appropriate regions.

In R_1, due to the redefining of variables in (6.1), the inner region R_2 appears as a line of unit length on the x-axis. The solution of (6.3), with this boundary, is

$$A_1^0(x,Y^0) = 1 - \frac{1+i}{2\sqrt{\pi K}} \int_0^x \frac{d\xi V(\xi)\exp(iKY^{0\,2}/2(x-\xi))}{(x-\xi)^{\frac{1}{2}}}, \qquad (6.8)$$

where

$$V(x) = \frac{\partial A_1^0}{\partial Y^0}(x,0_+) \qquad 0 < x < 1, \qquad (6.9)$$

because the problem is analogous to heat conduction in a semi-infinite rod with time-varying flux at the end $Y^0=0$. For details of the derivation see Appendix IIA; note that the x-coordinate is time-like in this interpretation. For matching purposes the small Y^0 limit of (6.8) is required, that is, from Appendix IIA,

$$A_1^0(x,Y^0) \to A(x) + V(x)|Y^0| + \mathcal{O}(Y^{0\,2}), \quad Y^0 \to 0 \qquad (6.10)$$

where

$$A(x) = 1 - \frac{1+i}{2\sqrt{\pi K}} \int_0^x d\xi V(\xi)(x-\xi)^{-\frac{1}{2}}. \qquad (6.11)$$

In R_2, equation (6.6) has the solution

$$A_1^i(x,Y^i) = a(x)\cos(\bar{k}Y^i), \qquad (6.12)$$

where $a(x)$ is, as yet, unknown.

On C the stretched y-coordinates have the values

$$\begin{aligned} Y^0 &= \pm\varepsilon^{1-\frac{\alpha}{2}} b(x) \\ Y^i &= \pm b(x), \end{aligned} \qquad (6.13)$$

so the continuity of potential condition (5.4) implies that

$$A(x) = a(x)\cos(\bar{k}b(x)) \ , \tag{6.14}$$

to leading order. The flux continuity condition (5.5) may be rewritten as

$$H\varepsilon^{-\delta}\left[\frac{\partial A^{(1)}(x,y)}{\partial Y^0}\varepsilon^{-\frac{\alpha}{2}} - \varepsilon b'(x)\left(iK\varepsilon^{-\alpha}A^{(1)}(x,y) + \frac{\partial A^{(1)}(x,y)}{\partial x}\right)\right]$$

$$= \varepsilon^{-1}\frac{\partial A^{(2)}(x,y)}{\partial Y^1} - \varepsilon b'(x)\left(iK\varepsilon^{-\alpha}A^{(2)}(x,y) + \frac{\partial A^{(2)}(x,y)}{\partial x}\right) \ , \tag{6.15}$$

where y is given by (5.10). Using the expansions (6.1c), (6.5c), (6.10) and (6.13) the leading order term of (6.15) is

$$HV(x) = -\bar{k}a(x)\sin(\bar{k}b(x)), \tag{6.16}$$

provided

$$\alpha + 2\delta = 2. \tag{6.17}$$

Assuming (6.17) is obeyed, (6.14) and (6.16) can be combined to give an integral equation for $V(x)$, namely,

$$A(x) = -\frac{H}{\bar{k}}V(x)\cot(\bar{k}b(x)) \ , \tag{6.18}$$

$A(x)$ being given in terms of $V(x)$ by (6.11). This is an Abel singular integral equation and may be solved by trapezoidal techniques outlined in §6.3.

Having obtained a leading order solution, (6.18) in conjunction with (6.10) and (6.12), it remains to be seen what effect the condition (6.17) has on the region of validity of the theory, in terms of the parameters h_1/h_2 and k_1. Firstly, for prominent sills (6.7a) also needs to be obeyed. Combining (6.7a) and (6.17) we find that $\alpha = \beta = \frac{2}{3}$, which verifies the

importance of the "special class of 'barely-submerged' islands" discussed in Mei and Tuck (1980; §4). A cursory glance at the remaining conditions (b) and (c) of (6.7), relating to canyons, shows their incompatibility with (6.17). Hence the parabolic approximation theory is *not formally valid for canyons* and it appears that it should only be used for barely-submerged sill geometries with the parameters

$$k_1 = \frac{h_1}{h_2} = O(\varepsilon^{-\frac{2}{3}}) \ . \qquad (6.19)$$

In practise the region of validity is larger than that described by (6.19). The reasons for this, as well as some explanation for the restricted validity, will be given in §6.3 from comparison with the results of the numerical model to be outlined in the next section.

6.2 Numerical Methods

This section will set out the solution of the singular integral equation (6.18) by numerical means, as in Mei and Tuck (1980), and also the scheme for direct solution of the scattering problem by a boundary integral technique. As the details of this latter approach have been given in chapter 2, here the problem will merely be set up.

We firstly consider the solution of (6.18). The technique used is described in depth in Weiss (1972), see also Tuck (1978). A summary only of the method will be given.

The interval over which we integrate, $(0,x)$ in this case, is divided into N segments of uniform size Δx. In each segment our unknown function $V(\xi)$ is assumed to vary linearly with ξ.

Then, from Weiss (1972; §4), the following lower triangular system for V at the end of each interval, V_n, $n=1,\ldots,N$, is found:

$$V_n = [-1+\mu\bar{W}_n V_0+\mu \sum_{j=1}^{n-1} V_j W_{n-j}]/[\frac{H}{\bar{k}}\cot(\bar{k}b_n)-\mu W_0] \qquad (6.20)$$

where

$$\mu = \frac{1+i}{2}\sqrt{\frac{\Delta x}{\pi K}} \quad , \qquad (6.21)$$

$V_n = V(n\Delta x)$, $x = n\Delta x$, $b_n = b(n\Delta x)$ and

$$W_0 = \frac{4}{3} \quad ,$$

$$W_j = \frac{4}{3}[(j+1)^{3/2}-2j^{3/2}+(j-1)^{3/2}] \qquad j=1,2,\ldots,n-1 \qquad (6.22)$$

$$\bar{W}_n = 2n^{1/2}-\frac{4}{3}[n^{3/2}-(n-1)^{3/2}], \qquad n=1,2,3,\ldots,N.$$

For the starting value V_0 we let $V(x)$ decay as x approaches zero so as to balance the cotangent in (6.18), that is,

$$\lim_{x\to 0} V(x)\cot(\bar{k}b(x)) = -\frac{\bar{k}}{\bar{H}} \quad . \qquad (6.23)$$

This results in

$$V_0 = 0, \qquad (6.24)$$

which means that (6.20) may be rewritten as

$$V_n = [-1+\mu \sum_{j=1}^{n-1} V_j W_{n-j}]/[\frac{H}{\bar{k}}\cot(\bar{k}b_n)-\mu W_0] \qquad n=1,\ldots,N. \qquad (6.25)$$

Note that if $V(x)$ is three times differentiable and $V'''(x)$ is bounded then, from Weiss (1972; theorem 4.1), this method is convergent of order two.

The technique outlined above has been thoroughly tested by Weiss and Mei and Tuck (1980) so (6.25) will be used without further

comment, other than to note that the term $-\mu W_0$ in the denominator acts as a damping term and stops infinite amplitude at resonance points.

We now turn to the boundary integral equation solution to (5.1). This technique expresses the potential in the two regions R_1 and R_2 by the integral equations

$$\bar{\phi}_1(\underset{\sim}{x}) = -\int_c \left(\bar{\phi}_1(\underset{\sim}{x}')\frac{\partial G_1(\underset{\sim}{x}';\underset{\sim}{x})}{\partial n} - G_1(\underset{\sim}{x}';\underset{\sim}{x})\frac{\partial \bar{\phi}_1(\underset{\sim}{x}')}{\partial n}\right) d\ell(\underset{\sim}{x}') \quad \underset{\sim}{x} \in \{R_1\text{-}C\} \quad (6.26a)$$

$$\phi_2(\underset{\sim}{x}) = \int_c \left(\phi_2(\underset{\sim}{x}')\frac{\partial G_2(\underset{\sim}{x}';\underset{\sim}{x})}{\partial n} - G_2(\underset{\sim}{x}';\underset{\sim}{x})\frac{\partial \phi_2(\underset{\sim}{x}')}{\partial n}\right) d\ell(\underset{\sim}{x}') \quad \underset{\sim}{x} \in \{R_2\text{-}C\}, \quad (6.26b)$$

where $\partial/\partial n$ is the outward normal derivative and G_1, G_2 are the Green's functions

$$\begin{aligned} G_1(\underset{\sim}{x}';\underset{\sim}{x}) &= -\frac{i}{4}H_0^{(1)}(k_1 r') \\ G_2(\underset{\sim}{x}';\underset{\sim}{x}) &= \frac{1}{4}Y_0(k_2 r') \ , \end{aligned} \qquad (6.27)$$

the notation being as in chapter 2.

For the potential on C the limiting process indicated in chapter 2 is used, multiplying the integrals in (6.26) by two, and altering them to their Cauchy principal-value form, denoted $\int$. The continuity conditions (5.4) and (5.5) are then used to find ϕ at any point on C.

To do this in practice the integrals must be discretized into N segments, as in equation (2.12), by considering ϕ and its derivative to be constant on a given segment and representable by their values at the segment's midpoint. Then, by writing the discretized integral equations as two matrix equations and using the continuity conditions, the potential may be rewritten as

$$\Psi_1 = -[E(A-I) - B(F-I)]^{-1} f, \tag{6.28}$$

where I is the $N\times N$ identity matrix,

$$\begin{aligned}
[\Psi_1]_j &= \bar{\phi}_1(\underset{\sim}{x}_j), \\
[A]_{j\,m} &= \frac{i}{2}\int_{\Delta\ell_m} \frac{\partial}{\partial n} H_0^{(1)}(k_1 r_j')\, d\ell(\underset{\sim}{x}'), \\
[B]_{j\,m} &= \frac{i}{2}\int_{\Delta\ell_m} H_0^{(1)}(k_1 r_j')\, d\ell(\underset{\sim}{x}'), \\
& \qquad\qquad j=1,\ldots,N;\ m=1,\ldots,N \qquad (6.29)\\
[E]_{j\,m} &= \frac{k_2^2}{2k_1^2}\int_{\Delta\ell_m} Y_0(k_2 r_j')\, d\ell(\underset{\sim}{x}'), \\
[F]_{j\,m} &= \frac{1}{2}\int_{\Delta\ell_m} \frac{\partial}{\partial n} Y_0(k_2 r_j')\, d\ell(\underset{\sim}{x}'), \\
[f]_j &= -(F-I)g + ik\, En_a .
\end{aligned}$$

The two vectors g, n_a are given by

$$\begin{aligned}
[g]_j &= e^{i k_1 x_j}, \\
& \qquad\qquad j=1,\ldots,N, \qquad (6.30)\\
[n_a]_j &= [n_x]_j\, [g]_j ,
\end{aligned}$$

where $\underset{\sim}{x}_j = (x_j, y_j)$ is the midpoint of the jth segment and n_x is the vector of the x-components of the normal at each segment's midpoint, and

$$r_j' = |\underset{\sim}{x}_j - \underset{\sim}{x}'|. \tag{6.31}$$

For this method to work the matrix $[E(A-I)-B(F-I)]$ must be non-singular.

To evaluate the integrals in (6.29) the numerical and analytic techniques outlined in §2.3 are used.

It is also required that the value of the potential be known at locations other than on C and to do this we discretize (6.26). This discretization is simpler as, knowing ϕ on C, only one of the expressions in (6.26) needs to be used for a given region;

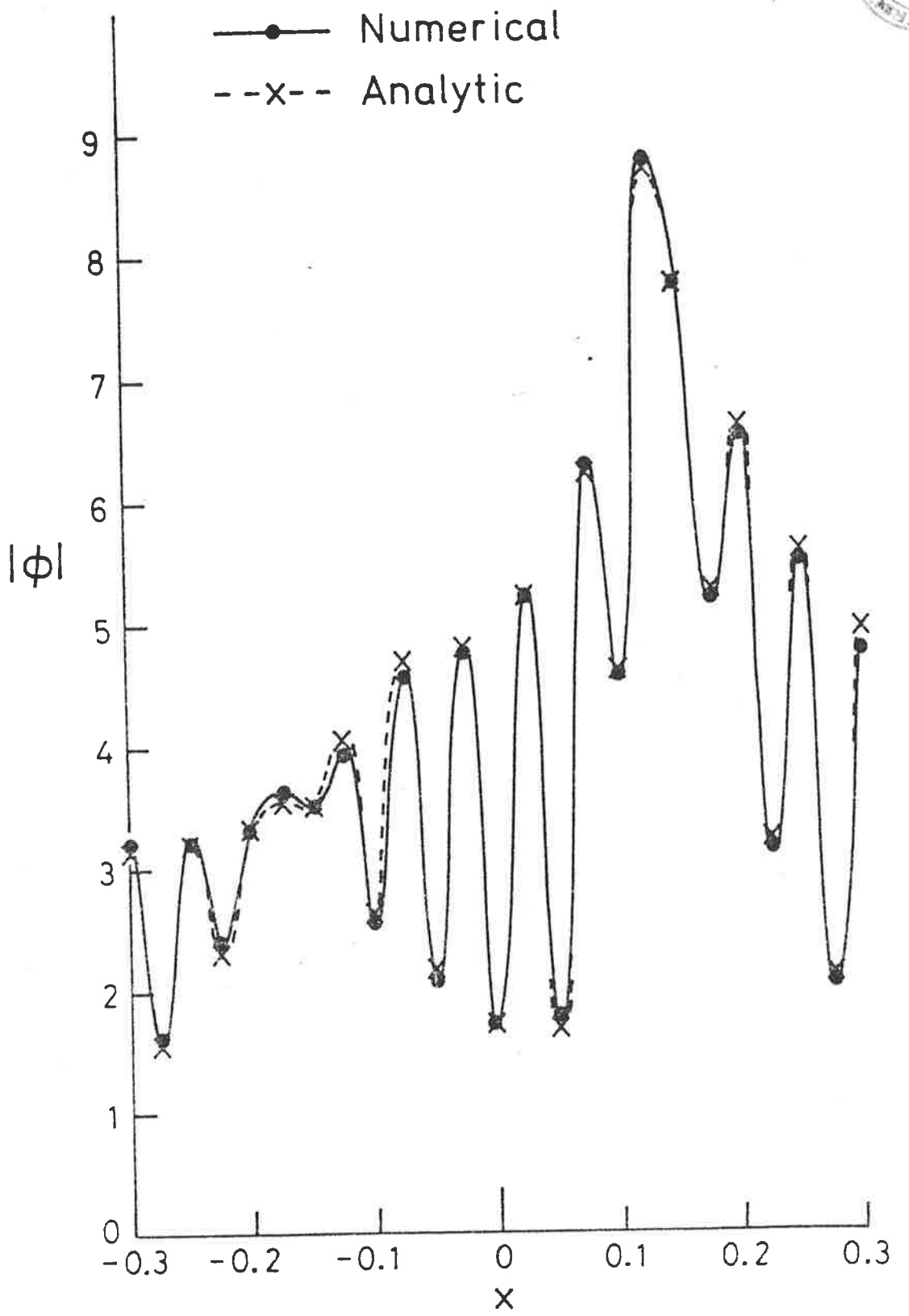

Figure 6.1: $|\phi|$ on centreline of circle of radius 0.325, $k_1 = 20$, $k_2 = 60$ (N=76).

also the integrals are easier to compute; see §2.4.

This numerical method, used only for contours symmetric about the x-axis thus reducing the size of the matrices in (6.28) by half, was tested on circular sills and canyons of various radii, because of the existence, for this geometry, of analytic solutions in terms of series of Bessel functions (see Appendix IIB and Longuet-Higgins (1967)). The agreement, with 10-15 segments per outer (k_1) wavelength, both inside the circle, where the amplitude is very oscillatory as in Figure 6.1, and on the boundary, was excellent. That is, no detectable difference between the numerical and series plots could be observed, except for some minor divergence on some of the internal amplitude peaks. This, of course, only applies for $k_1 \lesssim 30$, as for shorter waves a large number of segments were needed and storage problems arose.

From the preceding discussion it is clear that the model is reliable and will be of use in examining the validity of the parabolic approximation.

6.3 Comparison of Numerical Results and Parabolic Approximation Theory

Since Mei and Tuck (1980) examined the centreline amplitude of the velocity potential, that will be our basis of comparison. We also employ their example of a parabolic arc contour for C,

$$y = \pm\varepsilon b(x) = \pm 2\varepsilon x(1-x). \tag{6.32}$$

Note that this biconvex airfoil is not analytic at $x=0,1$, so the numerical method will not be as accurate at the ends as elsewhere. However, the errors involved are only small and local

as the numerical approximation essentially models a slightly different end-shape. This is verifiable by examining elliptic boundaries. It should also be noted that some 20 segments per wavelength were needed for 3-figure numerical convergence, due to the slenderness of C.

We first examine biconvex sills. An interesting result of the parabolic approximation theory is that resonance occurs over the sill if, from (6.18),

$$K^2 = \frac{\pi}{2Hb(x)} + n\pi \qquad n=0,1,2,\ldots \; . \tag{6.33}$$

Now, as $K^2 = O(1)$ by assumption, the formal theory implies that only the early stages of resonance can be described. This seems logical in view of the neglect of terms like $\partial A^{(2)}/\partial x$, since at resonance steep longitudinal, as well as transverse, gradients in $A^{(2)}$ are expected. Thus, curves such as those for $k_1 = 10,15$ in Mei and Tuck (1980; Fig. 3) will not be accurate*. This is borne out by the numerical results shown in Figures 6.2-6.4. The first of these shows that for k,h satisfying (6.19), when no resonance is observed, the parabolic approximation is accurate. Resonance, however, is not well described, although, as is evident from Figure 6.3, the position, if not the magnitude, of the first resonance peak is predicted fairly well. In fact the early stages of the bifurcation of this peak are also locationally predicted. For more complex resonance, as in Figure 6.4, even

---

*It should be noted that the legend of Mei and Tuck (1980; Fig. 3) appears to be incorrect. The sill should have parameters $\varepsilon=0.1$, $h_2/h_1=0.1$.

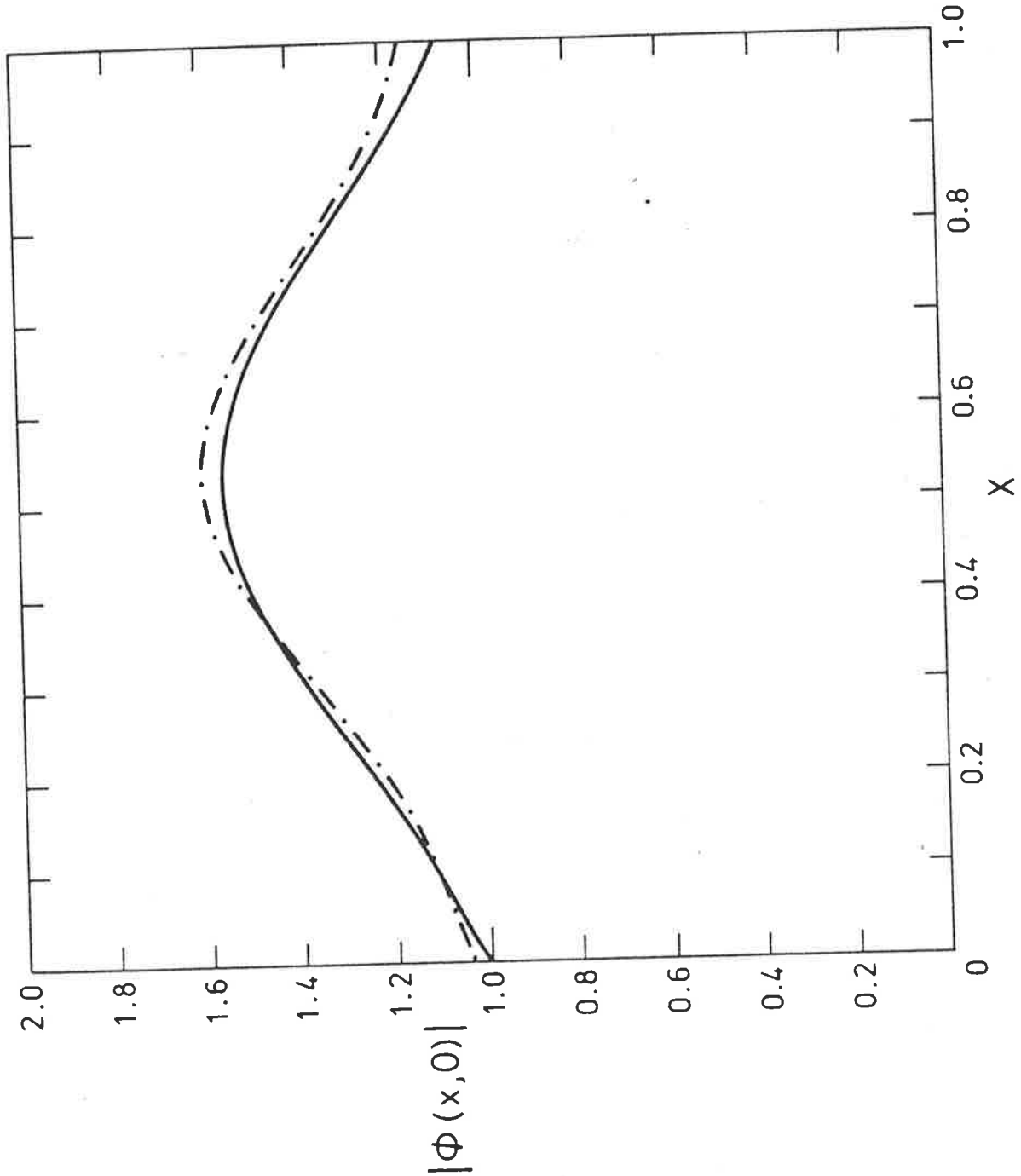

Figure 6.2: Comparison of the parabolic approximation (——) and the b.i.m. results (——·——) for a parabolic sill with parameters $\varepsilon = 0.1$, $k_1 = 5$, $h_1/h_2 = 9$.

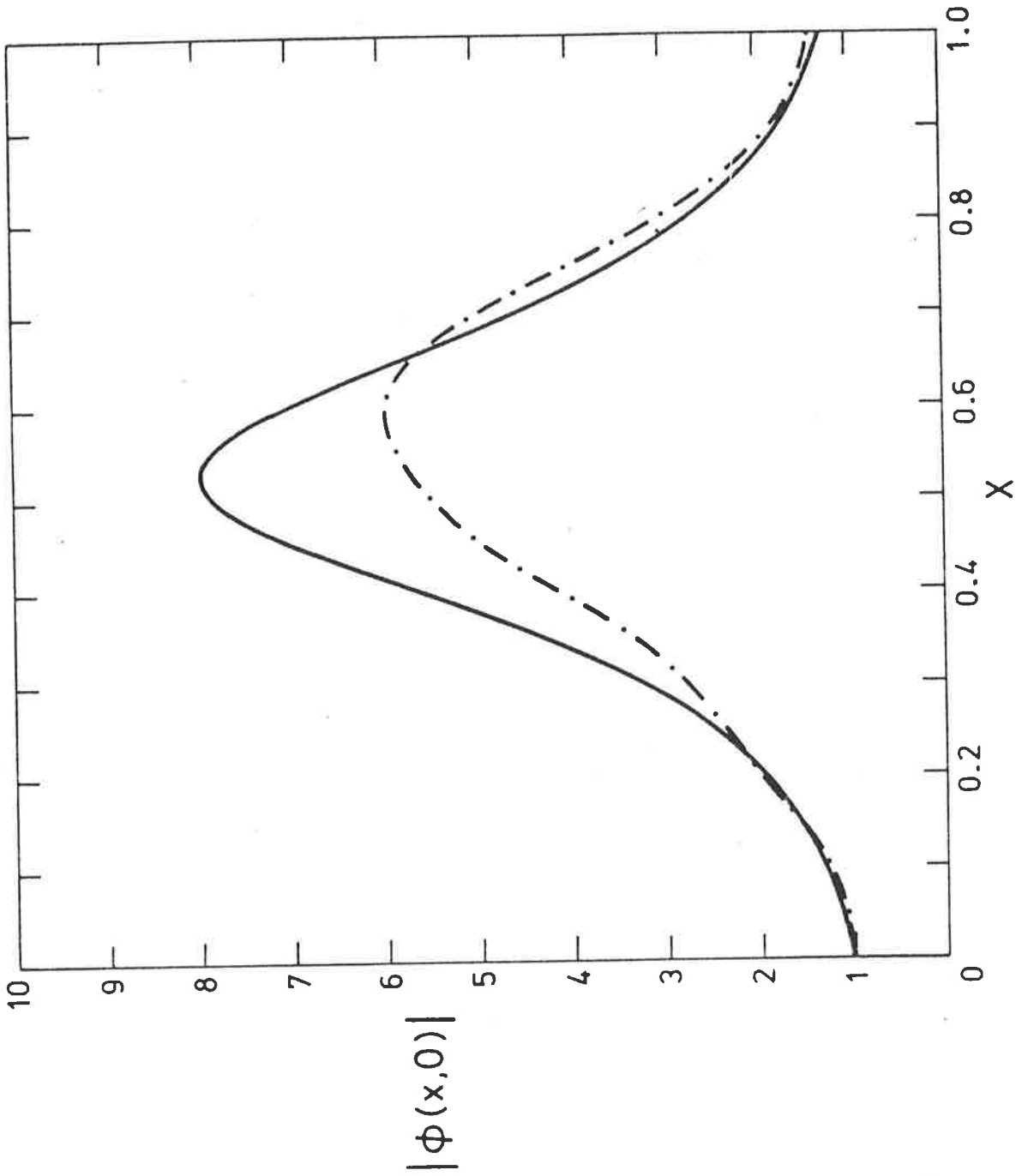

Figure 6.3: Same comparison as Figure 6.2 with new parameters $\varepsilon = 0.1$, $k_1 = 10$, $h_1/h_2 = 9$.

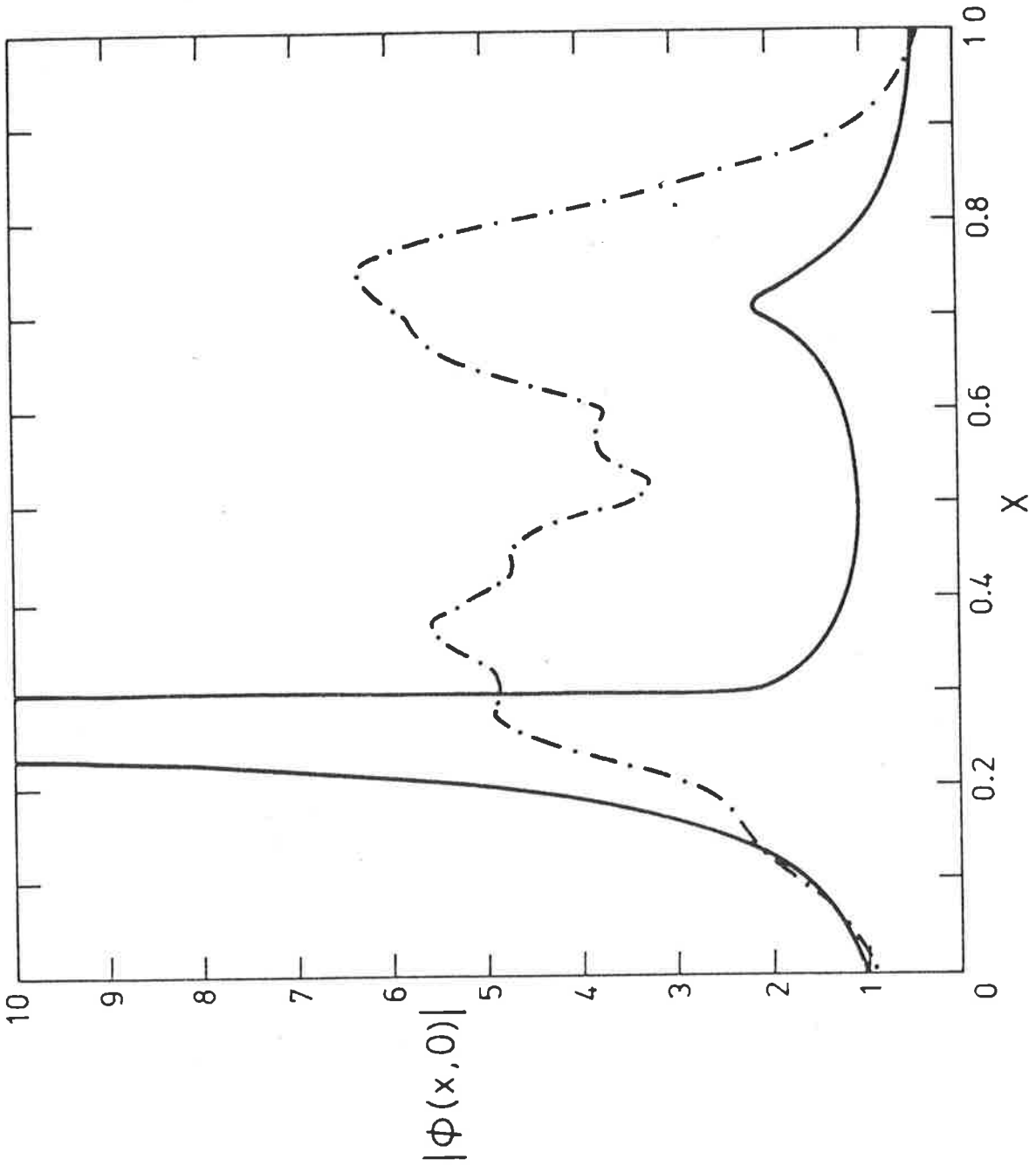

Figure 6.4: Same comparison as Figure 6.2 with new parameters $\varepsilon = 0.1$, $k_1 = 15$, $h_1/h_2 = 9$.

locational accuracy is lost however.

Turning our attention to canyons, it will be remembered that the theory of §6.1 predicted that the parabolic approximation is never valid. The veracity of this conclusion is confirmed in Figures 6.5 and 6.6. Once again a major reason why the parabolic approximation does not work well is that it predicts significant longitudinal $A^{(2)}$ gradients near the leading edge, while not including these terms in the theory. Also, the assumption that $|\phi| = O(1)$ at $x=0$ is not valid, especially with increasing canyon depth, as shown in Figure 6.6. The scattering cross-section for this case, Figure 6.7, reveals that the incident wave suffered significant side scattering as well as forward scattering, with the peak scatter occurring at an angle of 25° from the positive x-axis. This result is contrary to the parabolic approximation which assumes that scattering is predominantly *forward* directed. In Appendix IIC will be found a discussion of how the scattering cross-section is obtained from the boundary integral equation solution.

Figure 6.8 summarizes the conclusions concerning the "region of validity" of the parabolic approximation. This figure shows the parameter range (enclosed by a solid line) in which the parabolic approximation theory predicts an absolute error smaller than $\sim$10% of the total amplitude along the centreline of the submarine feature. Note that this is somewhat deceptive, as the area close to the H-axis has a *relative* error in the predicted disturbance much greater than 10%. However, because the amplitude is almost uniformly unity in the cases represented by this region, this

Figure 6.5: Comparison of the parabolic approximation (——) and the b.i.m. results (——·——) for a parabolic canyon with parameters $\varepsilon=0.1$, $k_1=20$, $h_1/h_2=0.5$.

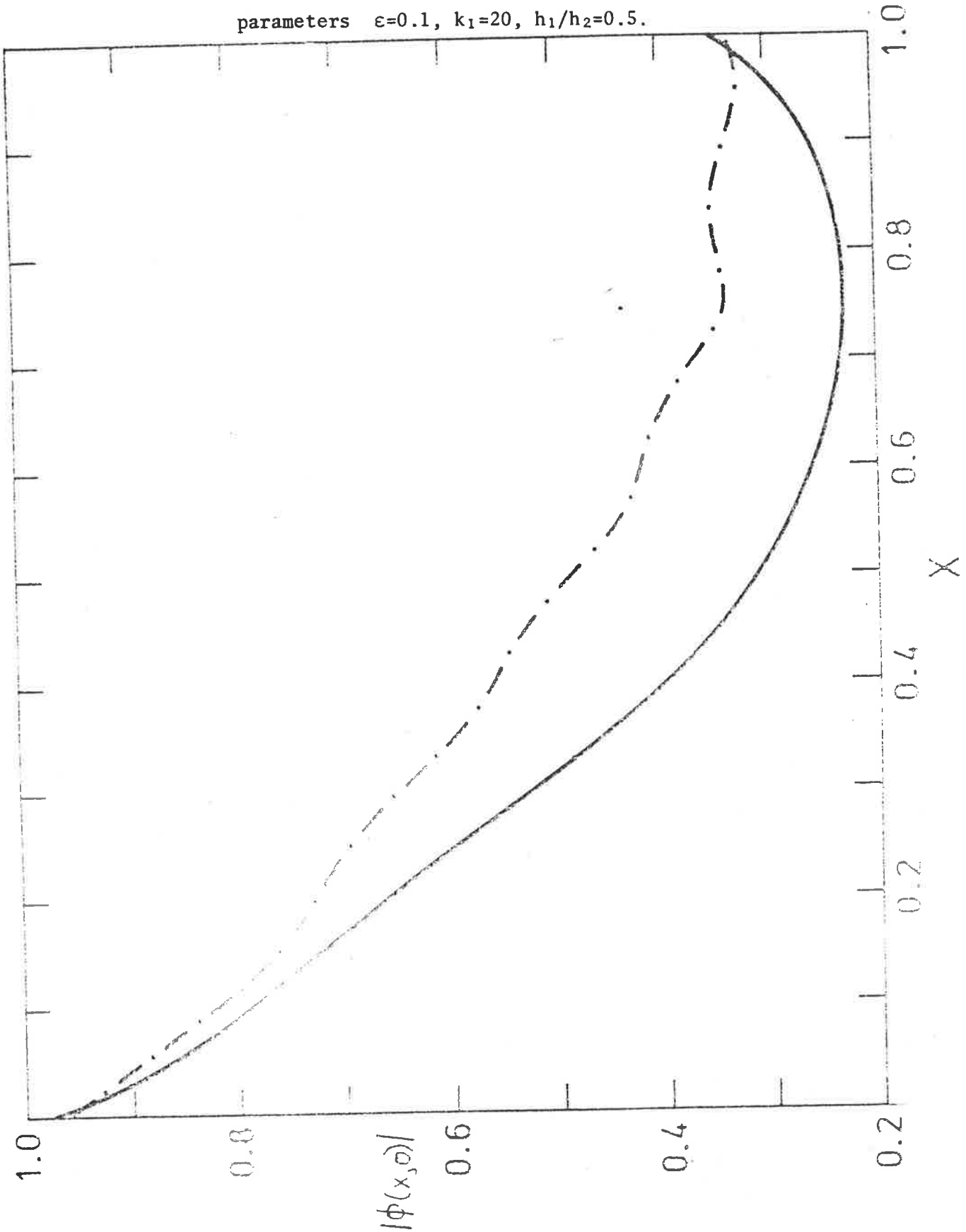

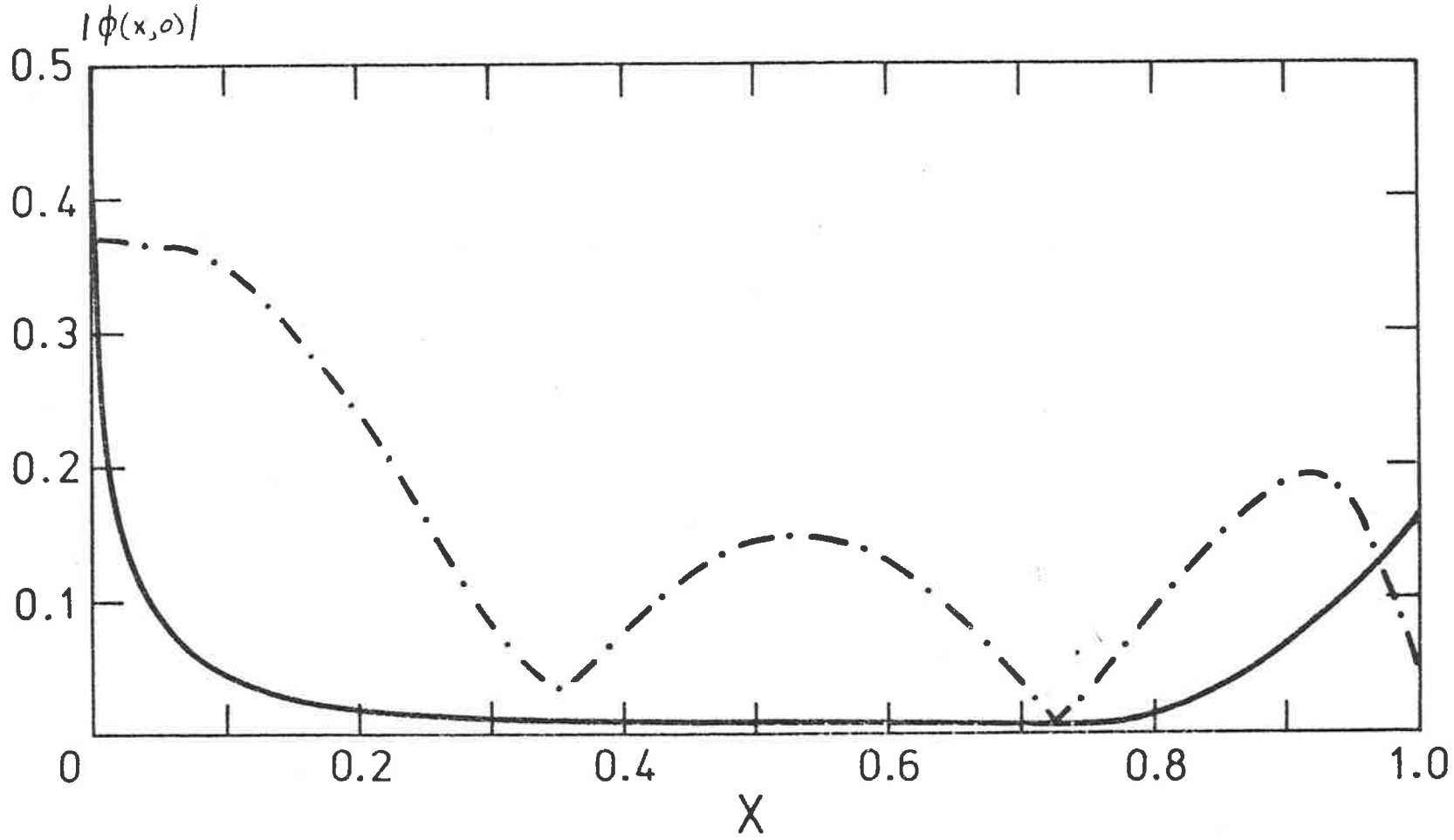

Figure 6.6: Same comparison as Figure 6.5 with new parameters $\varepsilon=0.1$, $k_1=20$, $h_1/h_2=0.025$.

Figure 6.7: Scattering cross-section for parabolic canyon with $\epsilon=0.1$, $k_1=20$, $k_2=\pi$.

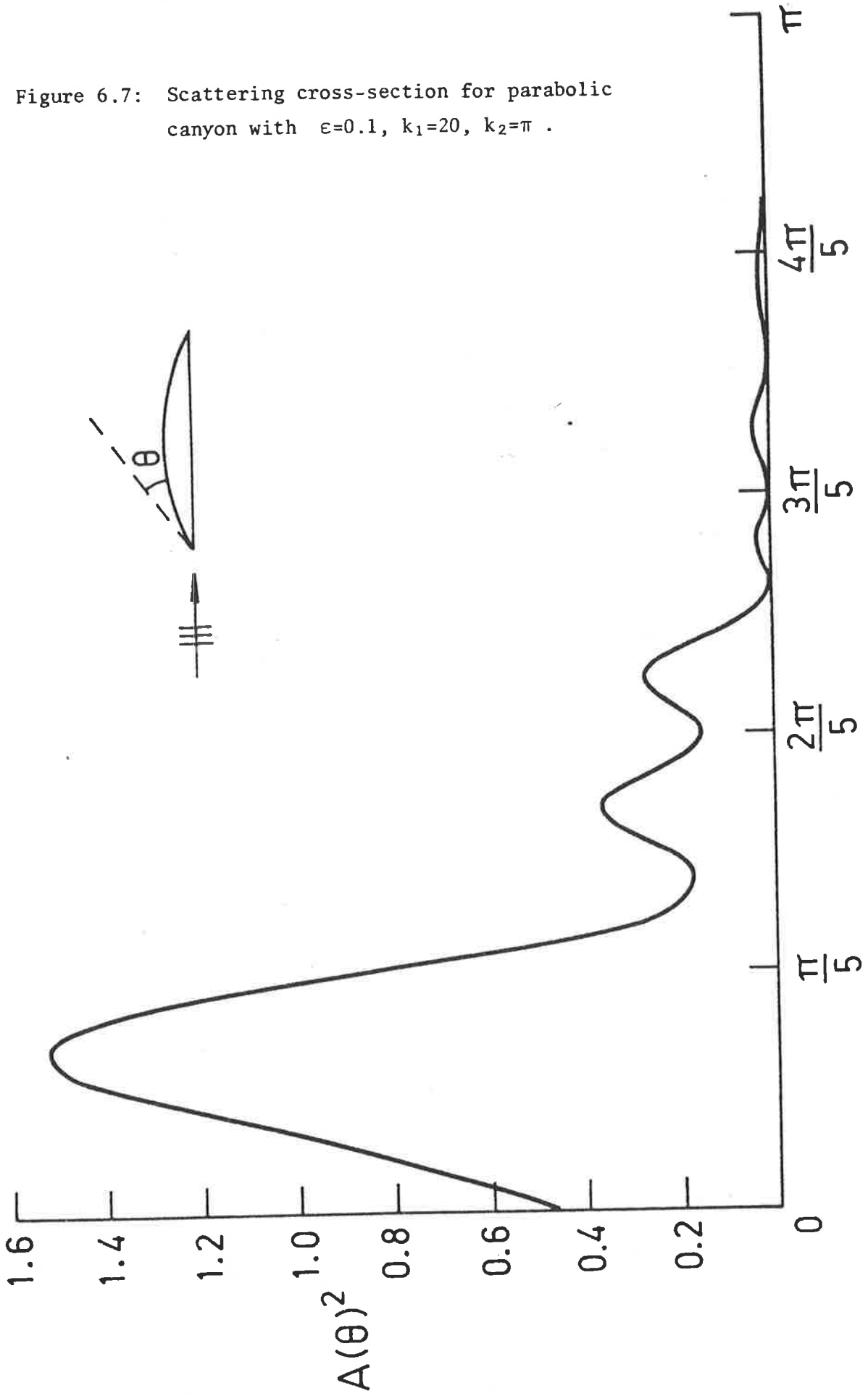

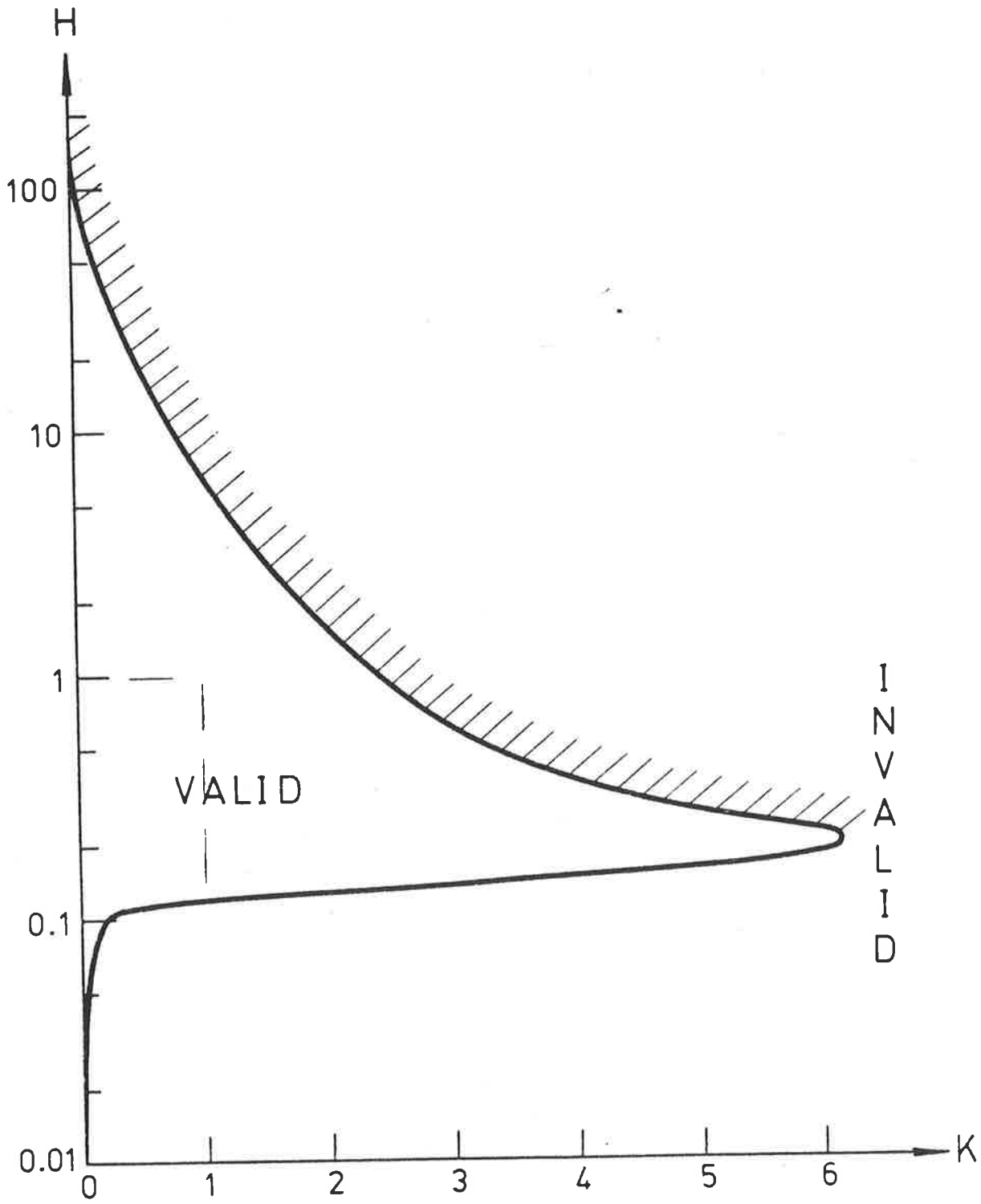

Figure 6.8: Region of validity of parabolic approximation in terms of $H = h_1\varepsilon^{2/3}/h_2$ and $K = k_1\varepsilon^{2/3}$. See text for explanation.

difference is not noticeable on any but a greatly magnified plot.

This figure, compiled from 43 parameter combinations with ε in the range $[0.05, 0.2]$, is only for a biconvex contour, but similar plots would be found for other boundaries. It indicates that the region defined by (6.19), whose approximate boundary is dashed, is the heart of the range of validity. In addition, the figure indicates that so long as resonance or steep gradients do not occur, the theory is useful. Thus, the spike along $H \simeq 0.2$ represents features where $h_1 \approx h_2$ and the resultant disturbance is small. Similarly, the graph asymptotes to the H axis as $k_1 \to 0$, for in this limit both the island and infinitely deep canyon problems have no disturbance. The other feature of this figure is the (striped) region which shows where resonance begins for sill scatterers. In this region, as shown above, the position, but not the magnitude, of resonance is well predicted.

It is also interesting to note that this figure suggests that scattering by islands does not obey the parabolic approximation, except in the degenerate case of $k_1 = 0$, this problem being described by the graph as $H \to \infty$. As will be shown in chapter 7, this suggestion is *not* correct for a range of non-trivial k_1.

CHAPTER 7

THE PARABOLIC APPROXIMATION FOR SCATTERING BY SLENDER OPAQUE BODIES

The parabolic approximation theory developed in the last chapter is here applied to the near-field of scattering by islands. It is shown that for a certain parameter range the theory compares well with numerical results computed using an adaptation of the b.i.e. method of §6.2. The theory is extended to second order. In addition to the situation when $b'(0)$ is finite the effect of letting this derivative be infinite will be examined.

7.1 Leading Order Theory

The near-field of the island described by (5.10) will be considered to consist of two regions, an inner space very close to the boundary of the obstruction and an outer region. The solution to (5.8a) will be examined in the two regions and matched across the undetermined boundary separating them. It will be assumed that

$$k = K\varepsilon^{-\alpha}, \quad 0 < \alpha < 2. \tag{7.1}$$

Note that in this theory the derivative of the body function $b(x)$ will be taken as finite at $x=0$ and $x=1$, the ends of the finite island.

If, in the outer region, we let $x = O(1)$ and, for some positive exponents γ,δ

$$\begin{aligned} y &= Y^0\varepsilon^{\gamma} \qquad 0 < \gamma < 1 \\ A^0 &= 1 + \varepsilon^{\delta}A_1^0(x,Y^0) + \varepsilon^{2\delta}A_2^0(x,Y^0) + \ldots \end{aligned} \tag{7.2}$$

then (5.8a) gives the leading order equation

$$2iK\frac{\partial A_1^0}{\partial x} + \frac{\partial^2 A^0}{\partial Y^{0\,2}} = 0, \tag{7.3}$$

if

$$\alpha = 2\gamma, \quad \alpha > \delta, \tag{7.4}$$

and the second order equation

$$2iK\frac{\partial A_2^0}{\partial x} + \frac{\partial^2 A_2^0}{\partial Y^{0\,2}} = 0. \tag{7.5}$$

Thus, from Appendix IIA, the outer solution is

$$A^0 = 1 - \frac{(1+i)}{2\sqrt{\pi K}} \sum_{\ell=1}^{2} \varepsilon^{\ell\delta} \int_0^x \frac{d\xi V_\ell(\xi) e^{i KY^{0\,2}/2(x-\xi)}}{\sqrt{x-\xi}} + O(\varepsilon^{3\delta}), \tag{7.6}$$

which has the limit as $Y^0 \to 0$ of

$$A^0 = 1 + \sum_{\ell=1}^{2} \varepsilon^{\ell\delta}(A_\ell(x) + Y^0 V_\ell(x)) + (\varepsilon^{3\delta}), \tag{7.7}$$

where

$$A_\ell(x) = -\frac{(1+i)}{2\sqrt{\pi K}} \int_0^x \frac{d\xi V_\ell(\xi)}{\sqrt{x-\xi}}, \qquad \ell=1,2. \tag{7.8}$$

In the inner region, let

$$\begin{aligned} y &= Y^i \varepsilon \\ A^i &= 1 + \varepsilon^{\beta} A_1^i(x,Y^i) + \varepsilon^{2\beta} A_2^i(x,Y^i) + \ldots \end{aligned} \tag{7.9}$$

so that the leading order equation to (5.8a) is

$$\frac{\partial^2 A_1^i}{\partial Y^{i\,2}} = 0 \tag{7.10}$$

and, if

$$\alpha + \beta < 2, \tag{7.11}$$

the second order equation is

$$\frac{\partial^2 A_2^i}{\partial Y^{i\,2}} = 0 \ . \qquad (7.12)$$

Equations (7.10) and (7.12) give the solutions

$$\begin{aligned} A_1^i &= a_1(x)Y^i + a_2(x) \\ A_2^i &= a_3(x)Y^i + a_4(x) \ , \end{aligned} \qquad (7.13)$$

the functions $a_i(x)$ to be specified later.

To perform the matching some of the $a_i(x)$ in (7.13) need to be determined from the boundary condition

$$\frac{\partial A}{\partial Y} = \varepsilon b'(x)(ikA + A_x) \qquad y = \varepsilon b(x), \qquad (7.14)$$

so, substituting (7.9) into (7.14),

$$\frac{\partial A_1^i}{\partial Y^i}(x, b(x)) = 0 \qquad (7.15)$$

is obtained as the boundary condition compatible with (7.10) and, if

$$2\beta + \alpha = 2, \qquad (7.16)$$

the second order boundary condition becomes

$$\frac{\partial A_2^i}{\partial Y^i}(x, b(x)) = iKb'(x) \ . \qquad (7.17)$$

Equations (7.15) and (7.17) imply that

$$\begin{aligned} a_1(x) &= 0 \\ a_3(x) &= iKb'(x) \ , \end{aligned} \qquad (7.18)$$

so the inner expansion may be written

$$A^i = 1 + \varepsilon^{\beta} a_2(x) + \varepsilon^{2\beta}(a_4(x) + iKb'(x)Y^i) + O(\varepsilon^{3\beta}). \qquad (7.19)$$

We now turn to the matching of the inner and outer solutions. Comparing (7.7) and (7.19), noting that $\beta = \delta$, it is seen that

$$a_2(x) = A_1(x)$$
$$a_4(x) = A_2(x) \qquad (7.20)$$
$$V_1(x) = iKb'(x).$$

Therefore to leading order the inner solution is

$$A^i = 1 - \frac{(i-1)}{2}\sqrt{\frac{K}{\pi}}\,\varepsilon^{1-\alpha/2}\int_0^x \frac{d\xi b'(\xi)}{\sqrt{x-\xi}} + O(\varepsilon^{2-\alpha}) \qquad (7.21)$$

and the outer solution is

$$A^0 = 1 - \frac{(i-1)}{2}\sqrt{\frac{K}{\pi}}\,\varepsilon^{1-\alpha/2}\int_0^x \frac{d\xi b'(\xi) e^{iKY^{02}/2(x-\xi)}}{\sqrt{x-\xi}} + O(\varepsilon^{2-\alpha}), \qquad (7.22)$$

if, from (7.1), (7.4) and (7.16),

$$\frac{2}{3} \leqslant \alpha < 2. \qquad (7.23)$$

7.2 Second Order Theory

From comparison of (7.21) with numerical results it was decided to extend this theory to second order to seek a better agreement between the two techniques. These comparisons will be shown in a later section. In the present discussion the second order theory will be presented, to be discussed with reference to the first order solutions and the numerical method in the later section.

There are two ways of approaching this second order theory, leading to solutions valid in different parameter ranges. Firstly, let $\alpha \geqslant 2\beta$, then the third order outer equation is

$$2iK\frac{\partial A_3^0}{\partial x} + \frac{\partial^2 A_3^0}{\partial Y^{02}} = 0, \qquad (7.24)$$

so that, using Appendix IIA, the inner expansion of the outer solution is now

$$A^0 = 1 + \varepsilon^{\beta}(A_1(x) + \varepsilon^{1-\alpha/2}Y^i V_1(x) - iKA_1'(x)\varepsilon^{2-\alpha}Y^{i\,2} + \ldots)$$

$$+ \varepsilon^{2\beta}(A_2(x) + \varepsilon^{1-\alpha/2}V_2(x)Y^i + \ldots) + \varepsilon^{3\beta}(A_3(x) + \ldots) + \ldots . \quad (7.25)$$

Similarly, the third order inner equation is

$$\frac{\partial^2 A_3^i}{\partial Y^{i\,2}} = -2iK\,\frac{\partial A_1^i}{\partial x}\,, \quad (7.26)$$

which has the solution

$$A_3^i = a_6(x) + a_5(x)Y_i - iKA_1'(x)Y_i^2\,. \quad (7.27)$$

From (7.14) the third order boundary condition is

$$\frac{\partial A_3^i}{\partial Y^i}\,(x,b(x)) = iKb'(x)A_1^i(x,b(x))\,, \quad (7.28)$$

which implies that

$$a_5(x) = iK[b'(x)A_1(x) + 2A_1'(x)b(x)]\,. \quad (7.29)$$

Therefore, comparing the inner expansion ((7.19) + (7.27)) with (7.25) it is found that, in addition to (7.20),

$$\begin{aligned} V_2(x) &= iK[b'(x)A_1(x) + 2A_1'(x)b(x)] \\ A_3(x) &= a_6(x)\,. \end{aligned} \quad (7.30)$$

As a result of this matching our second order inner solution is

$$A^i = 1 - \frac{(i-1)\sqrt{K}}{2\sqrt{\pi}}\,\varepsilon^{1-\alpha/2}\int_0^x \frac{d\xi b'(\xi)}{\sqrt{x-\xi}}$$

$$+ \varepsilon^{2-\alpha}\left\{iKb'(x)Y_i - \frac{(i-1)\sqrt{K}}{2\sqrt{\pi}}\int_0^x \frac{d\xi[b'(\xi)A_1(\xi)+2A_1'(\xi)b(\xi)]}{\sqrt{x-\xi}}\right\} + O(\varepsilon^{3-3\alpha/2}), \quad (7.31)$$

while the second order outer solution is

$$A^0 = 1 - \frac{(i-1)\sqrt{K}}{2\sqrt{\pi}}\varepsilon^{1-\alpha/2}\int_0^x \frac{d\xi b'(\xi)e^{iKY^{02}/2(x-\xi)}}{\sqrt{x-\xi}} - \frac{(i-1)\sqrt{K}}{2\sqrt{\pi}}\varepsilon^{2-\alpha}\int_0^x \frac{d\xi[b'(\xi)A_1(\xi)+2A_1'(\xi)b(\xi)]}{\sqrt{x-\xi}} + O(\varepsilon^{3-3\alpha/2}), \tag{7.32}$$

if

$$1 \leqslant \alpha < 2. \tag{7.33}$$

On the other hand, if $\alpha = \beta$ (or $\alpha=2/3$) then the second order outer equation is

$$2iK\frac{\partial A_2^0}{\partial x} + \frac{\partial^2 A_2^0}{\partial Y^{02}} = -\frac{\partial^2 A_1^0}{\partial x^2} \tag{7.34}$$

instead of (7.5). To solve (7.34) a particular integral $P_2(x,Y^0)$ is needed in addition to the complementary function (IIA.13). Using the principle of minimum singularity the Taylor series

$$P_2(x,Y^0) = c_2(x)Y_0^2 + c_3(x)Y_0^3 + \ldots \tag{7.35}$$

was assumed to represent the small Y^0 limit of $P_2(x,Y^0)$. Upon substituting (7.35) into (7.34) it is found that

$$\begin{aligned} c_2(x) &= -\frac{1}{2}A_1''(x) \\ c_3(x) &= -\frac{1}{6}V_2''(x) \end{aligned} \tag{7.36}$$

and that $c_j(x)$, $j > 3$, can be written in terms of lower order c_j. The third order outer equation is now

$$2iK\frac{\partial A_3^0}{\partial x} + \frac{\partial^2 A_3^0}{\partial Y^{02}} = -\frac{\partial^2 A_2^0}{\partial x^2} \tag{7.37}$$

which we will assume has the solution, for small Y^0, of

$$A_3^0(x,Y^0) = A_3(x) + P_3(x,Y^0) + O(Y^0). \tag{7.38}$$

The inner expansion of the outer solution is thus

$$A^0 = 1 + \varepsilon^{\beta}(A_1(x)+\varepsilon^{1-\alpha/2}V_1(x)Y^i - iK\varepsilon^{2-\alpha}A_1'(x)Y^{i\,2}+\ldots)$$
$$+ \varepsilon^{2\beta}(A_2(x)+\varepsilon^{1-\alpha/2}V_2(x)Y^i - \varepsilon^{2-\alpha}(\tfrac{1}{2}A_1''(x)+iKA_1'(x))Y^{i\,2}+\ldots) \qquad (7.39)$$
$$+ \varepsilon^{3\beta}(A_3(x)+P_3(x,0)+\ldots) + O(\varepsilon^{4\beta}) ,$$

and if the inner region is described by (7.10), (7.12) and (7.26) then matching (7.39) with the solutions to these equations gives us that (7.31) and (7.32) are once again the solutions in the inner and outer regions respectively.

As an example of the results obtained by this theory consider the biconvex island (6.32) which has an inner solution, upon evaluating the elementary integrals in (7.31), of

$$A^i = 1 - 2\varepsilon\sqrt{\frac{kx}{\pi}}(i-1)(1 - \frac{4x}{3}) + 4ik(\varepsilon x)^2(\frac{1}{8} - \frac{x}{12}) + O(\varepsilon^{3-3\alpha/2}), \qquad (7.40)$$

if $Y^i = b(x)$.

7.3 Theory for $\alpha=2$.

To date we have been concerned with $\alpha < 2$ in (7.1). However, when $\alpha=2$ some progress can be made. When this is true the first order inner equation is

$$2iK\frac{\partial A_0^i}{\partial x} + \frac{\partial^2 A_0^i}{\partial Y^{i\,2}} = 0 , \qquad (7.41)$$

if we do not begin our expansion with unity but with $A_0^i(x,Y^i)$. The corresponding boundary condition, from (7.14), is

$$\frac{\partial A_0^i}{\partial Y^i}(x,b(x)) = iKb'(x)A_0^i(x,b(x)) . \qquad (7.42)$$

This problem is not easily solved analytically but if the island coast is given by

$$y = \varepsilon\sqrt{x} \qquad (7.43)$$

then a similarity solution may be found, namely,

$$A_0^i\left(\frac{y}{\sqrt{x}}\right) = 1 - \frac{ik\varepsilon\int_\eta^\infty e^{ik\tau^2/2}d\tau}{(4e^{ik\varepsilon^2/8} + ik\varepsilon\int_{\varepsilon/2}^\infty e^{ik\tau^2/2}d\tau)} . \qquad (7.44)$$

This solution was found by Mei and Tuck (1980) but their equation (2.13) is incorrect.

It is of interest to note that (7.44) is the *exact* solution to irrotational time-harmonic flow past a parabola, not just an approximation. That is (7.44) is the solution to (5.8a) with the boundary condition $\partial\phi/\partial n = 0$ on the curve given by (7.43). This solution was found by Lamb (1906) and is reproduced by Jones (1964; p. 468). Note that A is constant on the boundary curve.

7.4 Local Expansion Near Curved Leading Edge

The theory of §7.1 and §7.2 breaks down locally where there is a curved end because $b'(x)$ becomes infinite in these regions. In this section a local expansion near a curved leading edge will be employed to overcome this problem. Note that the trailing edge cannot be so treated, as singularities of at least logarithmic severity still occur there. The removal of this singularity is a problem as yet unsolved.

For the purpose of demonstration the elliptic island

$$y = \pm\varepsilon\sqrt{x(1-x)} \qquad (7.45)$$

will be examined. However the theory is easily applied to other island shapes with a curved leading edge.

In an inner region near $x=0$ let

$$x = X^{\ell}\varepsilon^{a}$$
$$y = Y^{\ell}\varepsilon^{1+a/2} \qquad (7.46)$$
$$A^{\ell} = 1+\varepsilon^{\gamma}A_1^{\ell}(X^{\ell},Y^{\ell})+\varepsilon^{2\ell}A_2^{\ell}(X^{\ell},Y^{\ell})+\ldots$$

so that (7.45) may be expanded as

$$y = \varepsilon^{1+a/2}\sqrt{X^{\ell}}\left(1 - \frac{\varepsilon^{a}}{2}X^{\ell} - \varepsilon^{2a}\frac{X^{\ell 2}}{4} - \ldots\right) . \qquad (7.47)$$

Substituting these expansions into (5.8a) we obtain the leading order equation

$$\frac{\partial^2 A_1^{\ell}}{\partial Y^{\ell 2}} = 0 , \qquad (7.48)$$

if

$$0 < \alpha < 2, \quad 0 < a < 2, \qquad (7.49)$$

and, if

$$\gamma + \alpha < 2, \qquad (7.50)$$

our second order equation is of the same form as (7.48). Making the further assumptions

$$\alpha + 2\gamma = 2, \quad \alpha > a \qquad (7.51)$$

an inhomogeneous third order equation is obtained, namely,

$$\frac{\partial^2 A_3^{\ell}}{\partial Y^{\ell 2}} = - 2iK\frac{\partial A_1^{\ell}}{\partial X^{\ell}} . \qquad (7.52)$$

Solving these simple order equations gives the expansion

$$A^{\ell} = 1+\varepsilon^{\gamma}(d_1(X^{\ell})+d_2(X^{\ell})Y^{\ell})+\varepsilon^{2\gamma}(d_3(X^{\ell})+d_4(X^{\ell})Y^{\ell})$$
$$+\varepsilon^{3\gamma}(d_5(X^{\ell})+d_6(X^{\ell})Y^{\ell}-iKd_1'(X^{\ell})Y^{\ell 2}-\tfrac{i}{3}Kd_2'(X^{\ell})Y^{\ell 3})+O(\varepsilon^{4\gamma}) \qquad (7.53)$$

for the inner amplitude.

The boundary condition (7.14) may be expanded in terms of (7.46) and (7.47) to give the first three order boundary equations:

$$\frac{\partial A_1^{\ell}}{\partial Y^{\ell}}(X^{\ell},\sqrt{X^{\ell}}) = 0$$

$$\frac{\partial A_2}{\partial Y^{\ell}}(X^{\ell},\sqrt{X^{\ell}}) = +\frac{iK}{2\sqrt{X^{\ell}}} \tag{7.54}$$

$$\frac{\partial A_3^{\ell}}{\partial Y^{\ell}}(X^{\ell},\sqrt{X^{\ell}}) = +\frac{iKA_1^{\ell}}{2\sqrt{X^{\ell}}}(X^{\ell},\sqrt{X^{\ell}}) \ .$$

The last of these is valid only if the condition $\gamma < a$ holds, as well as (7.49)-(7.51). These boundary equations, when applied to the solutions of the appropriate order equations, give us that

$$\begin{aligned} d_2(X^{\ell}) &= 0 \\ d_4(X^{\ell}) &= iK/(2\sqrt{X^{\ell}}) \\ d_6(X^{\ell}) &= 2iKd_1'(X^{\ell})\sqrt{X^{\ell}} + \frac{iKd_1(X^{\ell})}{2\sqrt{X^{\ell}}} \ . \end{aligned} \tag{7.55}$$

The outer region is treated as in §7.1 so that the inner expansion of the outer solution becomes

$$\begin{aligned} A^0 = 1+\varepsilon^{\gamma}A_1(X^{\ell})+\varepsilon^{2\gamma}(Y^{\ell}V_1(X^{\ell})+A_2(X^{\ell}))+\varepsilon^{3\gamma}(A_3(X^{\ell}) \\ +V_2(X^{\ell})Y^{\ell}-iKA_1'(X^{\ell})Y^{\ell 2})+\ldots \ . \end{aligned} \tag{7.56}$$

Note that, from (7.2) $\delta = \gamma$ and, from the definition of $V_i(x)$, (IIA.3), $V_i(x) = \varepsilon^{-a/2}V_i(X^{\ell})$. If (7.53) is matched with (7.56) the following equalities are found:

$$\begin{aligned} d_1(X^{\ell}) &= A_1(X^{\ell}) \\ V_1(X^{\ell}) &= iK/(2\sqrt{X^{\ell}}) \\ d_3(X^{\ell}) &= A_2(X^{\ell}) \\ d_5(X^{\ell}) &= A_3(X^{\ell}) \\ V_2(X^{\ell}) &= 2iKA_1'(X^{\ell})\sqrt{X^{\ell}} + \frac{iKA_1(X^{\ell})}{2\sqrt{X^{\ell}}} \ . \end{aligned} \tag{7.57}$$

The leading edge inner solution is thus specified to second order as

$$A^{\ell} = 1 - \frac{(i-1)}{4}\sqrt{k\pi\varepsilon} - \frac{ik\varepsilon^2}{2}\left[\frac{\pi}{8} - \frac{Y^{\ell}}{\sqrt{X^{\ell}}}\right] + O(k^{3/2}\varepsilon^3) \quad (7.58)$$

for the island whose boundary is given by (7.45). Away from the leading edge (7.31) is valid and the two solutions are matched at the point where they possess the same value. Our outer solution is (7.32) for all x in the intermediate field of the island, however.

7.5 Boundary Integral Equation Method

As in Chapter 6, only the formulation of the b.i.e. technique will be specified here as the details were set out in Chapter 2.

The scattered wave potential in the ocean around the island is given by (6.26a) and on the coastline C itself

$$\bar{\phi}_1(\underset{\sim}{x}) = \frac{i}{2}\int_C \left[\bar{\phi}_1(\underset{\sim}{x}')\frac{\partial H_0^{(1)}(kr')}{\partial n} + ikn_{x'}e^{ikx'}H_0^{(1)}(kr')\right]d\ell(\underset{\sim}{x}'), \quad (7.59)$$

using the notation of Chapter 2 and §6.2, as there is a Neumann boundary condition on C. If (7.59) is discretised as in (2.12) then it may be rewritten as the matrix equation

$$\Psi_1 = (A-I)^{-1}Z \ , \quad (7.60)$$

where I is the $N\times N$ identity matrix, Ψ_1 and A are given in (6.29) and

$$Z = B\Psi_0 \ , \quad (7.61)$$

B also being given in (6.29) while

$$[\Psi_0]_j = -ikn_{x_j}e^{ikx_j} \ . \quad (7.62)$$

Note that (A-I) must be non-singular for (7.60) to be useful.

The integrals in (7.60) are evaluated using the analytic and numerical techniques outlined in §2.3.

As only islands symmetric about the x-axis may have the theory of this chapter applied to them, the size of the matrices in (7.60) could be reduced by half, which saved much storage space and c.p. time. The numerical method was tested on circular islands, as analytic solutions in terms of Bessel function series are available for this geometry (see Appendix IIB). The agreement between the two solutions on the coast of the island was excellent when 20 segments per wavelength were employed; so good in fact that the two could not be distinguished apart. The figure of 20 segments per wavelength was chosen because that is what will be generally used in the comparisons between the asymptotic and numerical methods in the next section.

7.6 Comparison of Numerical Results and Parabolic Approximation Theory

For the purpose of examining the theory of §§7.1, 7.2 the biconvex island whose boundary is given by (6.32) will be used. As was noted in §6.3, the numerical method will not be as accurate near $x=0,1$ due to the non-analyticity of the boundary curve at these points. However, the errors involved are only small.

Equation (7.40) gives A^i on the coast to second order so the modulus of this expression will be compared to $|\phi(\underset{\sim}{x})|$ along C. Three different (k,ε) pairs are examined in Figures 7.1-7.3. In each, the numerical results are compared with the first and second order asymptotic theories. The leading order theory

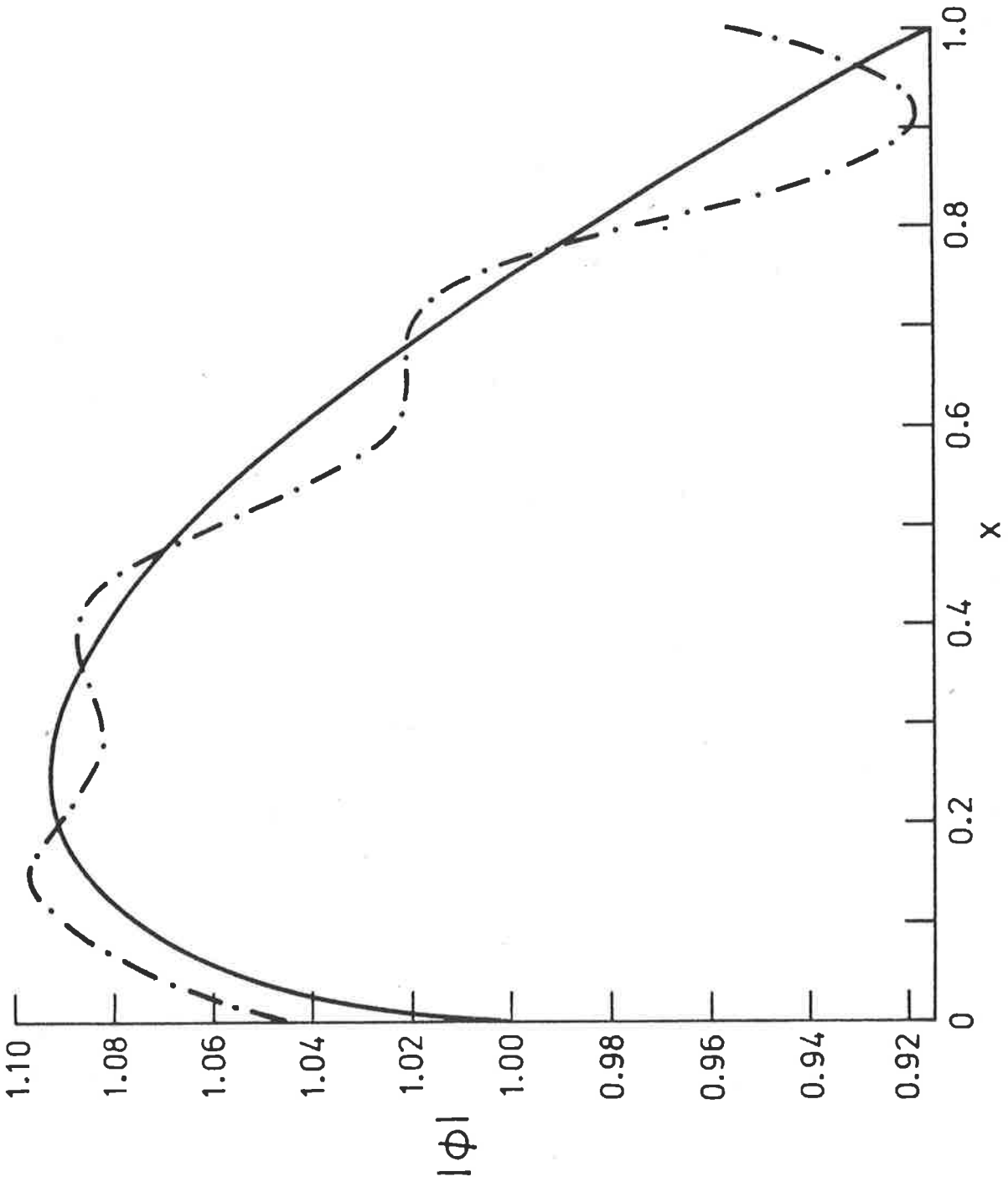

Figure 7.1: Biconvex island, k=10, ε=0.075. —·— coastal amplitude from b.i.e. method (N=41); —— coastal amplitude from 1st order par. approx. (2nd order indistinguishable from 1st).

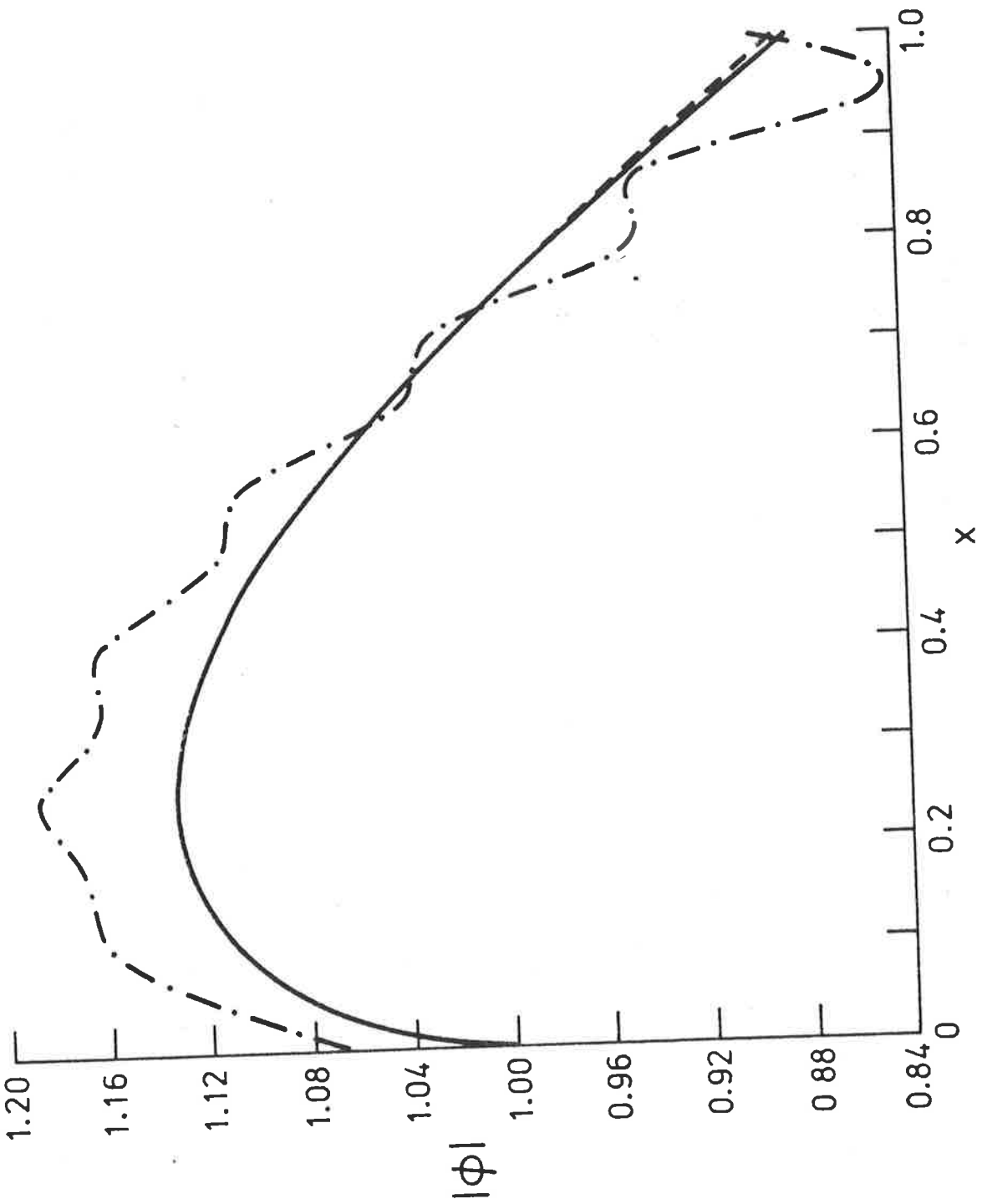

Figure 7.2: Biconvex island, k=20, ε=0.075. Same legend as Figure 7.1 with — — coastal amplitude from 2nd order par. approx. (N=76).

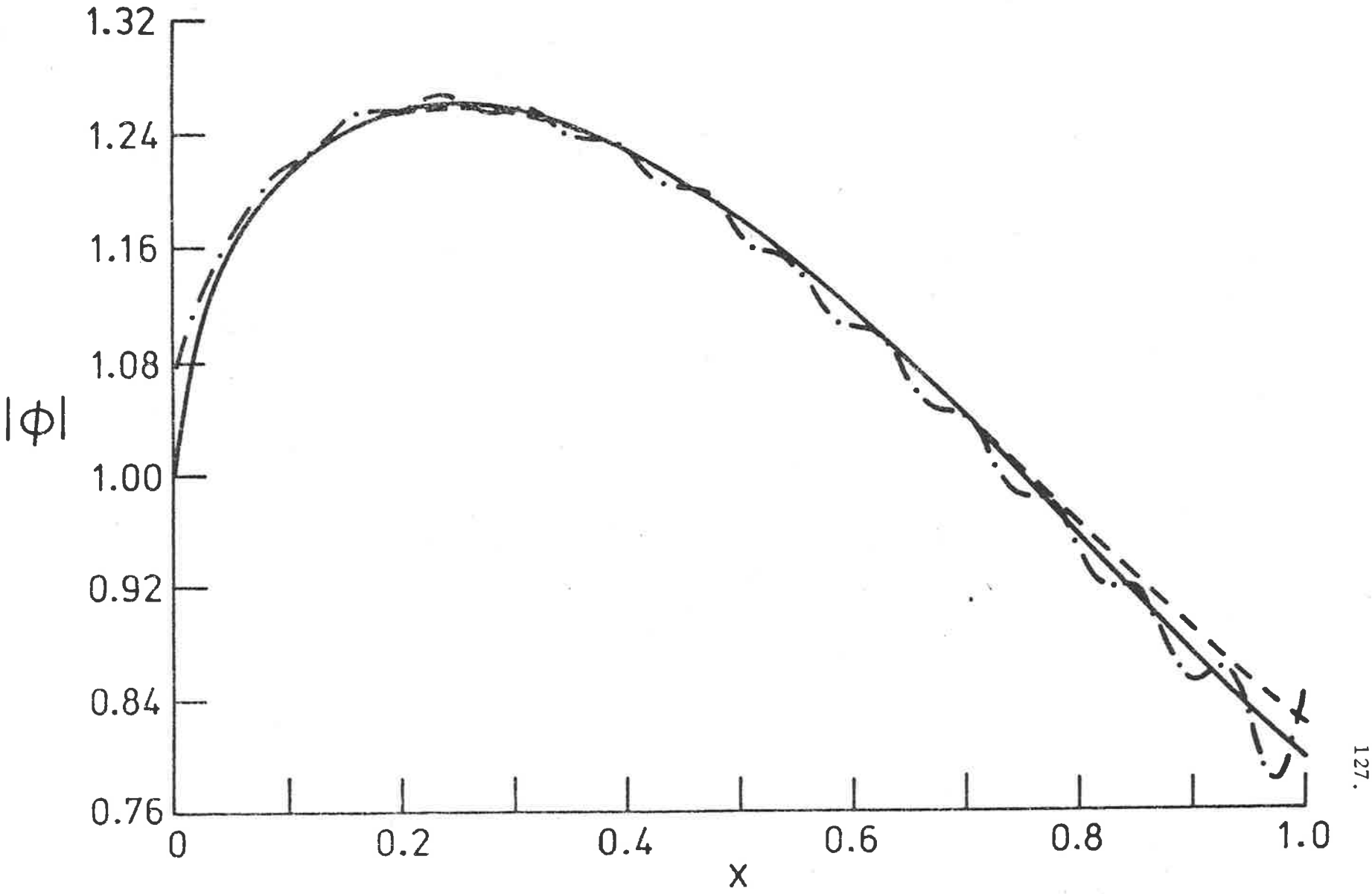

Figure 7.3: Biconvex island, k=40, ε=0.075. See Figure 7.2 for legend (N=151).

approximates the numerical curve fairly well in all cases, if the smaller amplitude waves in the numerical plots are smoothed. The second order was evaluated to attempt to model these waves but this did not occur. However, as $k\varepsilon$ gets larger these waves become smaller and the second order solution should give a good estimate of the amplitude. Examples only up to $k=40$ are given because of the large c.p. time required for larger k, but the trend in the figures illustrates how the second order solution will be useful in the upper part of the region of validity (7.33).

The waves superimposed on the mean amplitude in the numerical results have a wavelength very close to π/k, that is, half the wavelength of the incident plane wave. Their presence is as yet unexplained, but note that they are not always important; for example, an airfoil oriented so that its blunt end faces the oncoming flow does not produce such waves except of almost undetectable amplitude.

Islands with curved leading edges will now be examined. As §7.4 took as its example an elliptic island (7.45) this will also be used here. Choosing a body whose trailing edge is also curved will demonstrate how the theory breaks down in the vicinity of an infinite slope rear.

In Figures 7.4-7.6 the numerical model is compared to the first and second order solutions of the asymptotic theory for elliptic islands of various $k\varepsilon$. Note that the expression used for the latter curves away from the leading edge is

$$A = 1 - \frac{(i-1)\sqrt{k}}{2\sqrt{\pi}}\varepsilon[2E(\sqrt{x})-K(\sqrt{x})]+ik\varepsilon^2\left[\frac{1}{2}(1-2x)Y^i - \frac{1}{\sqrt{\pi}}\int_0^x\left\{\frac{E(\sqrt{\xi})(1-2\xi)+K(\sqrt{\xi})(\xi-\frac{3}{4})}{\sqrt{(1-\xi)\xi(x-\xi)}}\right\}d\xi\right], \tag{7.63}$$

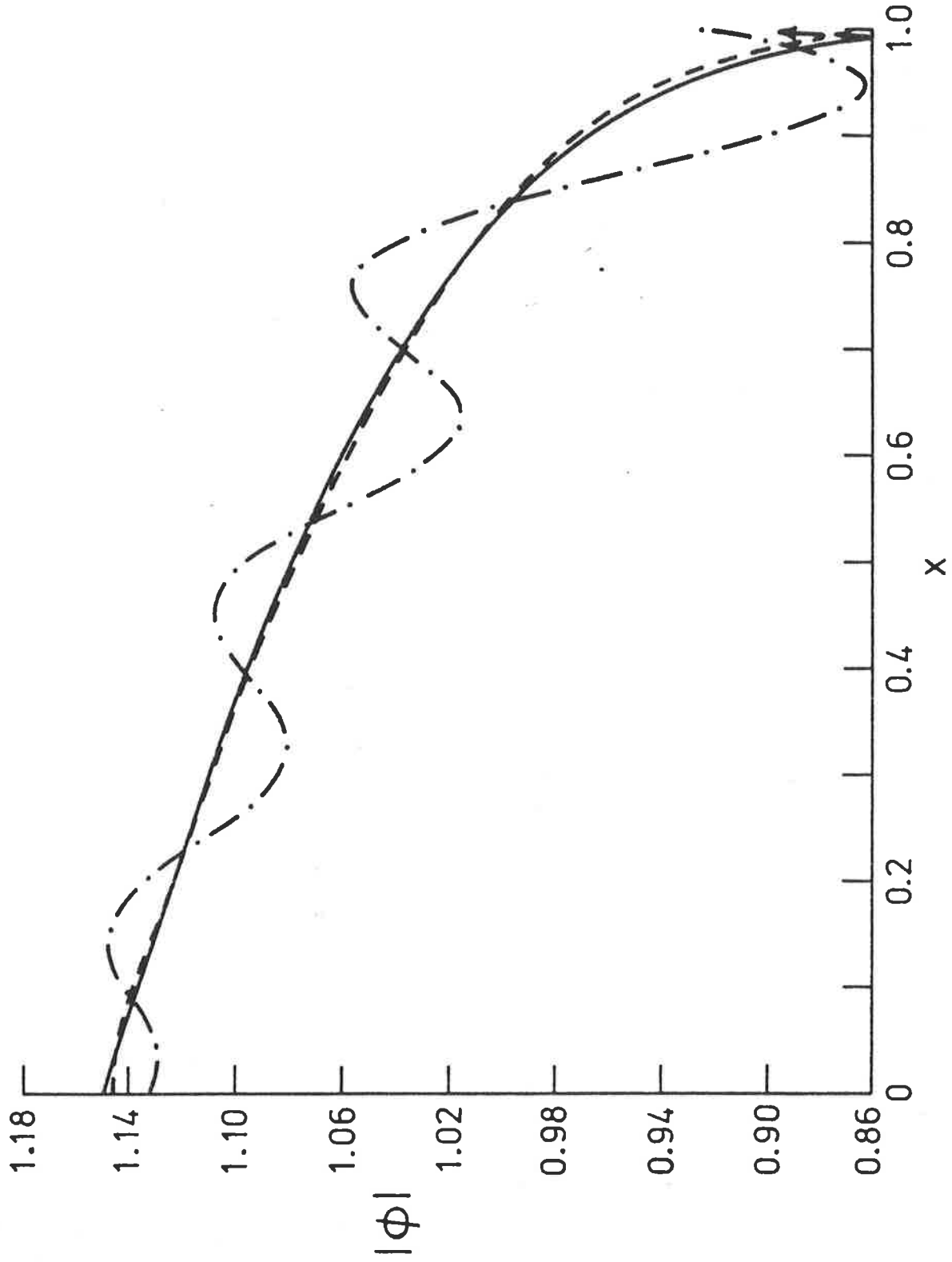

Figure 7.4: Elliptic island, k=10, ε = 0.1. See Figure 7.2 for legend. (N=76)

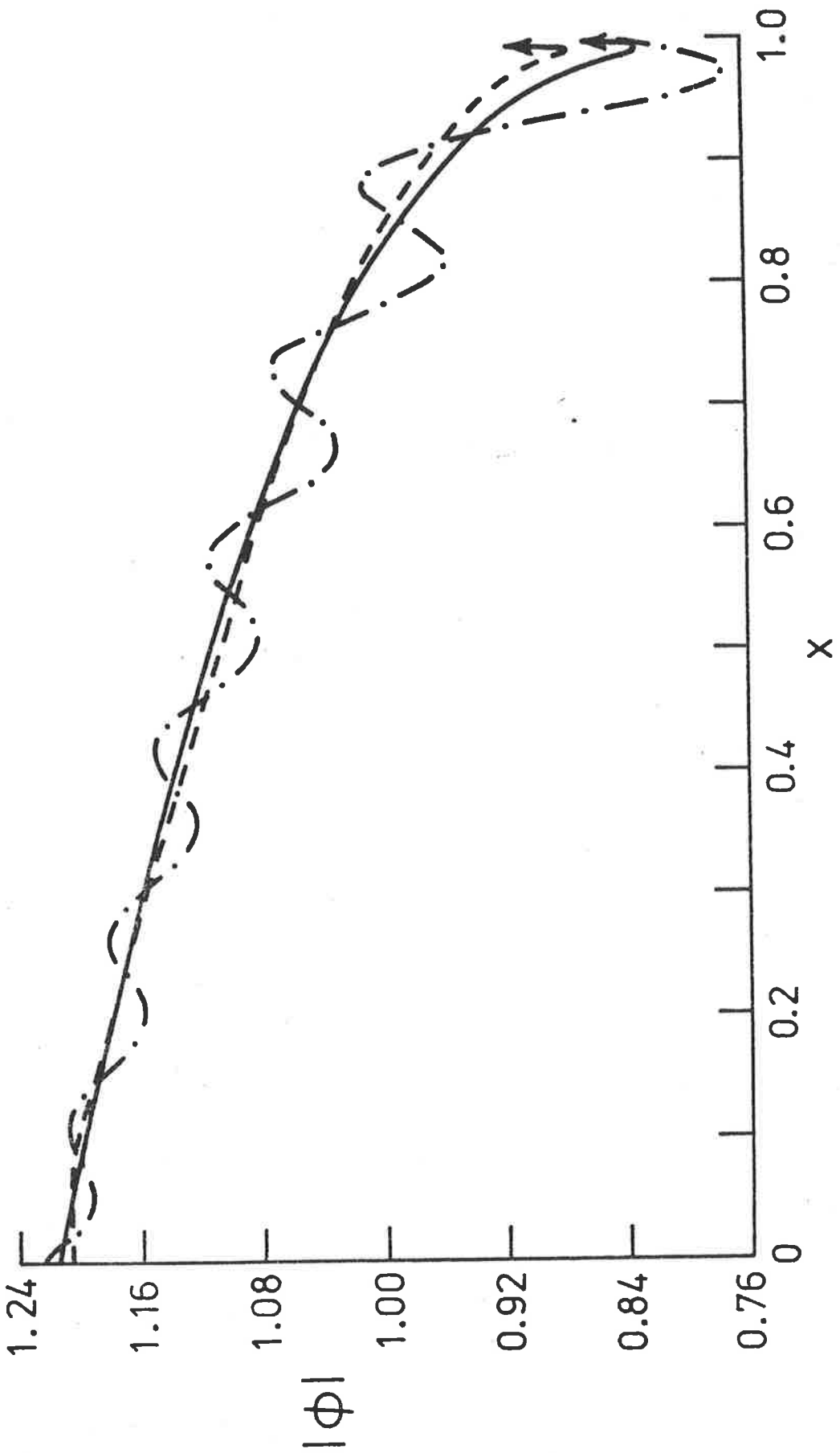

Figure 7.5: Elliptic island, k=20, ε=0.1. See Figure 7.2 for legend (N=76).

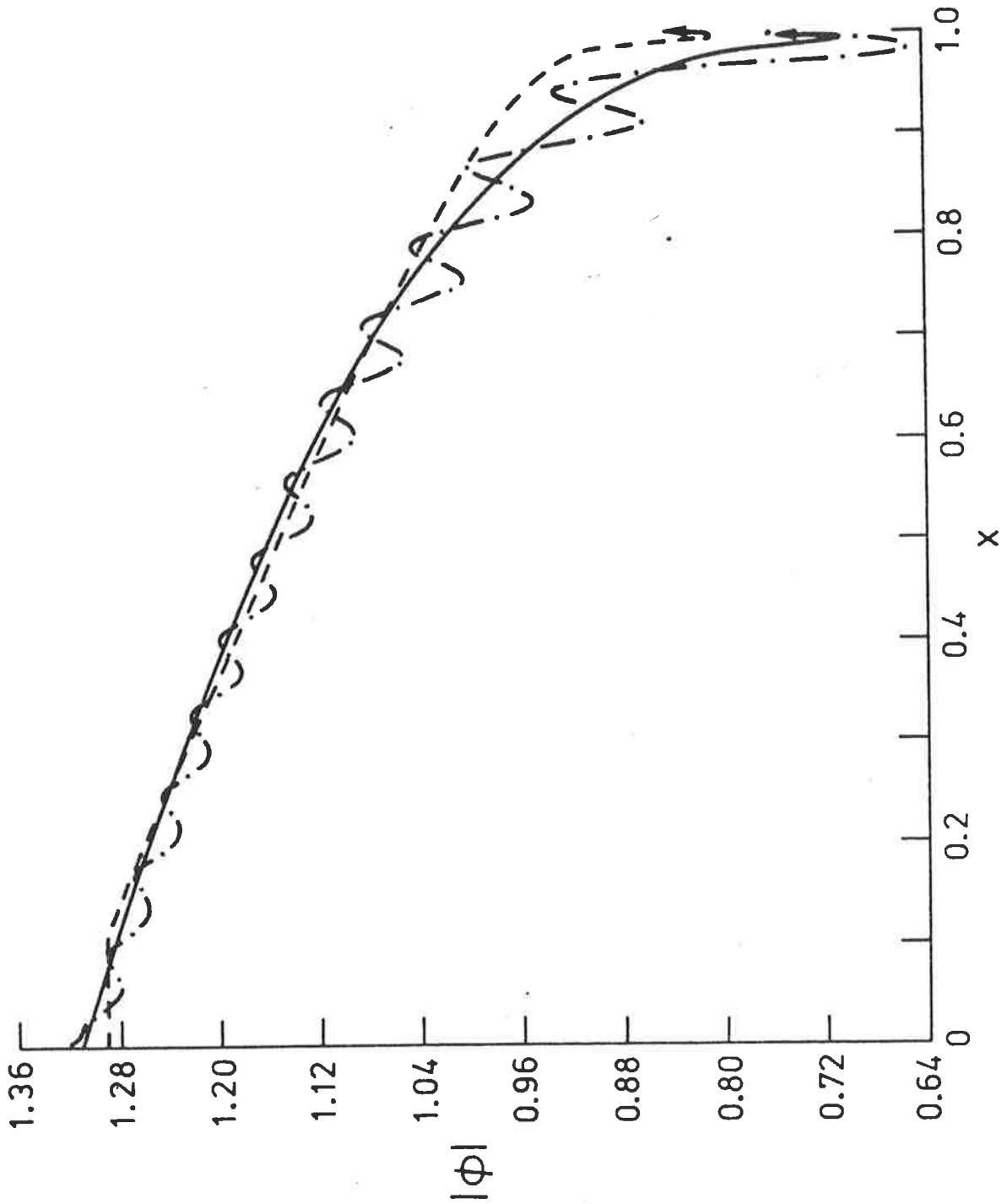

Figure 7.6: Elliptic island, k=40, ε=0.1. See Figure 7.2 for legend (N=76).

found from (7.31) with $E(x)$, $K(x)$ being complete Elliptic integrals as defined by Gradshteyn and Ryzhik (1980). The integral in (7.63) was evaluated numerically by quadrature formula 25.4.39 in Abramowitz and Stegun (1972).

As for the finite end-slope islands considered above, when $k\varepsilon$ is relatively small the first and second order asymptotic solutions differ little, as shown in Figure 7.4, and give an average of the numerical results, which exhibit a wave-like structure. Near the leading edge the effect of the theory of §7.4 is to smoothly guide the solution to its zero limit, at least for the first order solution. Note that the second order solution does not quite do this, but flattens the amplitude out for a small distance behind $x=0$. As the rear is approached, however, the asymptotic theory becomes singular. This does not become apparent, for this $k\varepsilon$ value, until very close to $x=1$.

If Figure 7.5 is next considered, where $k\varepsilon$ is now double its value in Figure 7.4, a similar picture is seen, except that the flattening of the second order solution extends to around $x=0.075$, instead of being confined to a very narrow region, and the second order solution appears more singular near the trailing edge. The overall impression of this figure is that the second order solution gives a slightly improved view of the mean amplitude to that of the first order solution for $x \lesssim 0.75$, while it diverges more for $x \gtrsim 0.9$. Note also that, as for finite end-slope islands, the amplitude of the perturbation to the mean numerical result is decreased as $k\varepsilon$ is increased, albeit slowly.

This is true in Figure 7.6 also, where $k\varepsilon$ is doubled once more. Most of the features noted of Figure 7.5 appear in this figure,

such as the flattening of the second order solution near the leading edge, and the unsatisfactory nature of the second order solution as $x \to 1$.

As indicated in (7.58), the first order leading edge solution is just the zero limit of the inner solution found using the techniques of §7.1. This is true for all island shapes. The second order leading edge solution acts as an amplitude stabilizer whose influence spreads as $k\varepsilon$ increases, due to the blunt end looking more like a parabolic island as the wavelength of the incident wave decreases.

To sum up, comparing numerical experiments with the asymptotic theory shows that the theory is useful in the range expected (7.23) but does not, in general, fully describe the numerical results. A wave perturbation is superimposed on the coastal amplitude of many islands, which is not predicted even by higher order theory, and difficulty is encountered at infinite slope trailing edges. However the trend of the amplitude (or a perturbation-wavelength spacial average) is given by the present theory, which would not, in any case, be expected to predict small-amplitude short-wavelength x-disturbances because of the assumption of small longitudinal gradients in the amplitude of e^{ikx} built into the theory. Note that the perturbation seems to be due to a reflection of the incoming waves from the trailing end of the island. Such a mechanism would explain the larger amplitude of the super-imposed wave near $x=1$ and the problems with convergence near this point. Reflection was also the reason why the parabolic approximation broke down in Chapter 6; however it has not, as yet, been able to be incorporated into the theory.

APPENDICES

APPENDIX IA

Contribution to Exterior Potential from Circle at Infinity

As in the uses of boundary integral techniques in Part II the outer curve at infinity is a complete circle rather than a semi-circle, the following proof is for that case but the proof also holds for any arc of the circle at infinity.

Theorem: The contribution to the exterior scattered potential, ϕ_s, from the circle at infinity, C, is zero $\Leftrightarrow$ Sommerfeld's radiation condition holds.

Proof:
$$\oint_C \left(G \frac{\partial \phi_s}{\partial n} - \phi_s \frac{\partial G}{\partial n}\right) d\ell = 0$$

$$\Leftrightarrow \lim_{kr \to \infty} \left\{ \int_0^{2\pi} \left(G \frac{\partial \phi_s}{\partial r} - \phi_s \frac{\partial G}{\partial r}\right) kr\, d\theta \right\} = 0$$

$$\Leftrightarrow \lim_{kr \to \infty} \left\{ \int_0^{2\pi} (kr)^{1/2} G \left\{ (kr)^{1/2} \left[\frac{\partial \phi_s}{\partial r} - ik\phi_s \right] \right\} - (kr)^{1/2} \phi_s \left\{ (kr)^{1/2} \left[\frac{\partial G}{\partial r} - ikG \right] \right\} d\theta \right\} = 0$$

$$\Leftrightarrow \lim_{kr \to \infty} \left[(kr)^{1/2} G \left\{ (kr)^{1/2} \left[\frac{\partial \phi_s}{\partial r} - ik\phi_s \right] \right\} - (kr)^{1/2} \phi_s \left\{ (kr)^{1/2} \left[\frac{\partial G}{\partial r} - ikG \right] \right\} \right] = 0$$

but $\phi_s \neq G$ and ϕ_s and G obey the same boundary conditions so

$$\Leftrightarrow \lim_{kr \to \infty} \left\{ (kr)^{1/2} \left[\frac{\partial \phi_s}{\partial r} - ik\phi_s \right] \right\} = 0,$$

which is Sommerfeld's radiation condition.

APPENDIX IB

Flow Through Holes

1. Introduction

The problem of incompressible flow through an aperture, satisfying certain conditions at infinity, is a difficult one in general, especially in three dimensions, but a number of geometries may be treated. Two dimensional theory is, of course, much simpler as conformal mapping may be used.

Researchers have been working on this problem for both compressible and incompressible flows since the last century and Rayleigh's pioneering work (1897). Some success was gained, as may be found from consulting Lamb (1932), and in recent years many approaches, generally restricted in aim, have been tried. For example, Tuck (1971), (1975) examined asymptotically the transmission of water waves through small apertures, while Memos (1980) discussed the flow through the opening between two walls inclined at an angle to each other. Ffowcs Williams (1972) looked at turbulent flow through a screen of circular apertures,, while Leppington and Levine (1973) extended this to elliptical apertures, in which the aperture dimension was much smaller than the spacing between the holes, which, in turn, was much smaller than the wavelength of the incident wave. De Smedt (1981a) has examined low frequency scattering through an aperture in a rigid screen, both numerically and analytically, in terms of pressure fields - he has also studied annular orifices (1981b). Sanchez-Hubert and Sanchez-Palencia (1982) have studied non-linear and viscous fluid flow through holes and the permeability of perforated walls. Some authors, such as Ingard (1953a) and Hirschwehr (1974), have adopted a classical approach and studied the Rayleigh end-correction.

M.S. Howe, who has been active in resonator theory, has also been prominent in the field of flow through apertures. He has looked at unsteady high Reynolds number flow through circular apertures (1979b) and at grazing flow through circular holes (1980a) and perforated screens (1980b). Unsteady flow has also been studied (1981b), (1981c).

The method presented here, following that of Tuck (1975), is still restricted in aim but is more comprehensive than most analytic results. The principal purpose is to find the parameters which play important roles in the cavity resonance theory presented in Chapters 3 and 4. Much of this work can also be found in Bigg and Tuck (1982) and Bigg (1982a).

2. Two Dimensional Theory

We need to solve

$$\nabla^2\bar{\phi} = 0 \tag{IB.1}$$

subject to

$$\frac{\partial\bar{\phi}}{\partial n} = 0 \tag{IB.2}$$

on the aperture boundaries and (3.2), or

$$\bar{\phi} \to \pm\frac{1}{\theta_\pm}\ln\left(\frac{r}{s}\right) , \tag{IB.3}$$

as $x \to \pm\infty$. Most examples of solutions up to now, and discussed in Tuck (1975), have had $\theta_+ = \theta_- = \pi$, that is, they correspond to openings in a plane wall. In particular, if the opening is a sharp-edged slit of width w, in a plane wall of zero thickness, then

$$s = \frac{w}{4} . \tag{IB.4}$$

In fact, the derivation, using elliptic coordinates, of this result in Tuck (1975) generalizes immediately to that for an opening consisting of a pair of hyperbolas, as sketched in Figure IB.1a, which has $\theta_+ = \theta_- < \pi^*$. Now s is exactly equal to one quarter of the distance between the *foci* of the hyperbolae, that is, if w is the actual width at the throat,

$$s = \frac{w}{4\sin(\theta_+/2)} \quad . \qquad (IB.5)$$

A plot of s/w against θ_+ is shown in Figure IB.2 as the solid line.

Another case in which the cavity aperture parameter s can be determined, at least semi-analytically is that in which the boundaries are straight-edged wedges as in Figure IB.3a. These two wedges, of angles $\alpha\pi$ and $\beta\pi$, have their vertices at D and H respectively. Without loss of generality, we may fix the location of H as the origin in the complex $z = x+iy$ plane, and also fix as vertical the left edge of the wedge with corner at H. The angles θ_- and θ_+ are as in §3.2, and of necessity

$$\theta_+ + \theta_- + \alpha\pi + \beta\pi = 2\pi \quad . \qquad (IB.6)$$

In what follows it will be convenient to set

$$\theta_- = \gamma\pi \quad . \qquad (IB.7)$$

The solution to (IB.1) is found by a Schwartz-Christoffel mapping to the upper half $\eta \geq 0$ of the $\zeta = \xi+i\eta$ plane, namely

---

*For an idea of the proof see the discussion of the 3D analogy.

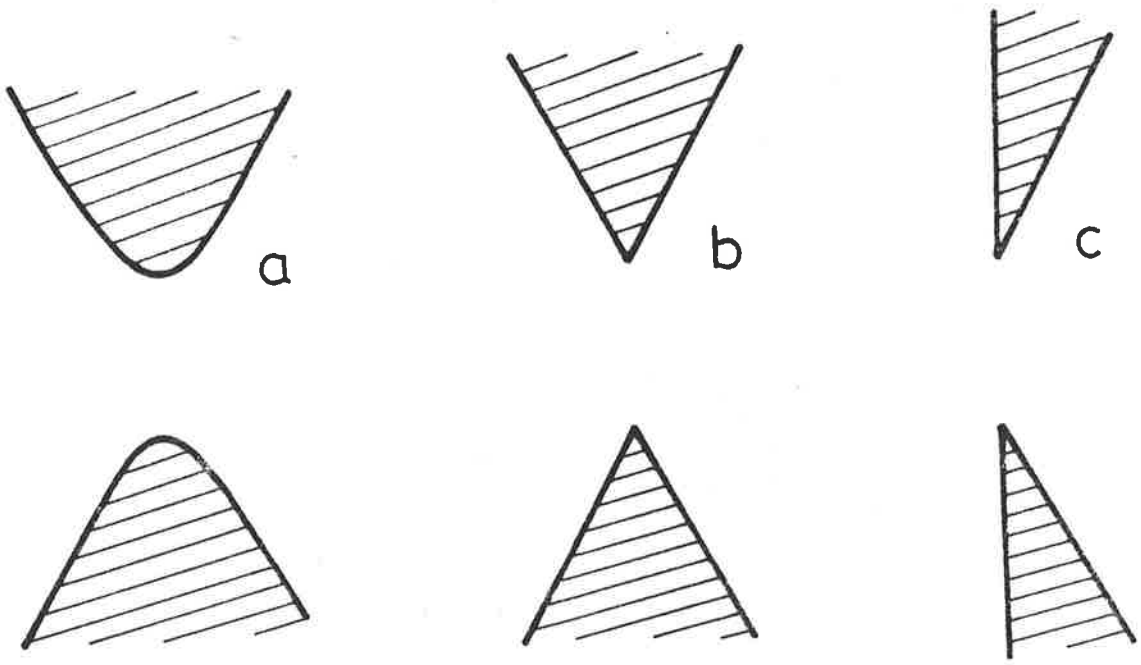

Figure IB.1: Special openings: (a) hyperbolic, (b) symmetric wedge, (c) wedge with $\theta_- = \pi$.

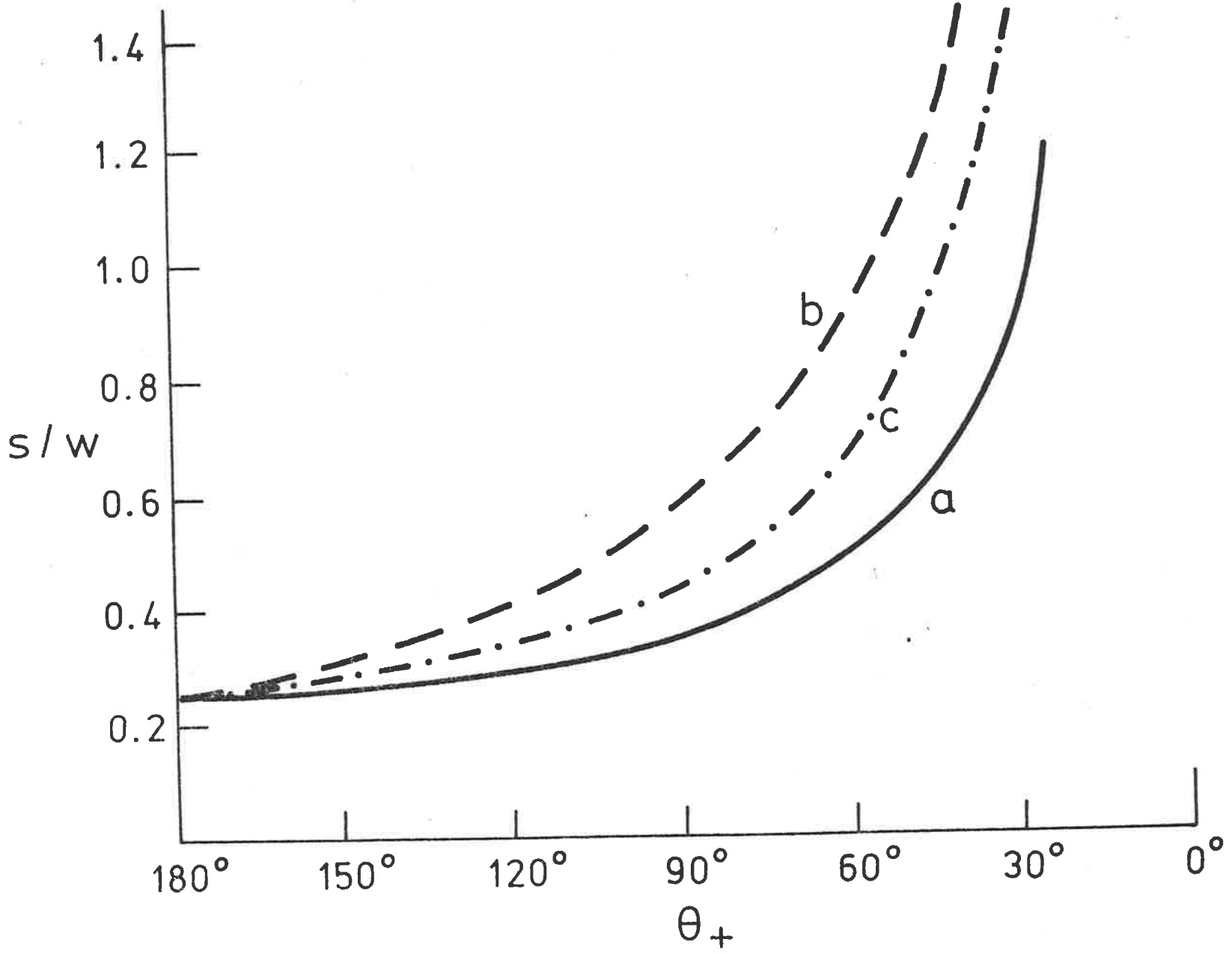

Figure IB.2: Effective size of openings of Figure IB.1.

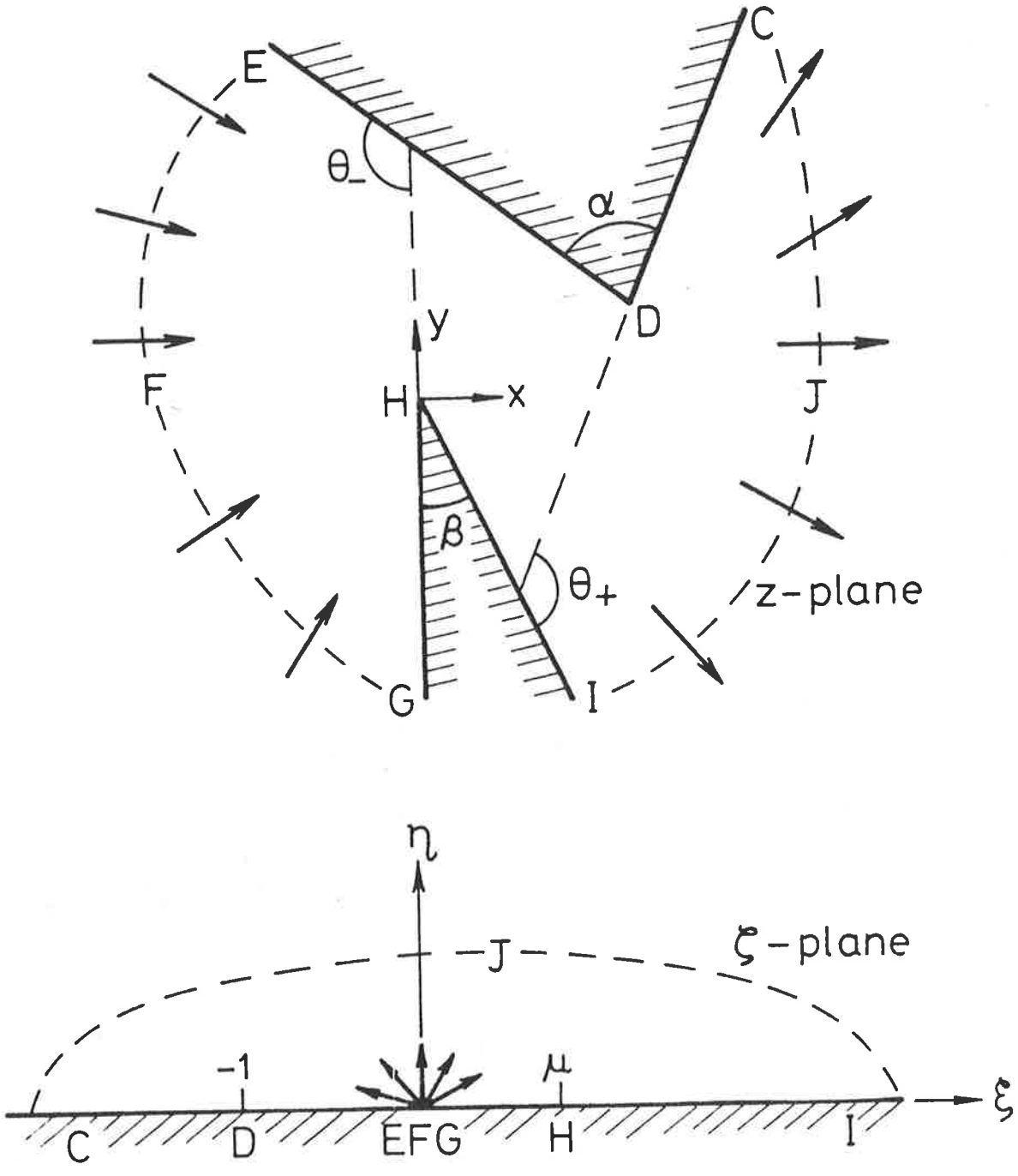

Figure IB.3: Conformal mapping of wedge-like openings.

$$\frac{dz}{d\zeta} = -ie^{i\beta\pi}\zeta^{-\gamma-1}(\zeta+1)^{1-\alpha}(\zeta-\mu)^{1-\beta}\ , \qquad \text{(IB.8)}$$

for some parameter μ as in Figure IB.3b. The corner points D and H are mapped to the points $\zeta = -1,\mu$ respectively. The overall length scale in this problem is arbitrarily determined by the fact that the constant multiplier in (IB.8) has unit magnitude.

The integral of (IB.8), for $\zeta = \xi+i0$ and $\xi < \mu$, satisfying $z(\mu) = 0$, is

$$z = -\frac{i\mu^{-\gamma-\beta}}{\gamma}(\xi^{-\gamma}-\mu^{-\gamma})+i\int_{\mu}^{\xi} t^{-\gamma-1}[(t+1)^{1-\alpha}(\mu-t)^{1-\beta}-\mu^{1-\beta}]dt. \qquad \text{(IB.9)}$$

Our main interest is in the location of the corner point D, which can be written as

$$z(-1) = i\mu^{1-\beta}[\mu^{-\gamma}F(\alpha,\beta,\mu) - e^{-i\gamma\pi}F(\beta,\alpha,1/\mu)], \qquad \text{(IB.10)}$$

where

$$F(\alpha,\beta,\mu) = \frac{1}{\gamma} - \int_0^1 t^{-\gamma-1}[(1+\mu t)^{1-\alpha}(1-t)^{1-\beta}-1]dt. \qquad \text{(IB.11)}$$

There is no difficulty in numerically evaluating F in (IB.11), and hence the coordinates of the point D. The method used here is to make the preliminary change of variable $t = \tau^{1/(1-\gamma)}$, which eliminates the algebraic singularity at $t=0$, and then use the mid-point rule. In the particular case $\mu=1$, $\alpha=\beta$, the function F reduces to a Beta-function, namely

$$F(\alpha,\alpha,1) = \frac{1-\alpha}{\gamma}\,B\left(1-\frac{\gamma}{2},\ 1-\alpha\right). \qquad \text{(IB.12)}$$

This special case yields an opening with symmetry about a line through the midpoint of HD.

The flow problem is solved in the ζ-plane by placing a source at the origin. That is, the complex potential is given by

$$\bar{f} = \bar{\phi} + i\bar{\psi}$$

$$= \frac{1}{\pi} \ln \zeta + \kappa \ , \qquad \text{(IB.13)}$$

for some constant κ. Now, as $\zeta \to 0$,

$$z \to -\frac{i}{\gamma}\mu^{1-\beta}\zeta^{-\gamma} + \text{constant} \qquad \text{(IB.14)}$$

so that

$$\bar{f} \to -\frac{1}{\theta_-} \ln\left(\frac{-\gamma z}{i\mu^{1-\beta}}\right) + \kappa \ . \qquad \text{(IB.15)}$$

This agrees with (IB.3) if

$$\frac{1}{\theta_-} \ln s = \kappa + \frac{1}{\theta_-} \ln\left(\frac{\mu^{1-\beta}}{\gamma}\right) \ . \qquad \text{(IB.16)}$$

Similarly, as $\zeta \to \infty$

$$z \to -\frac{ie^{i\beta\pi}\pi}{\theta_+} \zeta^{\theta_+/\pi} + \text{constant} \qquad \text{(IB.17)}$$

so that

$$\bar{f} \to \frac{1}{\theta_+} \ln\left(\frac{\theta_+ z}{-i\pi e^{i\beta\pi}}\right) + \kappa, \qquad \text{(IB.18)}$$

which agrees with (IB.3) if

$$-\frac{1}{\theta_+} \ln s = \kappa - \frac{1}{\theta_+} \ln\left(\frac{\pi}{\theta_+}\right) \ . \qquad \text{(IB.19)}$$

Subtraction of (IB.16) and (IB.19) to eliminate κ yields the required formula for s, namely

$$s = \pi\mu^{(1-\beta)\nu}\theta_+^{\nu-1}\theta_-^{-\nu} \ , \qquad \text{(IB.20)}$$

where

$$\nu = \frac{\theta_+}{(\theta_+ + \theta_-)} \,. \qquad \text{(IB.21)}$$

The problem is thus solved in an inverse manner by prescribing α,β,γ and μ. Results are wanted for s/w, where $w = |z(-1)|$, the distance between the corners H and D. Note that the length scale for the separate quantities s and w is arbitrarily set, by the choice of the mapping (IB.8), but this choice does not matter for their ratio.

Results for $\mu=1$, $\alpha=\beta$, plotted against θ_+ are shown in Figure IB.2. The dashed curve is for the opening of Figure IB.1b, which has a plane of symmetry along both the x- and y-axes, that is, $\theta_+ = \theta_-$, and the dashed chain-dotted curve is for $\theta_- = \pi$, that is, for an opening in a plane wall, as in Figure IB.1c. We recall that the solid curve corresponds to Figure IB.1a.

These results indicate that the effective size s of the opening is *increased* by decreasing the wall angles $\theta_\pm$ from π. This is most easily explained in terms of the hyperbolic opening, for which the controlling parameter is the interfocal distance, which exceeds the actual throat width. The increase is not rapid, but by the time the angle θ_+ reaches 90°, a 100-150% increase in s is predicted. On the other hand, as shown in Tuck (1975), wall thickness tends to *decrease* the opening parameter, providing θ_+ and θ_- remain at 180°.

3. Three Dimensional Theory

In three dimensions our governing equation is still (IB.1), subject to (IB.2) on the aperture boundaries, but now, as $z \to \pm\infty$, $\bar{\phi}$ must satisfy

$$\bar{\phi} \to \pm \frac{1}{\theta_{\pm}}\left[\left(\frac{1}{\bar{r}} - \frac{1}{\bar{s}}\right) - \gamma_{\pm}\ln\left(\frac{r \pm z}{\Omega}\right)\right] . \qquad \text{(IB.22)}$$

A few solutions for plane walls, where $\gamma_+ = \gamma_- = 0$ and $\theta_+ = \theta_- = 2\pi$, are available at present, mostly in Tuck (1975). For example, a circular opening of radius a in a plane wall has

$$s = \frac{2a}{\pi} . \qquad \text{(IB.23)}$$

Similarly, an elliptic hole with a semi-minor axis of length d and a semi-major axis of length a has

$$\frac{s}{2\sqrt{da}\pi} = \frac{\pi/2}{\sqrt{d/a}\,K(1-d^2/a^2)} , \qquad \text{(IB.24)}$$

where K is a complete elliptic integral. Another geometry for which an asymptotic solution exists is a cylindrical tube of length ℓ and radius a, shown in Figure IB.4b. Rayleigh (1896; p. 181) derives

$$s = \frac{a^2}{\ell+\frac{1}{2}\pi a} , \quad a \ll \ell . \qquad \text{(IB.25)}$$

Several other aperture geometries may be examined successfully and the rest of this section will be devoted to this investigation.

One of these geometries is that of Figure IB.4a, which consists of a pair of hyperbolas in the xz-plane rotated about the z-axis with $\theta_- = \theta_+$. An angle v in the xz-plane will be associated with this body, with

$$\theta_{\pm} = 2\pi(1-\cos v) . \qquad \text{(IB.26)}$$

Using oblate spheroidal coordinates, where

$$\begin{aligned} z &= a \cos\alpha \tan\delta \\ x &= a \sin\alpha \sec\delta, \end{aligned} \qquad \text{(IB.27)}$$

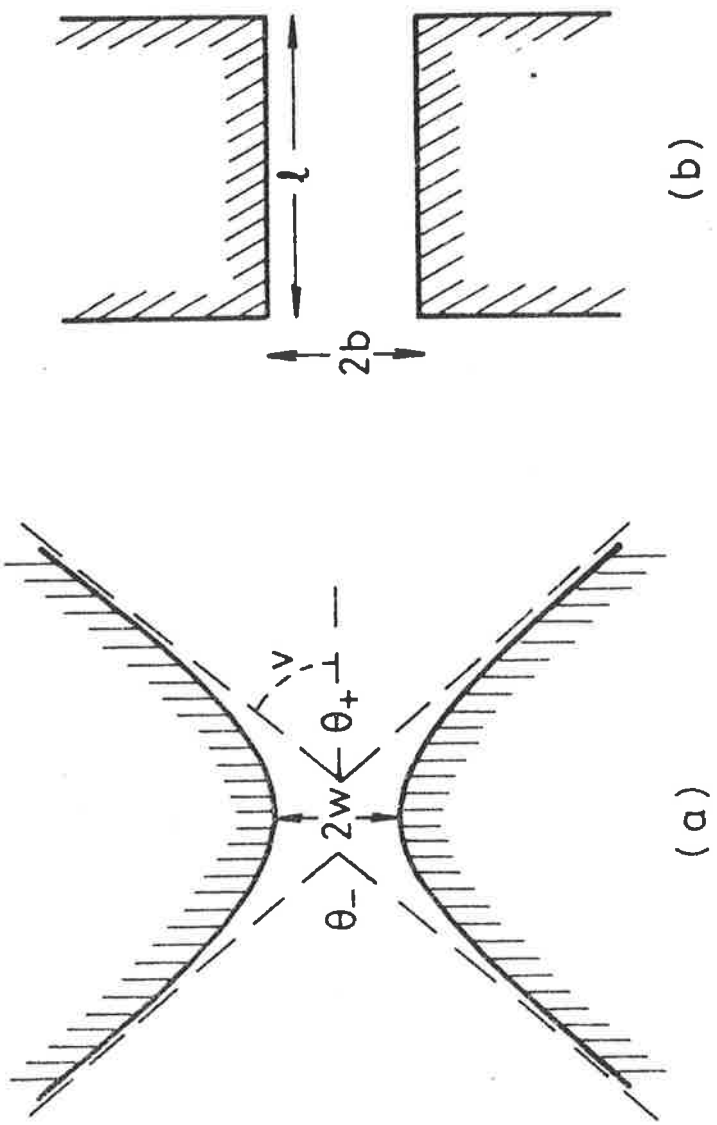

Figure IB.4: Special apertures, axisymmetric about z-axis. (a) rotated hyperbolas, $\theta_- = \theta_+$; (b) channel, $\theta_- = \theta_+ = 2\pi$.

Figure IB.5: Effective size s/W for rotated hyperbolas.

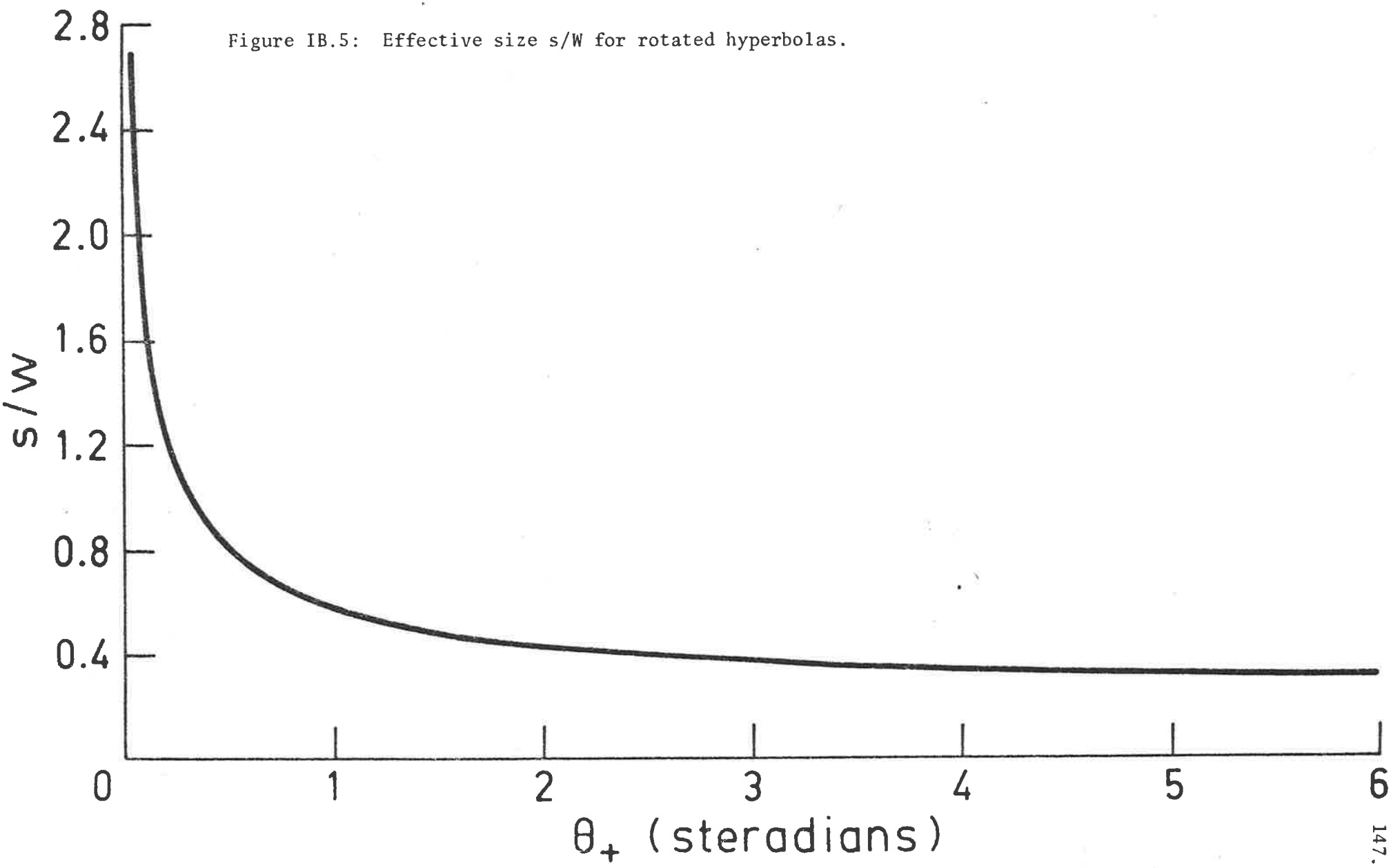

the opening surface is given by α = constant. To satisfy (IB.2) let

$$\bar{\phi} = \frac{\delta}{\theta_+ a} \quad . \tag{IB.28}$$

Then as $r \to \infty$,

$$\delta \to \pm\left(\frac{\pi}{2} - \frac{a}{r}\right)\mathrm{sgn}(z) + O(r^{-3}) \quad , \tag{IB.29}$$

which implies $s = 2a/\pi$. However, $2a$ is the interfocal distance and is given by

$$a = \frac{w}{2 \sin v} \quad , \tag{IB.30}$$

where w is the width of the opening, thus, using (IB.26),

$$s = \frac{w}{\sqrt{\theta_+ \pi} \cdot \sqrt{1 - \frac{\theta_+}{4\pi}}} \quad . \tag{IB.31}$$

Figure IB.5 depicts the variation of s/w with θ_+ for (IB.31). The main feature to note is the slow change of s/w with θ_+, which indicates that the shape of the opening does not have a great effect on s. This conclusion is supported by (IB.24), as shown in Tuck (1975; Figure 3).

We will now examine an orifice with curvature. Consider the axisymmetric opening geometry of Figure IB.6 which as $z \to \infty$, approaches a paraboloid of revolution. The potential in $z > 0$, for unit flow through the hole, can be treated by assuming that

$$-\left.\frac{\partial \phi}{\partial z}\right|_{z=0} = F(r_c) = \begin{cases} \dfrac{1}{2\pi a \sqrt{a^2 - r_c^2}} & r_c < a \\ f(r_c) & r_c > a. \end{cases} \tag{IB.32}$$

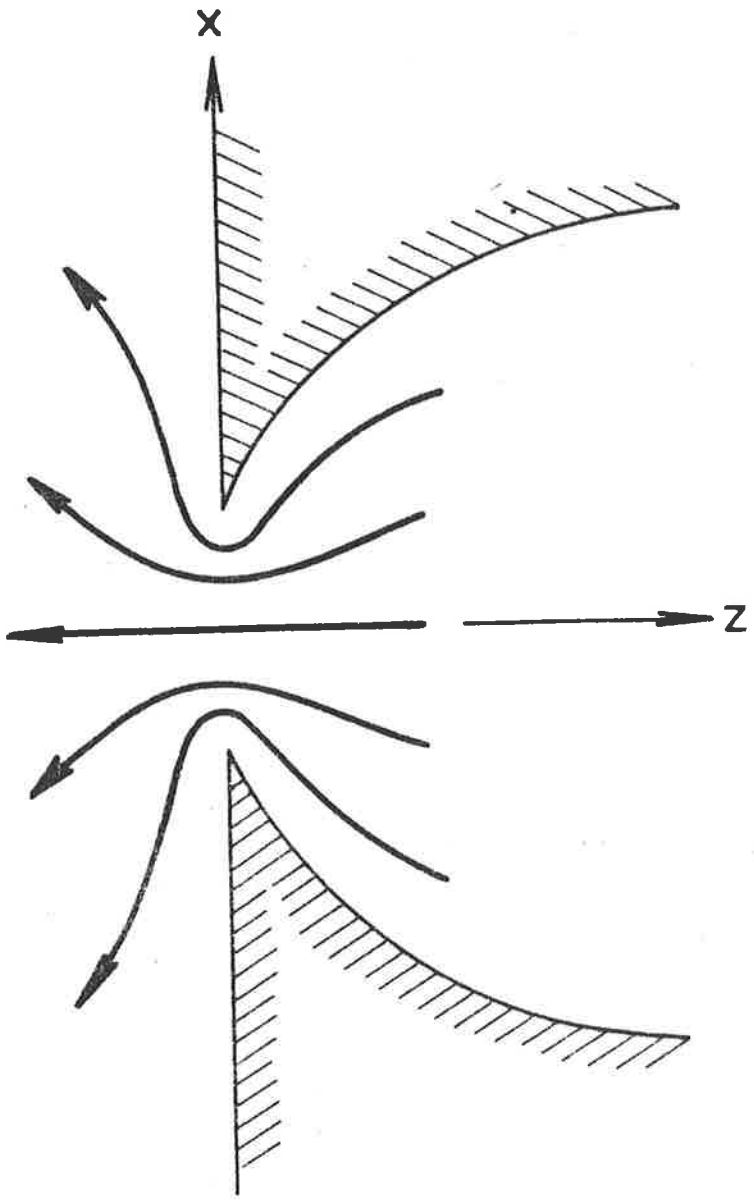

Figure IB.6: Opening geometry for limiting paraboloid.

Then, using Lamb (1932; §102, eq. 4),

$$\phi = \int_0^\infty e^{-pz} J_0(pr_c)\,dp \int_0^\infty F(\zeta) J_0(p\zeta)\,\zeta\,d\zeta, \qquad z \geqslant 0. \tag{IB.33}$$

If $f(r_c) = 0$, the problem is flow through a circular hole in a plane wall, which has the solution, upon evaluating (IB.33),

$$\phi = \frac{1}{2\pi a} \cdot \begin{cases} \arcsin\left(\dfrac{2a}{\sqrt{z^2+(a+r_c)^2}+\sqrt{z^2+(a-r_c)^2}}\right) - \dfrac{\pi}{2} & z > 0 \\ 0 & z=0,\ r_c < a \\ \operatorname{arcosec}\left(\dfrac{r_c}{a}\right) - \dfrac{\pi}{2} & z=0,\ r_c > a, \end{cases} \tag{IB.34}$$

where ϕ is scaled to zero in the aperture. Integrals 6.752.1 and 6.693.6 of Gradshteyn and Ryzhik (1980) can be used to obtain (IB.34).

If $f(r_c) \neq 0$ then

$$\phi = \phi_\rho + \phi_\varepsilon\,, \tag{IB.35}$$

where ϕ_ρ is the potential in (IB.34) and ϕ_ε is the potential due to the flow "through" the walls $r_c > w$. If the interior surface is given by $z = Z(r_c)$, then along $z=0$, allowing for unit flux,

$$\frac{\partial \phi}{\partial z} = \frac{\partial \phi_\varepsilon}{\partial z} = \frac{1}{2} Z'(r_c)\, \left.\frac{\partial \phi_\rho}{\partial r_c}\right|_{z=0}\,. \tag{IB.36}$$

However, from (IB.34),

$$\left.\frac{\partial \phi_\rho}{\partial r_c}\right|_{z=0} = \frac{-1}{2\pi r_c \sqrt{r_c^2 - a^2}}\,, \qquad r_c > a, \tag{IB.37}$$

so, in the right-half plane

$$\phi_\varepsilon = \frac{1}{4\pi}\int_0^\infty e^{-pz} J_0(r_c p)\,dp \int_a^\infty \frac{Z'(\zeta)}{\sqrt{\zeta^2-a^2}} J_0(p\zeta)\,d\zeta, \qquad z \geqslant 0. \quad \text{(IB.38)}$$

We are interested in all $Z(r_c)$ which approach the paraboloid of revolution

$$r_c^2 = \alpha z \quad \text{(IB.39)}$$

as $r_c \to \infty$, so consider

$$z = Z(r_c) = \frac{1}{\alpha}(r_c^2 - a^2) \quad . \quad \text{(IB.40)}$$

Substituting (IB.40) into (IB.38) and evaluating the second integral, using Gradshteyn and Ryzhik (1980, 6.554.3), we find that

$$\phi_\varepsilon = \frac{1}{2\pi\alpha}\int_0^\infty e^{-pz} J_0(pr_c)\frac{\cos pa}{p}dp \quad . \quad \text{(IB.41)}$$

This integral is divergent, but we may add a constant to (IB.41), as it is a potential, in such a way to cancel out the divergent element that is, integrating (IB.41) by parts

$$\phi_\varepsilon = \frac{1}{2\pi\alpha} \lim_{\ell \to 0} \{[\ln p(e^{-pz} J_0(pr_c)\cos pa]_\ell^\infty + \ln \ell +$$

$$\int_\ell^\infty \ln p e^{-pz}(zJ_0(pr_c)\cos pa + r_c J_1(pr_c)\cos pa + aJ_0(pr_c)\sin pa)dp\} \quad , \quad \text{(IB.42)}$$

where the $\ln \ell$ component cancels the divergent term in (IB.41). The integral remaining in (IB.42) cannot be evaluated, but as we are only interested in the difference between ϕ_ε as $r \to 0$, and $r \to \infty$, we may let $r_c = 0$ in (IB.42) and find that

$$\phi_\varepsilon = \frac{-1}{2\pi\alpha}[E_c + \ln(a^2+z^2)], \qquad r_c = 0, \quad \text{(IB.43)}$$

where E_c is Euler's constant, Gradshteyn and Ryzhik (1980; 4.441) being used in integrating (IB.42). Therefore, normalizing $\phi_\varepsilon|_{z=0}$ to 0,

$$\phi_\varepsilon \to \frac{-1}{2\pi\alpha} \ln\left(\frac{z}{a}\right) \quad \text{as} \quad z \to \infty \ . \tag{IB.44}$$

Equation (IB.22) indicates that

$$\phi \to \frac{1}{2\pi}\left[\left(\frac{1}{r} - \frac{1}{s}\right) - \frac{1}{\alpha} \ln\left(\frac{2z}{\Omega}\right)\right] \quad \text{as} \quad z \to \infty \tag{IB.45}$$

along the z-axis, as $\gamma_+ = \alpha^{-1}$ for (IB.39), so (IB.34) implies that

$$s = \frac{2a}{\pi} \ , \tag{IB.46}$$

the result (IB.23) without the added potential ϕ_ε, while (IB.44) implies that

$$\Omega = 2a. \tag{IB.47}$$

Thus the s parameter is seen to be associated with plane walls, while the Ω parameter describes the effect of curvature.

Other $Z(r_c)$ than (IB.40) may be studied by this method, for example, if

$$z = Z(r_c) = \frac{1}{\alpha}(r_c - a)^2 \tag{IB.48}$$

it can be shown that s is given by (IB.46) once more, while now

$$\Omega = 2ae^{-\pi/2} \ . \tag{IB.49}$$

APPENDIX IC

Determination of b for Special Cavities

1. Circular-sector Cavity

The normalization condition

$$\iint_{R_I} \phi_1 dxdy = 0 \qquad \text{(IC.1)}$$

must be applied to (3.39) in order to compute the shape parameter b. If the sector, enclosed by the arcs $\theta = \pm\theta_+$, is of radius a, then (IC.1) may be rewritten as

$$\int_0^a r\ln b dr = \int_0^a \left(r\ln r - \frac{r^3}{2a^3}\right)dr \qquad \text{(IC.2)}$$

which, using standard integrals, gives (3.40).

2. Circular cavity

For this case (IC.1) must be applied to (3.41). The circle being of radius a and defined by $r = 2a\cos\theta$, (IC.1) may be rewritten as

$$2\ln b\int_0^{\pi/2}\cos^2\theta d\theta = \int_0^{\pi/2}[2\cos^2\theta(\ln(2a\cos\theta) - \tfrac{1}{2}) + \tfrac{1}{3}\cos^4\theta]d\theta. \qquad \text{(IC.3)}$$

This can be reduced to

$$\ln b = \frac{2}{\pi}\left\{2\int_0^{\pi/2}\cos^2\theta\ln(\cos\theta)d\theta + \frac{\pi}{2}\ln 2a - \frac{\pi}{4} + \frac{\pi}{16}\right\} \qquad \text{(IC.4)}$$

and, using Gradshteyn and Ryzhik (1980; 4.387.9), namely,

$$\int_0^{\pi/2}\ln(\cos x)\cos^{2n}x dx = -\frac{(2n-1)!!}{2^n n!}\left\{\frac{\pi}{2}\ln 2 + \sum_{\ell=1}^{2n}\frac{(-1)^\ell}{\ell}\right\} \qquad \text{(IC.5)}$$

for n=1, equation (3.42) appears.

3. Rectangular cavity

Equation (3.43) may be rewritten as

$$\phi_1 = \frac{1}{2\pi}\,\mathrm{Re}\left\{\ln\left(\sinh\left(\frac{\pi(x+iy)}{2h}\right)\right)\right\} - \frac{x^2}{8hL} + \frac{1}{4hL}\sum_{n=0}^{\infty} a_n \cosh\frac{n\pi x}{h}\cdot\cos\frac{n\pi y}{h}\,, \qquad \text{(IC.6)}$$

where $\mathrm{Re}\{\ \}$ denotes the real part of the quantity in the brackets. This must satisfy

$$\nabla^2\phi_1 = -\frac{1}{4hL} \qquad \text{(IC.7)}$$

in R_1, the boundary conditions

$$\frac{\partial\phi_1}{\partial x} = 0 \quad \text{on} \quad x = 0, L$$
$$\frac{\partial\phi_1}{\partial y} = 0 \quad \text{on} \quad y = \pm h \qquad \text{(IC.8)}$$

and the limit condition

$$\phi_1 \to \frac{1}{2\pi}\ln\left(\frac{r}{b}\right) \quad \text{as} \quad r \to 0. \qquad \text{(IC.9)}$$

The Laplacians of the first and last terms of (IC.6) are zero so (IC.7) is easily satisfied. The logarithmic term of (IC.6) is the complex potential for a source placed halfway between two impermeable plates at $y=\pm h$, as shown in Lamb (1932; Article 64, point 4), so that it will obviously satisfy the boundary conditions on $x=0$, $y=\pm h$ and the singularity condition at $(0,0)$. The second term also manifestly obeys these conditions, as it vanishes as $r \to 0$. The last term of (IC.6) obeys the three boundary conditions and, when taken in conjunction with the logarithmic term, the condition (IC.9) clearly leads to (3.44).

However, the boundary condition $\partial\phi_1/\partial x = 0$ on $x=L$ still needs to be demonstrated and in the process values for a_n, $n=1,2,\ldots,$

will be derived. Now, as

$$\coth\left(\frac{\pi}{2h}(L+iy)\right) = \frac{\sinh\left(\frac{\pi L}{h}\right) - i\sin\left(\frac{\pi y}{h}\right)}{\cosh\left(\frac{\pi L}{h}\right) - \cos\left(\frac{\pi y}{h}\right)} , \qquad \text{(IC.10)}$$

$\partial\phi_1(L,y)/\partial x = 0$ may be written as

$$\sum_{n=1}^{\infty} A_n \cos\frac{n\pi y}{h} = \frac{Lh}{\pi}\left\{1 - \frac{\sinh\left(\frac{\pi L}{h}\right)}{\cosh\left(\frac{\pi L}{h}\right) - \cos\left(\frac{\pi y}{h}\right)}\right\} \qquad \text{(IC.11)}$$

where

$$A_n = na_n \sinh\left(\frac{n\pi L}{h}\right) . \qquad \text{(IC.12)}$$

If the denominator of the right-hand side of (IC.11) is converted into a geometric cosine series, that is,

$$\sum_{n=1}^{\infty} A_n \cos\frac{n\pi y}{h} = \frac{Lh}{\pi}\left\{1 - \tanh\left(\frac{\pi L}{h}\right)\sum_{\ell=0}^{\infty}\left(\frac{\cos\left(\frac{\pi y}{h}\right)}{\cosh\left(\frac{\pi L}{h}\right)}\right)^{\ell}\right\}, \qquad \text{(IC.13)}$$

then, using the orthogonality of the cosine functions, (IC.13) may be written as

$$A_n = -\frac{2hL}{\pi^2}\tanh\left(\frac{\pi L}{h}\right)\sum_{\ell=0}^{\infty}\left(\cosh\left(\frac{\pi L}{h}\right)\right)^{-\ell}\int_0^{\pi}\cos^{\ell}\tau\cos n\tau d\tau, \quad n \geqslant 1. \qquad \text{(IC.14)}$$

Upon use of Gradshteyn and Ryzhik (1980; 3.631.17) to evaluate the integral in (IC.14), the coefficients a_n, $n=1,2,\ldots,$ are defined as in (3.45).

To find a_0, and hence b through (3.44), the normalization condition (IC.1) is used, that is,

$$0 = -\frac{hL^3}{3} + 2a_0hL + \frac{2Lh}{\pi}\,\mathrm{Re}\left\{\int_{-h}^{h}\int_0^{L}\ln\left(\sinh\left(\frac{\pi(x+iy)}{2h}\right)\right)dxdy\right\} . \qquad \text{(IC.15)}$$

The last term in (IC.15), denoted I, is integrated by parts, and using the identity $\partial/\partial x = -i(\partial/\partial y)$ we obtain

$$\frac{\pi I}{2Lh} = \mathcal{R}e\left\{L\int_{-h}^{h} \ln\left(\sinh\left(\frac{\pi}{2h}(L+iy)\right)\right)dy + i\int_0^L x\ln\left[\frac{\sinh\left(\frac{\pi}{2h}(x+ih)\right)}{\sinh\left(\frac{\pi}{2h}(x-ih)\right)}\right]dx\right\} , \quad \text{(IC.16)}$$

which, upon expanding the hyperbolic functions in the second integral, becomes

$$\frac{\pi I}{2Lh} = \mathcal{R}e\left\{L\int_{-h}^{h} \ln\left(\sinh\left(\frac{\pi}{2h}(L+iy)\right)\right)dy\right\} - \frac{\pi L^2}{2} . \quad \text{(IC.17)}$$

The real part of the integrand in (IC.17) is given by

$$\mathcal{R}e\left\{\sinh\left(\frac{\pi}{2h}(L+iy)\right)\right\} = \frac{1}{2}\ln\left(\sinh^2\left(\frac{\pi L}{2h}\right)\cos^2\left(\frac{\pi y}{2h}\right)+\cosh^2\left(\frac{\pi L}{h}\right)\sin^2\left(\frac{\pi y}{2h}\right)\right)$$

$$= \frac{1}{2}\ln\left(\cosh^2\left(\frac{\pi L}{2h}\right)-\cos^2\left(\frac{\pi y}{2h}\right)\right) , \quad \text{(IC.18)}$$

so, making the change of variable $\tau = \pi y/2h$, (IC.17) becomes

$$\frac{\pi I}{2Lh} = -\frac{\pi L^2}{2} + \frac{hL}{\pi}\int_{-\pi/2}^{\pi/2} \ln(\alpha^2-\cos^2\tau)d\tau , \quad \text{(IC.19)}$$

where

$$\alpha = \cosh\left(\frac{\pi L}{2h}\right) > 1 . \quad \text{(IC.20)}$$

Integrating by parts, (IC.19) becomes

$$\frac{\pi I}{2Lh} = -\frac{\pi L^2}{2} + \frac{hL}{\pi}\left\{2\pi\ln\alpha - 2\int_0^{\pi/2} \frac{\tau\sin 2\tau}{\alpha^2-\cos^2\tau}\,d\tau\right\}, \quad \text{(IC.21)}$$

but, using Gradshteyn and Ryzhik (1980; 3.812.2), namely

$$\int_0^{\pi/2} \frac{x\sin 2x}{1+a\cos^2 x}\,dx = \frac{\pi}{a}\ln\left(\frac{1+\sqrt{1+a}}{2}\right) , \quad a > -1,\ a \neq 0, \quad \text{(IC.22)}$$

(IC.21) becomes

$$\frac{\pi I}{2Lh} = -\frac{\pi L^2}{2} + 2hL\ln\left(\frac{\cosh\frac{\pi L}{2h} + \sinh\frac{\pi L}{2h}}{2}\right) \quad . \qquad \text{(IC.23)}$$

Using the exponential identities for the hyperbolic functions (IC.23) becomes

$$I = L^3h - \frac{4L^2h^2}{\pi}\ln 2, \qquad \text{(IC.24)}$$

so, from (IC.15),

$$a_0 = -\frac{L^2}{3} + \frac{2Lh}{\pi}\ln 2 \ . \qquad \text{(IC.25)}$$

4. Inverse Method

For the second order potential

$$\phi_1 = \frac{1}{2\pi}\ln\left(\frac{r}{b}\right) = \frac{r^2}{4\pi a^2} - \frac{r^2\cos 2\theta}{4\pi a^2\lambda} \qquad \text{(IC.26)}$$

we need to solve the differential equation (3.50), or

$$\frac{dr}{d\theta} = \frac{\lambda}{r\sin 2\theta}\left(a^2 - r^2\left(1 + \frac{\cos 2\theta}{\lambda}\right)\right) \quad . \qquad \text{(IC.27)}$$

Multiplying both sides of (IC.27) by the integrating factor $\tan^{\lambda}\theta$ gives the exact differential equation

$$\frac{r}{\lambda}\tan^{\lambda}\theta\sin 2\theta dr + \left(r^2\left(1 + \frac{\cos 2\theta}{\lambda}\right) - a^2\right)\tan^{\lambda}\theta d\theta = 0 \ . \qquad \text{(IC.28)}$$

Thus, using the procedure for solving exact d.e.'s as set out in Kreyszig (1979, §1.5), we obtain (3.52). To evaluate b for a particular λ the expression (IC.26) must be integrated over the cavity either analytically or numerically.

APPENDIX ID

Semi-infinite Line Sources

1. Properties

Consider an inviscid fluid moving irrotationally in three dimensions which has a line of unit strength sources extending along the negative z-axis from the origin to $z = -\ell$. The velocity potential at a point $P(x,y,z)$ in this fluid is

$$\phi(P) = -\frac{1}{4\pi}\int_{-\ell}^{0} \frac{d\zeta}{\sqrt{\zeta^2-2z\zeta+r^2}} + C \ , \qquad \text{(ID.1)}$$

where

$$r = (x^2+y^2+z^2)^{\frac{1}{2}} \qquad \text{(ID.2)}$$

and C is any constant. We shall give C the special value

$$C = \frac{1}{4\pi} \ln 2\ell \ . \qquad \text{(ID.3)}$$

Equation (ID.1) can be rewritten as

$$\phi(P) = \frac{1}{4\pi}\left[\ln(r+z) + \ln\left|\frac{2\ell}{z+\ell+\sqrt{\ell^2+r^2+2z\ell}}\right|\right] \ . \qquad \text{(ID.4)}$$

If we now take the limit of (ID.4) as $\ell \to \infty$, keeping $r << \ell$, the potential reduces to

$$\phi(P) = \frac{1}{4\pi} \ln(r+z) \qquad \text{(ID.5)}$$

for the resulting semi-infinite line source. This result is interesting as it gives a logarithmic solution to Laplace's equation in three dimensional potential theory. Even though the

potential is known, see Whittaker and Watson (1958; §18.30), it does not seem to have been used extensively.

This axisymmetric potential has a corresponding Stoke's stream function of

$$\psi = \frac{1}{4\pi}(r+z) \ , \tag{ID.6}$$

with stream surfaces given by

$$16\pi^2\psi^2 + 8\pi\psi z = x^2+y^2 \ . \tag{ID.7}$$

Note that these stream surfaces are paraboloids of revolution, as are the equipotential surfaces given by

$$e^{8\pi\theta} - 2e^{4\pi\phi}z = x^2+y^2 \ . \tag{ID.8}$$

However, (ID.5) is *not* a separable solution of Laplace's equation in paraboloidal coordinates.

2. Potential due to a source on a curved surface

The logarithmic potential (ID.5) is useful in describing the near field of a source located on a curved surface which is locally axisymmetric.

Consider a region R, bounded by a surface S on which a point source is located at the origin O. The Neumann boundary condition

$$\nabla\phi.\underset{\sim}{n} = 0 \tag{ID.9}$$

is satisfied on S, except at O.

In the region $R_0 \subset R$ in the vicinity of O we assume that S is locally axisymmetric about a z-axis drawn through O normal

to S, the positive z-axis being in R_0. This part of S, denoted S_0, may be approximated by the paraboloid of revolution

$$x^2+y^2 = \alpha z, \quad \alpha > 0, \tag{ID.10}$$

so, on S_0, the normal is in the direction

$$\underset{\sim}{n} = (2x,2y,-\alpha) \ . \tag{ID.11}$$

We now let the potential in R_0 have the axisymmetric expansion

$$\phi = -\frac{1}{4\pi r} + \mu \ln(r+z) + O(1) \ , \tag{ID.12}$$

where μ, which has dimensions of inverse length, is yet to be determined. To obtain μ, the boundary condition (ID.9) is invoked on S_0, using (ID.11), to give

$$\mu\left(1 - \frac{2z}{r+z}\right) = \frac{z}{4\pi r^2} \ , \tag{ID.13}$$

but $r^2 = \alpha z+z^2$ on S_0 and as $z \to 0$ so

$$\mu \to \frac{1}{4\pi\alpha} \ . \tag{ID.14}$$

Thus, in S_0,

$$\phi = \frac{1}{4\pi}\left[-\frac{1}{r} + \frac{1}{\alpha}\ln(r+z)\right] + O(1) \ . \tag{ID.15}$$

This result shows that a source on a locally axisymmetric curved surface has properties combining those of an isolated point source extending from O along the axis of symmetry into the body.

APPENDIX IE

Parameter Determination for Special 3D Cavities

1. Conical Sector

The potential for this geometry is given by (4.42), that is

$$\phi_1 = \frac{r^2}{8\pi a^3} + \frac{1}{4\pi r} - \frac{1}{4\pi b_0} \quad . \tag{IE.1}$$

The normalization condition (4.30), that is

$$\iiint_V \phi_1 dV = 0 \ , \tag{IE.2}$$

is used to find b_0. So, substituting (IE.1) into (IE.2) gives

$$\int_0^{2\pi}\int_0^{a}\int_0^{v}\left(\frac{r^2}{2a^3} + \frac{1}{r}\right) r^2 \sin\varphi d\varphi dr d\psi = \frac{\theta_+ a^3}{3b_0} \tag{IE.3}$$

or, simplifying,

$$b_0^{-1} = \frac{6\pi}{\theta_+ a^3}(1 - \cos v)\left(\frac{a^2}{10} + \frac{a^2}{2}\right)$$

$$= \frac{9}{5a} \ , \tag{IE.4}$$

using (IB.26).

2. Circular Cylindrical Prism

The geometry of this cavity is shown in Figure IE.1a. We need to satisfy (4.39) or

$$\nabla^2\phi_1 = \frac{1}{2V} \tag{IE.5}$$

in the cavity, subject to (4.40) on the boundaries and

$$\phi_1 \to \frac{1}{4\pi}\left(\frac{1}{r} - \frac{1}{b_0}\right) \tag{IE.6}$$

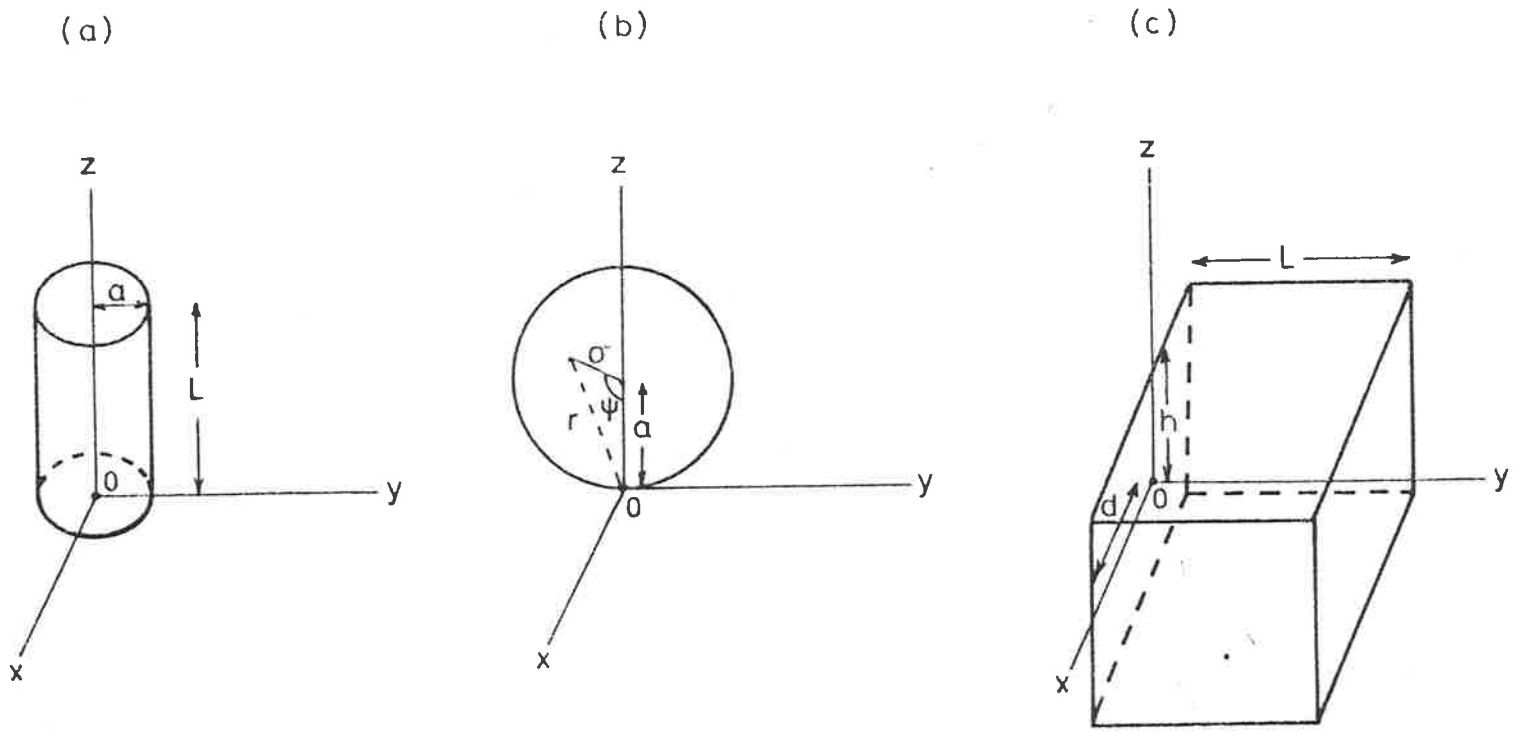

Figure IE.1: Cavities considered in §4.5; (a) circular cylinder, (b) sphere, (c) rectangular prism.

as $r \to 0$. It is easily seen that (4.44) satisfies all our criteria except $\partial\phi_1/\partial z = 0$ on $z=L$, thus this condition will be employed to find a_n and C.

Forcing this boundary condition on (4.44) means that

$$\sum_{n=1}^{\infty} A_n J_0\left(\frac{\alpha_n}{a} r_c\right) = \frac{1}{2\pi a} - \frac{aL}{4\pi(r_c^2+L^2)^{3/2}} , \qquad \text{(IE.7)}$$

where

$$A_n = \alpha_n a_n \sin\left(\frac{\alpha_n}{a} L\right) , \qquad n=1,2,\ldots . \qquad \text{(IE.8)}$$

Note that if, for some n,

$$L = \frac{\ell\pi a}{\alpha_n} , \qquad \ell=0,1,2,\ldots \qquad \text{(IE.9)}$$

we let that particular $a_n = 0$.

Using the orthogonality identity

$$\int_0^a r_c J_0\left(\frac{\alpha_n}{a} r_c\right) J_0\left(\frac{\alpha_\ell}{a} r_c\right) dr_c = \begin{cases} 0 & \ell \neq n \\ \dfrac{a^2}{2} J_1^2(\alpha_\ell) & \ell = n, \end{cases} \qquad \text{(IE.10)}$$

(IE.7) is simplified, by multiplying by $r_c J_0\left(\frac{\alpha_\ell}{a} r_c\right)$ and integrating from 0 to a with respect to r_c, to give

$$A_\ell = \frac{1}{a^2 J_1^2(\alpha_\ell)\pi}\left[\frac{1}{a}\int_0^a r_c J_0\left(\frac{\alpha_\ell}{a} r_c\right) dr_c - \frac{aL}{2}\int_0^a \frac{r_c J_0\left(\frac{\alpha_\ell}{a} r_c\right)}{(r_c^2+L^2)^{3/2}} dr_c\right], \quad \ell=1,2,\ldots . \qquad \text{(IE.11)}$$

Now, using Abramowitz and Stegun (1972; eq. 11.3.20), the first term in (IE.11) becomes $aJ_1(\alpha_\ell)/\alpha_\ell$ and the second term, upon integration by parts, gives

$$\frac{aL}{2}\int_0^a \frac{r_c J_0\left(\frac{\alpha_\ell}{a} r_c\right)}{(r_c^2+L^2)^{3/2}}\, dr_c = \frac{L}{2}\left[- \frac{J_0(\alpha_\ell)}{\sqrt{1+\left(\frac{L}{a}\right)^2}} + \frac{a}{L} - a\int_0^a \frac{J_1\left(\frac{\alpha_\ell}{a} r_c\right)}{\sqrt{r_c^2+L^2}}\, dr_c \right]. \qquad \text{(IE.12)}$$

However, making the change of variable $\tau = \frac{\alpha_\ell r_c}{a}$ in (IE.12) we find that (IE.11) becomes

$$A_\ell = \frac{1}{aJ_1^2(\alpha_\ell)\pi}\left[\frac{J_1(\alpha_\ell)}{\alpha_\ell} - \frac{1}{2} + \frac{\alpha_\ell L}{2a}\int_0^{\alpha_\ell} \frac{J_1(\tau)\, d\tau}{\sqrt{\tau^2+\left(\frac{\alpha_\ell L}{a}\right)^2}}\right], \quad \ell=1,2,\ldots, \qquad \text{(IE.13)}$$

as $J_0(\alpha_\ell) = 0$, and so (4.45) follows from (IE.8). The integral in (IE.13) is evaluated using Simpson's rule, as no simple expression could be found for it.

To find C the normalization condition (IE.2) is used, that is, from (4.44)

$$C = -\frac{1}{\pi a^2 L}\left[\frac{L^2}{12} + \frac{1}{2}\int_0^a\int_0^L \frac{r_c}{\sqrt{r_c^2+z^2}}\, dr_c\, dz + 2\pi \sum_{n=1}^{\infty} a_n \int_0^a r_c J_0\left(\frac{\alpha_n r_c}{a}\right) dr_c \int_0^L \cos\left(\frac{\alpha_n z}{a}\right) dz\right]. \qquad \text{(IE.14)}$$

Now using Abramowitz and Stegun (1972; eq. 11.3.20) again and evaluating the cosine integral, the last term of (IE.14) simplifies to

$$2\pi a^3 \sum_{n=1}^{\infty} \frac{a_n}{\alpha_n^2} \sin\left(\frac{\alpha_n L}{a}\right) J_1(\alpha_n) . \qquad \text{(IE.15)}$$

The other integral may be studied through the change of variable $u = r_c^2+z^2$ so that

$$\frac{1}{2}\int_0^a \int_0^L \frac{r_c}{\sqrt{r_c^2+z^2}}\, dr_c\, dz = \frac{1}{4}\int_0^L dz \int_0^a u^{-\frac{1}{2}} \frac{du}{dr_c}\, dr_c$$

$$= \frac{1}{2}\int_0^L (\sqrt{z^2+a^2} - z)\, dz \ . \qquad \text{(IE.16)}$$

If the change of variable $z = a\sinh\tau$ is now made in (IE.16) we find that

$$\frac{1}{2}\int_0^a \int_0^L \frac{r_c}{\sqrt{r_c^2+z^2}}\, dr_c\, dz = -\frac{L^2}{4} + \frac{a^2}{4}\left[\operatorname{arcsinh}\left(\frac{L}{a}\right) + \frac{L}{a}\cosh\left(\operatorname{arcsinh}\left(\frac{L}{a}\right)\right)\right]. \qquad \text{(IE.17)}$$

Thus substitution of (IE.15) and (IE.17) back into (IE.14) gives the expression (4.47) for C.

3. Spherical Cavities

A spherical cavity of radius a, with its aperture at the origin, will be considered. The orientation of the positive z-axis is into the cavity through the orifice, perpendicular to the limiting boundary at 0. It will be shown, using Legendre polynomial expansions for ϕ_1 in the resonator, that (4.50) is the potential inside the cavity.

Consider the coordinate system in Figure IE.1b. We must satisfy

$$\nabla^2\phi_1 = \frac{3}{8\pi a^3} \qquad \text{(IE.18)}$$

in R_1, such that

$$\left.\frac{\partial\phi_1}{\partial\sigma}\right|_{\sigma=a} = 0 \ , \qquad \text{(IE.19)}$$

except as $r \to 0$, where

$$\phi_1 \to \frac{1}{4\pi}\left(\frac{1}{r} - \frac{1}{b_0}\right) - \frac{1}{8\pi a}\ln\left(\frac{r+z}{\Lambda_0}\right) \quad . \tag{IE.20}$$

Let

$$\chi = \phi_1 - \frac{3\sigma^2\cos^2\psi}{16\pi a^3} \quad , \tag{IE.21}$$

then (IE.18) - (IE.20) become

$$\nabla^2\chi = 0 \quad , \tag{IE.22}$$

$$\frac{\partial\chi}{\partial\sigma} = -\left.\frac{3\sigma\cos^2\psi}{8\pi a^3}\right|_{\sigma=a} \quad , \qquad \psi\neq 0 \quad , \tag{IE.23}$$

and

$$\chi \to \frac{1}{4\pi}\left(\frac{1}{r} - \frac{1}{b_0}\right) - \frac{1}{8\pi a}\ln\left(\frac{r+z}{\Lambda_0}\right) - \frac{3}{16\pi a} \quad , \qquad r \to 0 \tag{IE.24}$$

respectively. To satisfy (IE.22) let

$$\chi = \frac{1}{4\pi r} + \sum_{n=0}^{\infty} a_n \sigma^n P_n(\cos\psi) \quad , \tag{IE.25}$$

where P_n are Legendre polynomials. Then (IE.23) implies that

$$\sum_{n=1}^{\infty} A_n P_n(\cos\psi) - \frac{1}{8\sqrt{2}\pi a^2(1-\cos\psi)^{1/2}} = -\frac{3\cos^2\psi}{8\pi a^2} \quad , \tag{IE.26}$$

where

$$A_n = n a^{n-1} a_n \quad , \qquad n=1,2,3,\ldots \quad . \tag{IE.27}$$

The orthogonality relation for Legendre polynomials, namely

$$\int_{-1}^{1} P_n(X) P_\ell(X)\,dX = \begin{cases} 0 & \ell\neq n \\ (n+\frac{1}{2})^{-1} & \ell=n \end{cases} \quad , \tag{IE.28}$$

may be invoked by multiplying (IE.26) by $P_\ell(\cos\psi)\sin\psi$ and

integrating from 0 to π with respect to ψ, making the change of variable $X = \cos\psi$, to give

$$A_n (n+\tfrac{1}{2})^{-1} = \frac{-3}{8\pi a^2} \int_{-1}^{1} X^2 P_n(X)\,dX + \frac{1}{8\pi\sqrt{2}a^2} \int_{-1}^{1} \frac{P_n(X)}{\sqrt{1-X}}\,dX, \quad n \geq 1, \tag{IE.29}$$

From Gradshteyn and Ryzhik (1980; 7.222.1) the first integral in (IE.29) vanishes for $n > 2$; for the remaining cases it is easily shown that

$$\int_{-1}^{1} X^2 P_n(X)\,dX = \begin{cases} 0 & n=1 \\ \frac{4}{15} & n=2. \end{cases} \tag{IE.30}$$

The second integral in (IE.29) takes the value $\sqrt{2}/(n+\frac{1}{2})$, as shown by Gradshteyn and Ryzhik (1980; 7.225.3). Therefore, (IE.29) becomes

$$a_n = \begin{cases} \dfrac{1}{8\pi n a^{n+1}} & n=1,3,4,\ldots \\ \dfrac{-1}{16\pi a^3} & n=2\ . \end{cases} \tag{IE.31}$$

To find a_0 the normalization condition (IE.2) will be employed. This condition, using (IE.21) and (IE.25), becomes

$$2\pi \int_0^{\pi}\int_0^{a} \left[\frac{\sigma^2 \sin\psi}{4\pi r} + \sigma^2 \sin\psi \sum_{n=0}^{\infty} a_n \sigma^n P_n(\cos\psi) + \frac{3\sigma^4}{16\pi a^3} \cos^2\psi \sin\psi\right] d\sigma\, d\psi = 0, \tag{IE.32}$$

the three terms of which we will denote I_1, I_2 and I_3 respectively. It is easily shown that

$$I_3 = \frac{3a^2}{40} \int_0^{\pi} \cos^2\psi \sin\psi\, d\psi = \frac{a^2}{20} \tag{IE.33}$$

but I_1 and I_2 are more complicated.

Using the change of variable $X = \cos\psi$, I_2 may be written as

$$I_2 = 2\pi \sum_{n=0}^{\infty} a_n \frac{a^{n+3}}{n+3} \int_{-1}^{1} P_n(X)dX \ , \qquad \text{(IE.34)}$$

but

$$\int_{-1}^{1} P_n(X)dX = \begin{cases} 0 & n \geq 1 \\ 2 & n = 0 \end{cases} , \qquad \text{(IE.35)}$$

so

$$I_2 = \frac{4\pi a_0 a^3}{3} \ . \qquad \text{(IE.36)}$$

Now r and σ are related by the expression

$$r = (\sigma^2+a^2-2a\sigma\cos\psi)^{\frac{1}{2}} \ , \qquad \text{(IE.37)}$$

so I_1 may be written as

$$I_1 = \frac{1}{2} \int_0^a \frac{\sigma^2}{\sqrt{2a\sigma}} d\sigma \int_0^{\pi} \frac{\sin\psi}{\sqrt{g-\cos\psi}} d\psi \ , \qquad \text{(IE.38)}$$

where

$$g = \frac{\sigma^2+a^2}{2a\sigma} \ . \qquad \text{(IE.39)}$$

If we let $\zeta = g-\cos\psi$, (IE.38) may be simplified to

$$I_1 = \frac{1}{\sqrt{2a}} \int_0^a \sigma^{3/2}[(g+1)^{\frac{1}{2}}-(g-1)^{\frac{1}{2}}]d\sigma \ , \qquad \text{(IE.40)}$$

which, upon substituting (IE.39) into (IE.40), reduces to

$$I_1 = \frac{a^2}{2} \ . \qquad \text{(IE.41)}$$

So, referring back to (IE.32), we find that

$$a_0 = -\frac{33}{80\pi a} \ . \qquad \text{(IE.42)}$$

Therefore, invoking (IE.21) and (IE.25),

$$\phi_1 = \frac{1}{4\pi r} + \frac{3\sigma^2\cos^2\psi}{16\pi a^3} - \frac{33}{80\pi a} + \frac{\sigma\cos\psi}{8\pi a^2} - \frac{\sigma^2 P_2(\cos\psi)}{16\pi a^3} + \frac{1}{8\pi a}\sum_{n=3}^{\infty}\left(\frac{\sigma}{a}\right)^n \frac{P_n(\cos\psi)}{n} \quad . \tag{IE.43}$$

This expression can be simplified, as the summation is connected to the Legendre polynomial generating function, that is, if

$$t = \frac{\sigma}{a} \quad . \tag{IE.44}$$

and

$$z = \cos\psi \tag{IE.45}$$

then

$$\int \frac{1}{t}\sum_{n=3}^{\infty} P_n(z)\,t^n\,dt = \sum_{n=3}^{\infty} P_n(z)\frac{t^n}{n} \quad . \tag{IE.46}$$

However, from Gradshteyn and Ryzhik (1980; 8.921),

$$\sum_{n=0}^{\infty} t^n P_n(z) = (1-2tz+t^2)^{-\frac{1}{2}}, \qquad |t| < 1 \ , \tag{IE.47}$$

so (IE.46) becomes

$$\sum_{n=3}^{\infty} P_n(z)\frac{t^n}{n} = \int\left[\frac{1}{t\sqrt{1-2tz+t^2}} - \frac{1}{t} - z - tP_2(z)\right]dt, \qquad |t| < 1 \ , \tag{IE.48}$$

which, upon use of Gradshteyn and Ryzhik (1980; 2.266), gives

$$\sum_{n=3}^{\infty} P_n(z)\frac{t^n}{n} = -\left\{tz + \frac{t^2}{2}P_2(z) + \ln\left(2-2zt+2\sqrt{1-2tz+t^2}\right)\right\}, \quad |t| < 1. \tag{IE.49}$$

Substituting (IE.49) into (IE.43) and changing the coordinates to a wholly aperture-centred system gives (4.50). Note, however, that this solution is only valid for $\sigma < a$ and on $\sigma = a$ we need another expression. Equation (IE.43) is still valid on this sphere, so a usable solution is obtained for $\sigma = a$ if $\sum_{n=3}^{\infty} P_n(\cos\psi)/n$ can be evaluated. In fact, Gradshteyn and Ryzhik (1980; 8.926.1)

gives us that

$$\sum_{n=3}^{\infty} \frac{P_n(\cos\psi)}{n} = -\ln(\sin\tfrac{\psi}{2}) - \ln(1+\sin\tfrac{\psi}{2}) - \cos\psi - \tfrac{1}{2}P_2(\cos\psi) \quad , \quad \text{(IE.50)}$$

so, on $\sigma = a$, where $r = a\sqrt{2-2\cos\psi}$, the potential is

$$\phi_1\Big|_{\sigma=a} = \frac{3\cos^2\psi}{16\pi a} + \frac{1}{4\pi a\sqrt{2-2\cos\psi}} - \frac{33}{80\pi a} - \frac{1}{8\pi a}(\ln[(\sin\tfrac{\psi}{2})(1+\sin\tfrac{\psi}{2})]+P_2(\cos\psi)). \quad \text{(IE.51)}$$

This, of course, gives a singularity at $\psi=0$, the aperture location.

4. Rectangular Prism

The geometry of this cavity is shown in Figure IE.1c. We must satisfy

$$\nabla^2\phi_1 = \frac{1}{8hdL} \quad \text{(IE.52)}$$

in R_I, subject to (4.40) on the boundaries, except at 0 where (IE.6) must be true. Using the ideas of Tuck (1975; §6) we know that the potential of a line of sinks spaced at intervals of $2d$ along the x-axis is

$$\phi_S = \frac{1}{4\pi r} + \frac{1}{4\pi}\sum_{\ell=1}^{\infty}\left\{\frac{1}{\sqrt{(x-\ell d)^2+y^2+z^2}} + \frac{1}{\sqrt{(x+\ell d)^2+y^2+z^2}} - \frac{2}{\ell d}\right\} . \quad \text{(IE.53)}$$

This potential gives us our two walls $x = \pm d$ and a similar row of sinks along the z-axis gives us $z = \pm h$. Thus, to satisfy all our conditions, except $\partial\phi_1/\partial y\Big|_{y=L} = 0$, we let ϕ_1 be given by (4.53).

To force the last boundary condition to hold we will choose appropriate a_n, $n=0,1,2,\ldots$. The procedure for doing this is

similar to that of the last section; that is, (4.53) is partially differential with respect to y and evaluated at $y=L$. Then the orthogonality of the cosine functions is invoked to find a_n, $n=1,2,\ldots,$ with a_0 evaluated by application of the normalization condition (IE.2). The details of this process will not be presented however, as the final expressions involve complicated integrals which must be evaluated numerically and were not investigated.

APPENDIX IIA

The Solution of Equation (6.3).

1. Solution of Outer Equation

Due to the stretching of the outer y-coordinate implicit in (6.1), the interior region R_2 appears to an observer in the outer region R_1 as a line of unit length along the x-axis. The problem to be solved may therefore be thought of as:

$$\frac{\partial}{\partial x} A_1^0(x,Y^0) - \frac{i}{2K} \frac{\partial^2}{\partial Y^{0^2}} A_1^0(x,Y^0) = 0 \quad \text{in} \quad R_2, \tag{IIA.1}$$

subject to

$$A_1^0(0,Y^0) = 1 \tag{IIA.2}$$

and

$$\frac{\partial}{\partial Y^0} A_1^0(x,0) = V(x) \ . \tag{IIA.3}$$

This system is a "heat" equation for a semi-infinite rod with "time"-varying flux at $Y^0=0$. To highlight this equivalence, in the following analysis we let

$$\begin{aligned} x &= t \\ Y^0 &= X \\ K &= \frac{i}{2K} \ . \end{aligned} \tag{IIA.4}$$

If

$$\psi = \frac{\partial}{\partial X} A_1^0(X,t) \tag{IIA.5}$$

then (IIA.1) becomes

$$\frac{\partial \psi}{\partial t} = K \frac{\partial^2 \psi}{\partial X^2} \ , \tag{IIA.6}$$

with the conditions (IIA.2) and (IIA.3) now

$$\left.\begin{aligned} \psi(0,t) &= V(t) \\ \psi(X,0) &= 0 \end{aligned}\right\} . \qquad \text{(IIA.7)}$$

From Carslaw (1921; §23) the solution to (IIA.6) and (IIA.7) is

$$\psi(X,t) = \frac{2}{\sqrt{\pi}} \int_{\frac{X}{2\sqrt{Kt}}}^{\infty} V\left(t - \frac{X^2}{4K\zeta^2}\right) e^{-\zeta^2} d\zeta , \qquad \text{(IIA.8)}$$

which, by the change of variable $\xi = t - X^2/(4K\zeta^2)$, may be written

$$\psi(X,t) = \frac{X}{2\sqrt{\pi K}} \int_0^t V(\xi) \exp\left(- \frac{X^2}{4K(t-\xi)}\right) \cdot (t-\xi)^{-3/2} d\xi . \qquad \text{(IIA.9)}$$

As (IIA.5) has the solution

$$A_1^0(X,t) = 1 - \int_X^{\infty} \psi(\zeta,t) d\zeta , \qquad \text{(IIA.10)}$$

then, substituting (IIA.9) into (IIA.10), we obtain

$$A_1^0(X,t) = 1 - \frac{1}{2\sqrt{\pi K}} \int_0^t \frac{d\xi V(\xi)}{(t-\xi)^{3/2}} \int_X^{\infty} d\zeta . \zeta \exp\left(- \frac{\zeta^2}{4K(t-\xi)}\right). \qquad \text{(IIA.11)}$$

The second integral in (IIA.11) may be evaluated through the change of variable $u = \zeta^2/[4K(t-\xi)]$ to give

$$A_1^0(X,t) = 1 - \sqrt{\frac{K}{\pi}} \int_0^t \frac{d\xi V(\xi)}{\sqrt{t-\xi}} \exp\left(- \frac{X^2}{4K(t-\xi)}\right) . \qquad \text{(IIA.12)}$$

Thus, upon reverting to our original variables, the solution to (IIA.1) is

$$A_1^0(x,Y^0) = 1 - \frac{(1+i)}{2\sqrt{\pi K}} \int_0^x \frac{d\xi V(\xi)}{\sqrt{x-\xi}} \exp(iKY^{0\,2}([2(x-\xi)]) \quad , \quad \text{(IIA.13)}$$

which is equation (6.8) .

2. Expansion of Equation (6.8) for Small Y^0

As we are interested, for matching purposes, in the limit of (IIA.13) as R_2 is approached, the small Y^0 expansion of this equation is required. So, taking a Taylor series expansion of (IIA.13),

$$A_1^0(x,Y^0) = A_1^0(x,0) + \frac{\partial A_1^0(x,0)}{\partial Y^0}|Y^0| + \frac{1}{2}\frac{\partial^2 A_1^0(x,0)}{\partial Y^{0\,2}} Y^{0\,2} + O(Y^{0\,3}). \quad \text{(IIA.14)}$$

However,

$$A_1^0(x,0) = A(x) = 1 - \frac{(1+i)}{2\sqrt{\pi K}} \int_0^x \frac{d\xi V(\xi)}{\sqrt{x-\xi}} \quad , \quad \text{(IIA.15)}$$

the first derivative at $Y^0=0$ is given by (IIA.3) and, using (IIA.1),

$$\frac{\partial^2 A_1^0(x,0)}{\partial Y^{0\,2}} = -2KiA'(x) \quad , \quad \text{(IIA.16)}$$

so (IIA.14) may be written as

$$A_1^0(x,Y^0) = A(x) + V(x)|Y^0| - iKA'(x)Y^{0\,2} + O(Y^{0\,3}) \quad . \quad \text{(IIA.17)}$$

APPENDIX IIB

Solutions for Circular Topography

1. Circular Sills and Canyons

Consider a plane wave incident on a circular submerged feature of uniform depth h_2 and radius a in an ocean of depth h_1. A vertical cylinder connects the two regions, as in §5.2. The incident wave has a velocity potential given by equation (5.2) and the governing equations in the two regions are Helmholtz equations, as shown by (5.1). Sommerfeld's radiation condition (5.3) holds at infinity, and at C, the boundary between the outer region R_1 and the inner region R_2, there are two boundary conditions, namely, continuity of potential (5.4) and continuity of flux (5.5).

As solutions to this problem we will try

$$\phi_1(x,y) = e^{ik_1x} + \sum_{n=0}^{\infty} b_n H_n^{(1)}(k_1r)\cos n\theta \quad \text{in } R_1 \qquad \text{(IIB.1a)}$$

and

$$\phi_2(x,y) = \sum_{n=0}^{\infty} c_n J_n(k_2r)\cos n\theta \quad \text{in } R_2, \qquad \text{(IIB.1b)}$$

where b_n, c_n, $n=0,1,\ldots$ are to be determined, r,θ are polar coordinates centred at the centre of the circle and $J_n, H_n^{(1)}$ are the usual Bessel functions of order n (see Abramowitz and Stegun (1972; Chapter 9)). To use the continuity conditions we must be able to write e^{ik_1x} in terms of a series of Bessel functions; using Gradshteyn and Ryzhik (1980, Eq. 8.511.4) this may be done to give

$$e^{ik_1x} = J_0(k_1r) + 2\sum_{n=1}^{\infty} i^n J_n(k_1r)\cos n\theta \,. \qquad \text{(IIB.2)}$$

If the potential continuity condition (5.4) is invoked then we find that

$$J_0(k_1a)+b_0H_0^{(1)}(k_1a)+\sum_{n=1}^{\infty}(b_nH_n^{(1)}(k_1a)+2i^nJ_n(k_1a))\cos n\theta = \sum_{n=0}^{\infty}c_nJ_n(k_2a)\cos n\theta\ , \qquad \text{(IIB.3)}$$

and invoking the flux continuity condition (5.5) gives

$$k_1^{-1}\{J_0'(k_1a)+\sum_{n=1}^{\infty}[2i^nJ_n'(k_1a)+b_nH_n^{(1)}(k_1a)]\cos n\theta+b_0H_0^{(1)\prime}(k_1a)\} = k_2^{-1}\sum_{n=0}^{\infty}c_nJ_n'(k_2a)\cos n\theta\ . \qquad \text{(IIB.4)}$$

By equating coefficients of $\cos n\theta$, $n=0,1,2,\ldots$, on both sides of (IIB.3) and (IIB.4) a series of equations is formed. Manipulating the two equations for $n=0$ leads to expressions for b_0 and c_0, namely,

$$c_0 = \frac{H_0^{(1)}(k_1a)J_1(k_1a)-J_0(k_1a)H_1^{(1)}(k_1a)}{\frac{k_1}{k_2}J_1(k_2a)H_0^{(1)}(k_1a)-J_0(k_2a)H_1^{(1)}(k_1a)}\ , \qquad \text{(IIB.5a)}$$

$$b_0 = \frac{c_0J_0(k_2a)-J_0(k_1a)}{H_0^{(1)}(k_1a)}\ , \qquad \text{(IIB.5b)}$$

while consideration of the equations for general non-zero n leads to

$$c_n = 2i^n\left[\frac{H_n^{(1)\prime}(k_1a)J_n(k_1a)-J_n'(k_1a)H_n^{(1)}(k_1a)}{J_n(k_2a)H_n^{(1)\prime}(k_1a)-\frac{k_1}{k_2}J_n'(k_2a)H_n^{(1)}(k_1a)}\right] \quad n=1,2,\ldots, \qquad \text{(IIB.6a)}$$

$$b_n = \frac{\frac{k_1}{k_2}c_nJ_n'(k_2a)-2i^nJ_n'(k_1a)}{H_n^{(1)\prime}(k_1a)} \qquad n=1,2,\ldots\ . \qquad \text{(IIB.6b)}$$

Thus we have a series expression for the potential both inside and outside the circular region. Computations involving these series will be discussed in §IIB.3.

2. Circular Islands

The problem of scattering by a circular island of radius a is similar to that described in the preceding section, with $h_2=0$. This means that we only have to find the potential in the outer region R_1, with the boundary condition, from (5.5), of

$$\frac{\partial \phi_1}{\partial r}(a,\theta) = 0 . \qquad \text{(IIB.7)}$$

In R_1 let

$$\phi_1(x,y) = e^{ik_1x} + \sum_{n=0}^{\infty} d_n H_n^{(1)}(k,r)\cos n\theta , \qquad \text{(IIB.8)}$$

where d_n, $n=0,1,2,\ldots$ are to be determined. Because e^{ik_1x} can be represented by Bessel functions, as shown by (IIB.2), the condition (IIB.7) may be invoked to give

$$k_1 J_0'(k_1a) + 2k_1 \sum_{n=1}^{\infty} i^n J_n'(k_1a)\cos n\theta + k_1 \sum_{n=0}^{\infty} d_n H_n^{(1)\prime}(k_1a)\cos n\theta = 0. \qquad \text{(IIB.9)}$$

Upon equating coefficients of $\cos n\theta$, $n=0,1,2,\ldots$ in (IIB.9) it is found that

$$d_0 = -J_1(k_1a)/H_1^{(1)}(k_1a) , \qquad \text{(IIB.10a)}$$

$$d_n = \frac{-2i^n\left[J_{n-1}(k_1a) - \frac{n}{k_1a}J_n(k_1a)\right]}{H_{n-1}^{(1)}(k_1a) - \frac{n}{k_1a}H_n^{(1)}(k_1a)} \qquad n=1,2,\ldots , \qquad \text{(IIB.10b)}$$

so the potential ϕ_1 is representable as a series.

3. Computation

To use the series (IIB.1) and (IIB.8) it is necessary to be able to evaluate $J_n(x)$ and $Y_n(x)$ of arbitrary integer order and then sum the terms in each series until each additional term contributes less than some small quantity, typically of the order of $k_1 a \times 10^{-8}$. The Bessel functions for $n=0,1$ may be easily found by use of the polynomial approximations in Abramowitz and Stegun (1972; §9.4), however, while the higher order functions may be computed from recurrence relations such as in A. & S. (1972; §9.1.27) there are values of the argument for which this technique is unstable. Thus, the procedure set out in A. & S. (1972; §9.12, Example 1) is employed when $n > x$. This procedure essentially uses the recurrence relation in the direction of decreasing n, when it *is* stable. Of course, in this method enough Bessel functions were evaluated for convergence to occur before the highest order function used was needed.

For all $k_1 a$ examined convergence was rapid, generally requiring less than 40 terms, however for $k_1 a$ larger than about 70 the method would become very expensive.

APPENDIX IIC

The Scattering Cross-section

From Sommerfeld's radiation condition (5.3), as $r \to \infty$ then the scattered wave will be of the form

$$\bar{\phi}_1(r,\theta) \sim B(\theta) e^{ik_1 r}/r^{\frac{1}{2}} , \qquad \text{(IIC.1)}$$

where $B(\theta)$ is known as the scattering cross-section of the scatterer. This function essentially shows the directions in which most of the scattered wave radiates.

To find $B(\theta)$ from equation (6.26a) a discretization procedure similar to that described in §6.2 is used, with the additional assumption that as r' is very large then over a segment $H_0^{(1)}(k_1 r')$ and $\partial H_0^{(1)}(k_1 r')/\partial n$ are virtually constant and representable by their large argument asymptotic forms (see Abramowitz and Stegun (1972; eq. 9.2.3)). The radius r' is also approximated by

$$r' \sim (r^2 - 2x\xi - 2y\eta)^{\frac{1}{2}}$$

$$= r\left[1 - \frac{x\xi}{r^2} - \frac{y\eta}{r^2}\right] + O\left(\frac{1}{r}\right) , \qquad \text{(IIC.2)}$$

where the segment midpoint is (x,y), the point approaching infinity is (ξ,η) and

$$r^2 = x^2 + y^2 = O(1) . \qquad \text{(IIC.3)}$$

Using these approximations, and assuming that $\phi_1(x,y)$ on C is already known from numerical computation, an approximation to $B(\theta)$ may be found.

BIBLIOGRAPHY

M. Abramowitz and I.A. Stegun (eds.), 1972. *Handbook of Mathematical Functions* (Dover, New York).

M. Alster, 1972. "Improved calculation of resonant frequencies of Helmholtz resonators", *J. Sound Vib.* 24, 63-85.

R.S. Arthur, 1946. "Refraction of water waves by islands and shoals with circular bottom-contours", *Trans. Amer. Geophys. Union* 27, 168-177.

R.S. Arthur, 1951. "The effect of islands on surface waves", *Bull. Scripps Ocean. Inst.* (Tech. Series) 6, 1-24.

R. Barakat, 1963. "Diffraction of plane waves by an elliptic cylinder", *J. Acoust. Soc. Amer.* 35, 1990-1996.

C. Berhault, 1980. "An integro-variational method for interior and exterior free surface flow problems", *Appl. Ocean Res.* 2, 33-38.

J.C.W. Berkhoff, 1972. "Computation of combined refraction-diffraction", *Proc. 13th Coast. Eng. Conf.* 1, 471-490.

E.N. Bernard and A.S. Vastano, 1977. "Numerical computation of tsunami response for island systems", *J. Phys. Oceanogr.* 7, 389-395.

G.R. Bigg, 1979. "Tsunami: an analysis and review of the phases of a tsunami's history", Honours thesis, Dept. Applied Math., University of Adelaide.

G.R. Bigg, and E.O. Tuck, 1982. "Two dimensional resonators with small openings", *J. Austral. Math. Soc. Ser. B.* 24, 2-27.

G.R. Bigg, 1982a. "The three dimensional cavity resonator", *J. Sound Vib.* 85(2), to appear Nov.-Dec. 1982.

G.R. Bigg, 1982b. "Semi-infinite line sources and locally axisymmetric surfaces", *Int. J. Math. Educ. Science Technol.* 13, 463-466.

H.K. Brock, R.N. Buchal and C.W. Spofford, 1977. "Modifying the sound-speed profile to improve the accuracy of the parabolic-equation technique", *J. Acoust. Soc. Amer.* 62, 543-552.

S.M. Candel, 1979. "Numerical solution of wave scattering problems in the parabolic approximation", *J. Fluid Mech.* 90, 465-507.

G.F. Carrier, 1966. "Gravity waves on water of variable depth", *J. Fluid Mech.* 24, 641-659.

H.S. Carslaw, 1921. *Introduction to the Mathematical Theory of the Conduction of Heat in Solids* (MacMillan, London, 2nd ed.).

L.G. Chambers, 1965. "On long waves on a rotating earth", *J. Fluid Mech.* 22, 209-216.

H.S. Chen and C.C. Mei, 1973. "Wave forces on a stationary platform of elliptical shape", *J. Ship Res.* 17, 61-71.

H.S. Chen and C.C. Mei, 1976. "Oscillations and wave forces in a man-made harbour in the open sea", *Proc. 10th Symp. Naval Hydro.*, 573-594.

M.H.T. Chen, 1976. "Various models of environmental effects of tsunamis", *Crit. Rev. Env. Control* 6, 131-154.

P.L. Christiansen, 1974. "Diffraction of gravity waves by large islands", *Proc. 14th Coast. Eng. Conf.* 1, 601-614.

P.L. Christiansen, 1976. "Diffraction of gravity waves by ray methods", *Lect. Notes Phys.* 64, 28-38.

J. Corones, 1975. "Bremmer series that correct parabolic approximations", *J. Math. Anal. Appl.* 50, 361-372.

E.E. Covert, 1970. "An approximate calculation of the onset velocity of cavity oscillations", *J. Amer. Inst. Aeronaut. Astronaut.* 8, 2189-2194.

A. Cummings, 1973. "Acoustics of a wine bottle", *J. Sound Vib.* 31, 331-343.

R. De Smedt, 1981a. "Low frequency scattering through an aperture in a rigid screen - some numerical results", *J. Sound Vib.* 75, 371-386.

R. De Smedt, 1981b. "Sound penetration through a thin circular ring", *J. Sound Vib.* 75, 387-396.

S.F. Dotsenko and L.V. Cherkesov, 1979. "On the diffraction of a surface gravitational wave over a small irregularity of the bottom", *J. App. Math. Mech.* 43, 684-692.

C. Eckart, 1952. "The propagation of gravity waves from deep to shallow water", *Nat. Bur. Stand. Circ.* 521, 165-173.

S.A. Elder, 1978. "Self-excited depth-mode resonance for a wall-mounted cavity in turbulent flow", *J. Acoust. Soc. Amer.* 64, 877-890.

O. Faltinsen, 1972. "Wave forces on a restrained ship in head-sea waves", *Proc. 9th Symp. Naval Hydro.*, 1763-1844.

J.E. Ffowcs Williams, 1972. "The acoustics of turbulence near sound-absorbent liners", *J. Fluid Mech.* 51, 737-749.

C.J.R. Garrett, 1970. "Bottomless harbours", *J. Fluid Mech.* 43, 433-449.

J. Geer, 1968. "Uniform asymptotic solutions for potential flow around a thin airfoil and the electrostatic potential about a thin conductor", *SIAM J. Appl. Math.* 16, 75-101.

J. Geer, 1974. "Uniform asymptotic solutions for the two-dimensional potential field about a slender body", *SIAM J. Appl. Math.* 26, 539-553.

J. Geer, 1975. "Uniform asymptotic solutions for potential flow about a slender body of revolution", *J. Fluid Mech.* 67, 817-827.

J. Geer, 1978. "The scattering of a scalar wave by a slender body of revolution", *SIAM J. Appl. Math.* 34, 348-370.

J. Geer, 1980. "Electromagnetic scattering by a slender body of revolution: axially incident plane wave", *SIAM J. Appl. Math.* 38, 93-102.

I.S. Gradshteyn and I.M. Ryzhik, 1980. *Table of Integrals, Series, and Products* (Academic Press, London, 4th ed., English trans. ed. by A. Jeffrey).

E.J. Hamilton and V. Kerdemelidis, 1982. "Transmission through slits formed by inclined planes", *IEEE Trans. Ant. Prop.* AP-30, 199-204.

J.L. Hammack, 1972. "Tsunamis - a model of their generation and propagation", *Cal. Inst. Tech. W.M. Keck Lab. Hydraul. Water Res. Rep.* KH-R-28, 1-261.

R.A. Handelsman and J.B. Keller, 1967. "Axially symmetric potential flow around a slender body", *J. Fluid Mech.* 28, 131-147.

P. Haren and C.C. Mei, 1981. "Head sea diffraction by a slender raft with application to wave power absorption", *J. Fluid Mech.* 104, 505-526.

R.F. Harrington, 1982. "Resonant behaviour of a small aperture backed by a conducting body", *IEEE Trans. Ant. Prop.* AP-30, 205-212.

H. von Helmholtz, 1860. "Theorie der Luftschwingungen in Röhten mit offenen Enden", *Crelle* 57, 1-72.

E. Hirschwehr, 1974. "Theoretical and experimental investigation of the mouth-correction for resonance absorbers", *Acustica* 30, 241-246.

K. Honda, T. Terada and D. Isitani, 1908. "On the secondary undulations of oceanic tides", *Phil. Mag. Ser.* 6, 15, 88-126.

J.R. Houston, R.D. Carver and D.G. Markle, 1977. "Tsunami-wave elevation frequency of occurrence for the Hawaiian Islands", *U.S. Army Eng. Waterways Exp. Stat., Vicksburg Miss. Rep.* H-77-16.

J.R. Houston, 1978. "Interaction of tsunamis with the Hawaiian Islands calculated by a finite element numerical model", *J. Phys. Oceanogr.* 8, 93-102.

M.S. Howe, 1975. "Contributions to the theory of aerodynamic sound, with application to excess jet noise and the theory of the flute", *J. Fluid Mech.* 71, 625-673.

M.S. Howe, 1976. "On the Helmholtz resonator", *J. Sound Vib.* 45, 427-440.

M.S. Howe, 1979a. "The influence of grazing flow on the acoustic impedance of a cylindrical wall cavity", *J. Sound Vib.* 67, 533-544.

M.S. Howe, 1979b. "On the theory of unsteady high Reynolds number flow through a circular aperture", *Proc. Roy. Soc. Ser.* A 366, 205-223.

M.S. Howe, 1980a. "On the diffraction of sound by a screen with circular apertures in the presence of a low Mach number grazing flow", *Proc. Roy. Soc. Ser.* A 370, 523-544.

M.S. Howe, 1980b. "The influence of vortex shedding on the diffraction of sound by a perforated screen", *J. Fluid Mech.* 97, 641-653.

M.S. Howe, 1981a. "The role of displacement thickness fluctuations in hydroacoustics, and the jet-drive mechanism of the flue organ pipe", *Proc. Roy. Soc. Ser.* A 374, 543-568.

M.S. Howe, 1981b. "On the theory of unsteady shearing flow over a slot", *Phil. Trans. Roy. Soc. Ser.* A 303, 151-180.

M.S. Howe, 1981c. "The influence of mean shear on unsteady aperture flow, with application to acoustical diffraction and self-sustaining cavity oscillations", *J. Fluid Mech.* 109, 125-146.

J.N. Hunt and R.E. Baddour, 1981. "The diffraction of non-linear progressive waves by a vertical cylinder", *Quart. J. Mech. Appl. Math.* 34, 69-87.

L.S. Hwang and E.O. Tuck, 1970. "On the oscillations of harbours of arbitrary shape", *J. Fluid Mech.* 42, 447-464.

U. Ingard, 1953a. "On the theory and design of acoustic resonators", *J. Acoust. Soc. Amer.* 25, 1037-1061.

U. Ingard, 1953b. "The near field of a Helmholtz resonator exposed to a plane wave", *J. Acoust. Soc. Amer.* 25, 1062-1067.

J.D. Isaacs, E.A. Williams and C. Eckart, 1951. "Total reflection of surface waves by deep water", *Trans. Amer. Geophys. Union* 32, 37-40.

E.V. Jansson, 1977. "Acoustical properties of complex cavities. Prediction and measurement of resonance properties of violin-shaped and guitar-shaped cavities", *Acustica* 37, 211-221.

D.S. Jones, 1974. *The Theory of Electromagnetism* (Pergamon Press, Oxford).

I.G. Jonsson, O. Skovgaard and O. Brink-Kjaer, 1976. "Diffraction and refraction calculations for waves incident on an island", *J. Mar. Res.* 34, 469-496.

J.B. Keller, 1962. "Geometrical theory of diffraction", *J. Opt. Soc. Amer.* 52, 116-130.

L.E. Kinsler and A.R. Frey, 1962. *Fundamentals of Acoustics* (Wiley, New York, 2nd ed.).

E. Kreyszig, 1979. *Advanced Engineering Mathematics* (Wiley, New York, 4th ed.).

H.W. Krieger, 1943. "Island peoples of the Western Pacific; Micronesia and Melanesia", *Smithsonian Inst. War Background Stud.* 16.

G.A. Kriegsmann and E.W. Larsen, 1978. "On the parabolic approximation to the reduced wave equation", *SIAM J. Appl. Math.* 34, 200-204.

G.A. Kriegsmann, 1979. "An illustrative model describing the refraction of long water waves by a circular island", *J. Phys. Oceanogr.* 9, 607-611.

A.D.K. Laird, 1955. "A model study of wave action on a cylindrical island", *Trans. Amer. Geophys. Union* 36, 279-285.

H. Lamb, 1906. "On Sommerfeld's diffraction problem; and on reflection by a parabolic mirror", *Proc. London Math. Soc.* 4, 190-203.

H. Lamb, 1932. *Hydrodynamics* (Cambridge Univ. Press, London, 6th ed.).

C.C. Lautenbacher, 1970. "Gravity wave refraction by islands", *J. Fluid Mech.* 41, 655-672.

J.-J. Lee, 1969. "Wave induced oscillations in harbours of arbitrary shape", *Cal. Inst. Tech. W.M. Keck Lab. Hydraul. Water Res. Rep.* KH-R-20, 1-266.

J.-J. Lee, 1971. "Wave induced oscillations in harbours of arbitrary geometry", *J. Fluid Mech.* 45, 375-394.

M.A. Leontovich and V.A. Fock, 1946. "Solution of the problem of propagation of electromagnetic waves along the earth's surface by the method of the parabolic equation", *J. Phys. U.S.S.R.* 10, 13-24.

F.G. Leppington and H. Levine, 1973. "Reflexion and transmission at a plane screen with periodically arranged circular or elliptical apertures", *J. Fluid Mech.* 61, 109-127.

D. Lewis, 1978. *The Voyaging Stars* (Collins, London).

M.S. Longuet-Higgins, 1967. "On the trapping of wave energy round islands", *J. Fluid Mech.* 29, 781-821.

M.S. Longuet-Higgins, 1969. "On the trapping of long-period waves round islands", *J. Fluid Mech.* 37, 773-784.

M.S. Longuet-Higgins, 1970. "Steady currents induced by oscillations round islands", *J. Fluid Mech.* 42, 701-720.

P. Lorrain and D.R. Corson, 1970. *Electromagnetic Fields and Waves* (Freeman, San Francisco, 2nd ed.).

C. Lozano and R.E. Meyer, 1976. "Leakage and response of waves trapped by round islands", *Phys. Fluids* 19, 1075-1088.

H. Maruo and N. Sasaki, 1975. "On the wave pressure acting on the surface of an elongated body fixed in head seas", *Sel. Pap. J. Soc. Naval Arch. Japan* 13, 34-42.

F. Mattioli, 1978a. "Some integral formulations of the scalar Helmholtz equation", *Lett. Nuovo Cimento Ser. 2* 21, 288-290.

F. Mattioli, 1978b. "Wave induced oscillations in harbours of variable depth", *Comp. Fluids* 6, 161-172.

F. Mattioli and S. Tinti, 1979. "Discretization of harbour resonance problem", *Proc. Amer. Soc. Civ. Eng., J. Waterways, Port, Coast Ocean Div.* 105, 464-469.

F. Mattioli and S. Tinti, 1980. "Response of coastal harbours", *Int. J. Num. Meth. Eng.* 15, 296-301.

F. Mattioli, 1981. "Element integral approach for water waves", *Comp. Fluids* 9, 181-203.

J.J. McCoy, 1977. "A parabolic theory of stress wave propagation through inhomogeneous linearly elastic solids", *J. Appl. Mech.* 44 , 462-468.

S.T. McDaniel, 1975. "Parabolic approximations for underwater sound propagation", *J. Acoust. Soc. Amer.* 58, 1178-1185.

C.C. Mei, 1979. "Grazing incidence of short elastic waves on a slender cavity", *Wave Motion* 1, 113-122.

C.C. Mei and E.O. Tuck, 1980. "Forward scattering by long thin bodies", *SIAM J. Appl. Math.* 39, 178-191.

C.D. Memos, 1980. "Energy transmission by surface waves through an opening", *J. Fluid Mech.* 97, 557-568.

R.E. Meyer and J.F. Painter, 1979. "Wave trapping with shore absorption", *J. Eng. Maths.* 13, 33-45.

R.E. Meyer, 1979. "Theory of water wave refraction", *Adv. Appl. Mech.* 19, 53-141.

R.E. Meyer, 1980. "Exponential Asymptotics", *SIAM Rev.* 22, 213-224.

J.W. Miles and W.H. Munk, 1961. "Harbor paradox", *Amer. Soc. Civ. Eng., J. Waterways Harb. Div.* 87, 111-130.

J.W. Miles and F. Gilbert, 1968. "Scattering of gravity waves by a circular dock", *J. Fluid Mech.* 34, 783-793.

J.W. Miles, 1971. "Resonant response of harbours: an equivalent-circuit analysis", *J. Fluid Mech.* 46, 241-265.

J.W. Miles, 1974. "Harbor seiching", *Ann. Rev. Fluid Mech.* 6, 17-35.

J.W. Miles and Y.K. Lee, 1975. "Helmholtz resonance of harbours", *J. Fluid Mech.* 67, 445-464.

J.W. Miles, 1981a. "Non-linear Helmholtz oscillations in harbours and coupled basins", *J. Fluid Mech.* 104, 407-418.

J.W. Miles, 1981b. "Diffraction of gravity waves by a barrier reef", *J. Fluid Mech.* 109, 115-123.

W. Möhring, 1982. "Finite rank acoustic scattering problems", *J. Acoust. Soc. Amer.* 71, 5-8.

T. Moimoi, 1967. "Long waves around a circular island [I]", *Bull. Earthquake Res. Inst.* 45, 345-357.

D.J. Nefske, J.A. Wolf and L.J. Howell, 1982. "Structural-acoustic finite element analysis of the automobile passenger compartment: a review of current practice", *J. Sound Vib.* 80, 247-266.

P.A. Nelson, N.A. Halliwell and P.E. Doak, 1981. "Fluid dynamics of a flow excited resonance, Part I: experiment", *J. Sound Vib.* 78, 15-38.

R.L. Panton and J.M. Miller, 1975a. "Resonant frequencies of cylindrical Helmholtz resonators", *J. Acoust. Soc. Amer.* 57, 1533-1535.

R.L. Panton and J.M. Miller, 1975b. "Excitation of a Helmholtz resonator by a turbulent boundary layer", *J. Acoust. Soc. Amer.* 58, 800-806.

H.D. Pite, 1977. "The excitation of damped waves diffracted over a submerged circular sill", *J. Fluid Mech.* 82, 621-641.

L.S. Pocinki, 1950. "The application of conformal transformations to ocean wave refraction problems", *Trans. Amer. Geophys. Union* 31, 856-866.

J. Proudman, 1914. "Diffraction of tidal waves on flat rotating sheets of water", *Proc. London Math. Soc. Ser. 2* 14, 89-102.

D.G. Provis, 1976. "Experimental studies of wave refraction", *Lect. Notes Phys.* 64, 39-45.

A.C. Radder, 1979. "On the parabolic equation method for water-wave propagation", *J. Fluid Mech.* 95, 159-176.

M. Rahman, 1981. "Numerical response of an arbitrarily shaped harbour", *Appl. Math. Modelling* 5, 109-121.

Lord Rayleigh, 1870. "On the theory of resonators", *Phil. Trans. Roy. Soc.* 161, 77-118.

Lord Rayleigh, 1896. *Theory of Sound: Volume II* (MacMillan, London, 2nd ed.).

Lord Rayleigh, 1897. "On the passage of waves through apertures in plane screens and allied problems", *Phil. Mag.* 43, 259-272.

P.B. Rhines, 1969. "Slow oscillations in an ocean of varying depth - Part 1. Abrupt topography, Part 2. Islands and seamounts", *J. Fluid Mech.* 37, 161-205.

J.H. Richmond, 1965. "Scattering by a dielectric cylinder of arbitrary cross section shape", *IEEE Trans. Ant. Prop.* AP-13, 334-341.

M. Roseau, 1976. *Asymptotic Wave Theory* (North-Holland, Amsterdam).

J. Sanchez-Hubert and E. Sanchez-Palencia, 1982. "Acoustic fluid flow through holes and permeability of perforated walls", *J. Math. Anal. Appl.* 87, 427-453.

R.P. Shaw, 1974. "Time harmonic waves scattered by obstacles in an infinite inhomogeneous medium", *J. Acoust. Soc. Amer.* 56, 1354-1360.

R.P. Shaw and W. Falby, 1978. "Febie - a combined finite element - boundary integral equation method", *Comp. Fluids* 6, 153-160.

R.P. Shaw, 1979. "Boundary integral equation methods applied to wave problems", *Developments in Boundary Element Methods - 1* (eds. P.K. Banerjee and R. Butterfield), (Applied Science, London), 121-153.

M.C. Shen, R.E. Meyer and J.B. Keller, 1968. "Spectra of water waves in channels and around islands", *Phys. Fluids* 11, 2289-3304.

M.C. Shen and J.B. Keller, 1975. "Uniform ray theory of surface, internal and acoustic wave propagation in a rotating ocean or atmosphere", *SIAM J. Appl. Math.* 28, 857-875.

R. Smith and T. Sprinks, 1975. "Scattering of surfaces waves by a conical island", *J. Fluid Mech.* 72, 373-384.

J.J. Stoker, 1957. *Water Waves* (Interscience, New York).

W.C. Summerfield, 1969. "On the trapping of wave energy by bottom topography", *Horace Lamb Cent. Oceanogr. Res. Pap.* 30, 1-214.

W.C. Summerfield, 1972. "Circular islands as resonators of long-wave energy", *Phil. Trans. Roy. Soc. Ser. A* 272, 361-402.

C.K.W. Tam and P.J.W. Block, 1978. "On the tones and pressure oscillations induced by flow over rectangular cavities", *J. Fluid Mech.* 89, 373-399.

P.K. Tang and W.A. Sirignano, 1973. "Theory of a generalized Helmholtz resonator", *J. Sound Vib.* 26, 247-262.

F.D. Tappert, 1977. "The parabolic approximation method", *Lect. Notes Phys.* 70, 224-287.

E.O. Tuck, 1971. "Transmission of water waves through small apertures", *J. Fluid Mech.* 49, 65-74.

E.O. Tuck, 1975. "Matching problems involving flow through small holes", *Adv. Appl. Mech.* 15, 89-158.

E.O. Tuck, 1978. "Numerical quadratures of trapezoidal type for inverse square root singularities, with applications to Abel integral equations", *Dept. of Appl. Math., Uni. Adel., Rep.* T7801.

E.O. Tuck, 1980. "The effect of a submerged barrier on the natural frequencies and radiation damping of a shallow basin connected to open water", *J. Austral. Math. Soc. Ser. B* 22, 104-128.

A.C. Vastano and R.O. Reid, 1967. "Tsunami response for islands: verification of a numerical procedure", *J. Mar. Res.* 25, 129-139.

G.N. Watson, 1919. "The diffraction of electric waves by the earth", *Proc. Roy. Soc. Ser. A* 95, 83-99.

R. Weiss, 1972. "Product integration for the generalized Abel equation", *Math. Comp.* 26, 177-190.

E.T. Whittaker and G.N. Watson, 1958. *A Course in Modern Analysis* (Cambridge University Press, Cambridge, 4th ed. re-issue).

Captain Winkler, 1899. "On sea charts formerly used in the Marshall Islands with notices on the navigation of these islanders in general", *Ann. Rep. Smithsonian Inst.*, 487-508.

D.K.P. Yue and C.C. Mei, 1980. "Forward diffraction of Stokes waves by a thin wedge", *J. Fluid Mech.* 99, 33-52.

B.T. Zinn, 1970. "A theoretical study of non-linear damping by Helmholtz resonators", *J. Sound Vib.* 13, 347-356.

C. Zwikker and C.W. Kosten, 1949. *Sound Absorbing Materials* (Elsevier, New York).